

**The PRMT5 complex: Composition, adapter proteins and new
interaction partners**

Inaugural-Dissertation

zur Erlangung des Doktorgrades
der Mathematisch-Naturwissenschaftlichen Fakultät
der Heinrich-Heine-Universität Düsseldorf

vorgelegt von

Jan Cox

aus Geldern

Düsseldorf, Dezember 2021

aus dem Institut für Molekulare Medizin I
der Heinrich-Heine-Universität Düsseldorf

Gedruckt mit der Genehmigung der
Mathematisch-Naturwissenschaftlichen Fakultät der
Heinrich-Heine-Universität Düsseldorf

Berichtersteller:

1. Prof. Dr. Sebastian Wesselborg
2. Prof. Dr. Lutz Schmitt

Tag der mündlichen Prüfung: 25.03.2022

Table of Contents

1	Abstract.....	II
2	Zusammenfassung.....	III
3	List of figures.....	V
4	Abbreviations.....	VI
5	Introduction.....	1
5.1	mRNA splicing and U snRNP biosynthesis.....	1
5.2	Post-translational modification of proteins.....	3
5.2.1	Protein phosphorylation.....	3
5.2.2	Protein arginine methylation.....	5
5.2.3	The protein arginine methyltransferases (PRMTs).....	6
5.3	Composition of the PRMT5 complex.....	8
5.3.1	PRMT5 and WD45 form the core complex.....	8
5.3.2	pICln and RioK1 – the adapter proteins of PRMT5.....	9
5.3.3	NF90 – the new methylation target.....	11
6	Aims.....	13
7	Publications.....	14
7.1	Chapter 1 - An essential role of the autophagy activating kinase ULK1 in snRNP biogenesis.....	15
7.2	Chapter 2 - NF90 – A new interaction partner of the PRMT5-WD45-RioK1 complex is highly methylated in the cell.....	56
8	Discussion.....	79
8.1	Impaired splicing and autophagy - associations between ULK1, AMPK, and mTOR 79	
8.2	PRMT5-RioK1 and mTOR.....	81
8.3	Protein arginine methylation of NF90 – a fully methylated substrate.....	82
8.4	Conclusions and further perspectives.....	83
9	Bibliography.....	84
10	Acknowledgments.....	92
11	Declaration.....	94

1 Abstract

This thesis focuses on the composition of the Protein Arginine Methyltransferase 5 (PRMT5) complex and the search for new interaction partners. In addition to PRMT5, the complex consists of the WD Repeat Domain 45 protein (WD45) and the adapter proteins RIO Kinase 1 (RioK1) or the Chloride Conductance Regulatory Protein (pICln). PRMT5 belongs to the protein arginine methyltransferase family and catalyzes the post-translational symmetric dimethylation of proteins. In this process, two methyl groups of the methyl group donor S-adenosylmethionine (SAM) are transferred to one nitrogen each of the guanidinium group in the side chain of arginine.

Chapter 1 focuses on the PRMT5-WD45-pICln complex, which plays an important role in the biogenesis of spliceosomal small uridine-rich nuclear ribonucleoproteins (U snRNPs). U snRNPs are RNA-protein complexes consisting of a small nuclear RNA (snRNA) and the seven Sm proteins B, D1, D2, D3, E, F and G. For successful assembly of U snRNPs, post-translational modifications such as methylations and phosphorylations of various proteins are necessary. pICln plays a crucial role in this process as an assembly chaperone and recruits the Sm proteins D1 and D2 to PRMT5 where SmD1 is symmetrically dimethylated. Together with Sm E, F, and G a stable precursor ring structure, the so-called 6S complex, is formed. pICln also recruits the Sm proteins D3 and B to PRMT5 for symmetrically dimethylation. The 6S complex and the pICln, SmB, D3 complex are then transferred onto the SMN complex, which assembles the heptameric Sm protein ring onto the snRNAs. We identified pICln as a novel substrate of the Uncoordinated [unc-51] Like Kinase 1 (ULK1). ULK1 phosphorylates pICln at the ULK1 specific serines 193, 195, and 197 in the C-terminus. The phosphorylation of pICln at these sites leads to ring opening of the 6S precursor structure at the SmG-pICln contact surface, allowing a successful assembly of the final U snRNP. In addition to its role in autophagy, we were able to describe here a novel regulatory function of ULK1 in U snRNP biogenesis.

Chapter 2 focuses on RioK1, which is antagonistic to pICln and acts as a general adapter protein by recruiting new interaction partners independently of snRNP biogenesis, thereby increasing the substrate diversity of PRMT5. We discovered the nuclear factor 90 (NF90) as a new substrate of the PRMT5-WD45-RioK1 complex. NF90 contains several RG-rich repeats in the C-terminus, which are typical methylation motifs of PRMT5. We demonstrated that the arginines at positions 644, 649, 653, and 655 are preferentially methylated and that NF90 is fully methylated in the cell under native conditions.

2 Zusammenfassung

Diese Arbeit befasst sich mit der Zusammensetzung des Protein-Arginin-Methyltransferase 5 (PRMT5) Komplexes und der Suche nach neuen Interaktionspartnern. Neben PRMT5 besteht der Komplex aus dem WD Repeat Domain 45 Protein (WD45) und den Adapterproteinen RIO Kinase 1 (RioK1) oder dem Chlorid Conductance Regulatory Protein (pICln). PRMT5 gehört zur Familie der Protein-Arginin-Methyltransferasen und katalysiert die posttranslationale symmetrische Dimethylierung von Proteinen. Dabei werden zwei Methylgruppen des Methylgruppendonors S-Adenosylmethionin (SAM) auf je ein Stickstoff der Guanidiniumgruppe in der Seitenkette von Arginin übertragen.

Kapitel 1 befasst sich mit dem PRMT5-WD45-pICln-Komplex, der eine wichtige Rolle bei der Biogenese von spliceosomalen *small uridine-rich nuclear ribonucleoproteins* (U snRNPs) spielt. U snRNPs sind RNA-Protein-Komplexe, die aus einer *small nuclear RNA* (snRNA) und den sieben Sm-Proteinen B, D1, D2, D3, E, F und G bestehen. Für die erfolgreiche Biogenese von U snRNPs sind posttranslationale Modifikationen wie Methylierungen und Phosphorylierungen verschiedener Proteine erforderlich. pICln spielt in diesem Prozess eine entscheidende Rolle als Assemblierungs-Chaperon und rekrutiert die Sm-Proteine D1 und D2 zu PRMT5, wo SmD1 symmetrisch dimethyliert wird. Zusammen mit Sm E, F und G wird eine stabile Vorläufer-Ringstruktur, der so genannte 6S-Komplex, gebildet. pICln rekrutiert ebenfalls die Sm-Proteine D3 und B, welche durch PRMT5 symmetrisch dimethyliert werden. Der 6S-Komplex und der pICln, SmB, D3-Komplex werden dann auf den SMN-Komplex übertragen, der den heptameren Sm-Proteinring auf der entsprechenden snRNA zusammenbaut. Wir identifizierten pICln als ein neues Substrat der *Uncoordinated [unc-51] Like Kinase 1* (ULK1). ULK1 phosphoryliert pICln an den ULK1-spezifischen Serinen 193, 195 und 197 im C-Terminus. Die Phosphorylierung von pICln an diesen Stellen führt zur Ringöffnung der 6S-Vorläuferstruktur an der SmG-pICln-Kontaktfläche, was einen erfolgreichen Zusammenbau des fertigen U snRNPs ermöglicht. Zusätzlich zu seiner Rolle in der Autophagie konnten wir hier eine neue regulatorische Funktion von ULK1 in der U snRNP-Biogenese beschreiben.

Kapitel 2 befasst sich mit dem zu pICln antagonistischen RioK1, das als allgemeines Adapterprotein fungiert, indem es neue, von der snRNP Biogenese unabhängige, Interaktionspartner rekrutiert und dadurch die Substratvielfalt von PRMT5 erhöht. Wir entdeckten *nuclear factor 90* (NF90) als neues Substrat des PRMT5-WD45-RioK1-Komplexes. NF90 enthält mehrere RG-reiche Wiederholungen im C-Terminus, die typische Methylierungsmotive von PRMT5 sind. Wir konnten zeigen, dass die Arginine an den

Positionen 644, 649, 653 und 655 bevorzugt methyliert werden und NF90 in der Zelle unter nativen Bedingungen vollständig methyliert vorliegt.

3 List of figures

Figure 1: Schematic structure of a U snRNP with U snRNA and the heptameric ring of Sm proteins.....	2
Figure 2: Structure of S-Adenosyl methionine (SAM).....	5
Figure 3: Delocalized positive charge in the guanidinium group of arginine.....	5
Figure 4: Different types of protein arginine methylation catalyzed by PRMTs.....	7
Figure 5: Known functions and composition of the PRMT5 complex.....	10
Figure 6: RG-rich sites in the amino acid sequence of the known PRMT5 substrate nucleolin.....	11

*Figure 4 and Figure 5 were created with BioRender.com

Chapter 1

Figure 1: ULK1 interacts directly with the PRMT5 complex independent of its role in autophagy.....	27
Figure 2: ULK1 phosphorylates pICln in the C-terminal region on residues S193, S195, and S197.....	29
Figure 3: ULK1 dependent phosphorylation of pICln regulated binding of pICln towards SmG.....	32
Figure 4: Phosphorylation of pICln by ULK1 alters the structure of the 6S complex.....	35
Figure 5: Phosphorylated pICln is not able to build the 6S complex and to promote the subsequent Sm protein transfer onto the SMN complex.....	38
Figure 6: Decrease of endogenous ULK1 results in a decreased number of Cajal bodies.....	39
Figure 7: ULK1 phosphorylation of pICln regulates UsnRNP biogenesis.....	41
Figure 8: Schematic illustration summarizing the new role of ULK1 in the UsnRNP assembly.....	43
SD Figure 1: rULK1 interacts directly with rpICln in vitro.....	50
SD Figure 2: Western Blot of size exclusion chromatography of wild type HEK293T and HEK293T ULK1-siRNA knockdown S100 extracts.....	51
SD Figure 3: Composition and activity of the PRMT5-complex with pICln phosphomutants in reference to pICln wt.....	52
SD Figure 4: Inhibition of ULK1 results in a decreased number of Cajal bodies.....	53
SD Figure 5: ATG3 deficient cells are capable for UsnRNP biogenesis.....	54
SD Figure 6: Sequence alignment of human pICln.....	55

Chapter 2:

Figure 1: NF90 interacts with the PRMT5-WD45-RioK1 complex.....	65
Figure 2: The C-terminus of NF90 is methylated by PRMT5.....	67
Figure 3: NF90 arginine mutants and in vivo inhibitor studies.....	69
SD Figure 1: Quantitative binding studies of NF90, PRMT5, WD45, and RioK1.....	78

4 Abbreviations

(v/v)	volume per volume
(w/v)	weight per volume
[32P]-ATP	32-P (phosphate) adenosine triphosphate, radioactive
[32P]-UTP	32-P (phosphate) uridine triphosphate, radioactive
[35S]-methionine	35-S (sulfur) methionine, radioactive
[3-H]-SAM	3-H (tritium) S-Adenosyl methionine, radioactive
μg	microgram
μl	microliter
μM	micromolar
AA	amino acid
AB	amido black
ADMA	asymmetric dimethylarginine
Adox	adenosine dialdehyde
ADP	adenosine diphosphate
ALS	amyotrophic lateral sclerosis
AMPK	AMP-activated protein kinase
AR	autoradiography
ATG	autophagy-related
ATP	adenosine triphosphate
AUC	analytical ultracentrifugation
bp	base pair
BSA	bovine serum albumin
CB	cajal bodies
CS	coomassie blue staining
CTD	C-terminal domain
DKO	double knockout
DMEM	Dulbecco's modified Eagle's medium
DMSO	dimethyl sulfoxide
DNA	deoxyribonucleic acid
DPBS	Dulbecco's phosphate-buffered saline
DRBM	double-stranded RNA-binding motif
dsRNA	double-stranded RNA
DTT	dithiothreitol

DZF	domain associated with zinc fingers
DZF	domain associated with zinc fingers
<i>E. coli</i>	<i>Escherichia coli</i>
e.g.	<i>exempli gratia</i> (for example)
EBSS	Earle's Balanced Salt Solution
EDTA	ethylenediaminetetraacetic acid
EGTA	ethylene glycol-bis(β -aminoethyl ether)-tetraacetic acid
FCS	fetal calve serum
Fig.	figure
FIP200	focal adhesion kinase-interacting protein of 200 kDa
g	gram
GFP	green fluorescent protein
GSH	glutathione
GST	glutathione S-transferase
h	hour
HEK293	human embryonic kidney 293 cells
HPLC	high-performance liquid chromatography
ILF3	interleukin enhancer-binding factor 3
IP	immunoprecipitation
IPTG	isopropyl β -D-1-thiogalactopyranoside
JMJD6	jumonji domain-containing 6 protein
k. dom.	kinase domain
K_D	dissociation constant
kDa	kilodaltons
LB	lysogeny broth
LC-MS	liquid chromatography-mass spectrometry
MBP	myelin basic protein
mCi	microcurie
MDa	mega dalton
MEF	mouse embryonic fibroblast
MEP50	methylosome protein 50
mg	milligram
min	minutes
ml	milliliter

mM	millimolar
MMA	monomethylarginine
MMTS	methylmethanethiosulfonate
ms	millisecond
MST	microscale thermophoresis
mTOR	mechanistic target of rapamycin
mTORC1	mTOR complex 1
NF90	nuclear factor 90
NFAT	nuclear factor of activated T-cells
Ni-NTA	nickel nitrilotriacetic acid
nl	nanoliter
NLS	nuclear localization signal
nM	nanomolar
nm	nanometer
NMR	nuclear magnetic resonance
pICln	chloride conductance regulatory protein
PRMT	protein arginine N-methyltransferase
PRMT5	protein Arginine Methyltransferase 5
PTM	post-translational modification
PTM	post-translational modification
Raptor	regulatory-associated protein of mTOR
RG-rich	arginine-glycine-rich
RioK1	right open reading frame Kinase 1
rpm	revolutions per minute
RT	room temperature
S100	cytoplasm extract
SAH	S-adenosyl-L-homocysteine
SAM	S-adenosyl methionine
SB	super broth
SDMA	symmetric dimethylarginine
SDS	sodium dodecyl sulfate
SDS-PAGE	sodium dodecyl sulphate-polyacrylamide gel electrophoresis
siRNA	small interfering RNA
SMA	spinal muscular atrophy

SMN	survival of motor neuron
snRNA	small nuclear RNA
SPR	surface plasmon resonance
starv.	starvation
SV	sedimentation velocity
TFA	trifluoroacetic acid
U	enzyme unit
U snRNP	small uridine-rich nuclear ribonucleoproteins
ULK1	uncoordinated [unc-51] Like Kinase 1
WB	western blot
WD45	WD repeat domain 45 protein
wt	wild type

Amino Acid	Three letter code	One letter code
Alanine	Ala	A
Arginine	Arg	R
Asparagine	Asn	N
Aspartic acid	Asp	D
Cysteine	Cys	C
Glutamic acid	Glu	E
Glutamine	Gln	Q
Glycine	Gly	G
Histidine	His	H
Isoleucine	Ile	I
Leucine	Leu	L
Lysine	Lys	K
Methionine	Met	M
Phenylalanine	Phe	F
Proline	Pro	P
Serine	Ser	S
Threonine	Thr	T
Tryptophan	Trp	W
Tyrosine	Tyr	Y
Valine	Val	V

5 Introduction

Proteins play an important role in all cellular signaling pathways and functions. Initially, it was assumed that one gene encodes for one protein with one function (Beadle and Tatum, 1941). Today, it is known that several mechanisms at the transcriptional and translational levels significantly increase protein diversity (Bludau and Aebersold, 2020).

Basically, the human genome consists of approx. 20,000 genes (Bludau and Aebersold, 2020). Through alternative splicing, alternative transcription initiation, and alternative polyadenylation, the resulting transcriptome reaches a number of approx. 80,000 - 100,000 transcripts (de Klerk and t Hoen, 2015, Bludau and Aebersold, 2020). Of these mechanisms, RNA splicing is by far the most important (Wang et al., 2008). It is estimated that 86% of all human genes are spliced, resulting in at least two or more mRNA transcripts, making splicing the major contributor to transcriptome diversity (Wang et al., 2008, Bludau and Aebersold, 2020). At the proteome level, mechanisms such as alternative translation initiation or termination and post-translational modifications (PTMs) of proteins can further increase protein diversity (Bludau and Aebersold, 2020). However, alternative translations play only a minor role, since over 90% of the 5' start codon and the first stop codon are used (Bludau and Aebersold, 2020). Post-translational modifications of proteins are thus mainly responsible for diversity at the proteome level. They lead to an enormous complexity of the human proteome, which can grow to an estimated 1,000,000 protein variants (Jensen, 2004, Virág et al., 2020, de Klerk and t Hoen, 2015). Alternative splicing together with PTMs are therefore the two most important processes, allowing proteins encoded by one gene to appear in different modified forms with different properties and functions in the eukaryotic cell. This allows a significant expansion of the functional spectrum of proteins without a substantial increase in the size of the genome.

5.1 mRNA splicing and U snRNP biosynthesis

Before a fully synthesized mRNA is exported from the nucleus and serves as a template for protein translation in the cytoplasm, the pre-RNA undergoes three main processing steps. Already during transcription by polymerase II, the pre-RNA is provided with a 7-methylguanosine at the 5' end (Shatkin, 1976, Galloway and Cowling, 2019). This so-called CAP structure prevents the mRNA from fast degradation and is an important export signal (Galloway and Cowling, 2019). After transcription, the pre-RNA is polyadenylated and a tail of adenines is added to the 3' end. This Poly(A)tail serves to stabilize the mRNA and is also

important for its export to the cytoplasm (Stewart, 2019). Furthermore, eukaryotes have evolved a process called splicing. This is necessary because eukaryotic pre-RNA consists of protein-coding regions, the exons, and non-coding regions the introns (Hoskins and Moore, 2012). These noncoding regions are removed during the maturation of the final mRNA by splicing (Berget et al., 1977, Chow et al., 1977). Through alternative splicing, eukaryotes

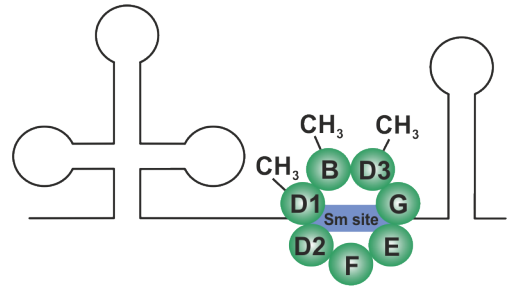


Figure 1: Schematic structure of a U snRNP with U snRNA and the heptameric ring of Sm proteins. SmB, SmD1, and SmD3 are symmetrically dimethylated by PRMT5.

are moreover able to combine different exons and thus translate a pre-RNA into different variants of mRNA. For this purpose, more than 100 proteins form a multi-protein complex that is several megadaltons in size and is called spliceosome (Hoskins and Moore, 2012). The spliceosome is formed by uridine-rich small nuclear ribonucleoproteins (U snRNPs). Each U snRNP consists of an RNA part, the small nuclear RNA (snRNA), and seven proteins, the Sm proteins or LSm proteins (like Sm) (Figure 1) (Gruss et al., 2017). So far, six U snRNPs named after the incorporated snRNA are known but only the five U snRNPs U1, U2, U4, U5, and U6 form the spliceosome (Kambach et al., 1999, Matera and Wang, 2014, Gruss et al., 2017). Except for U6 snRNP, all U snRNPs consist of the seven Sm proteins B/B', D1, D2, D3, E, F, and G (Figure 1) (Gruss et al., 2017). The biogenesis of snRNPs takes place in both the nucleus and cytoplasm, requiring the shuttling of components between the two compartments (Matera and Wang, 2014). The U snRNA is first transcribed in the nucleus and then exported to the cytoplasm. The Sm proteins are translated directly in the cytoplasm, where they are assembled to a heptameric ring and transferred to the snRNA (Figure 1) (Kambach et al., 1999). In the assembly of this heptameric ring structure, both PRMT5 and pICln play important roles. pICln acts as an assembly chaperone (Chari et al., 2008). It directly captures the Sm proteins D1 and D2 stored at the ribosome and recruits them to PRMT5 where SmD1 is symmetrically dimethylated (Paknia et al., 2016, Gruss et al., 2017, Brahms et al., 2000). Together with Sm E, F, and G a stable hexameric precursor ring structure, the so-called 6S complex, is formed (Zhang et al., 2011, Grimm et al., 2013). Likewise, pICln recruits the Sm proteins D3 and B to PRMT5, where they undergo symmetric dimethylation (Brahms et al., 2001, Brahms et al., 2000, Meister et al., 2001b, Friesen et al., 2001b). The 6S complex containing pICln, SmD1, D2, E, F, and G and the pICln, SmB, D3 complex are then transferred onto the SMN complex (Chari et al., 2008). For this transfer, symmetric dimethylation of SmB, SmD1, and SmD3 by PRMT5 is important, since SMN binds preferentially to the dimethylated RG-rich regions of these Sm proteins (Friesen et al., 2001a, Brahms et al., 2001). At the SMN complex, ATP-dependent

assembly of the heptameric ring then occurs (Meister et al., 2001a). pICln leaves the complex and the ring is built onto the snRNA (Chari et al., 2008). Together with SMN, the U snRNP is shuttled into the nucleus and transferred to cajal bodies (CB) for maturation (Matera and Wang, 2014, Gruss et al., 2017). The mRNA spliced by the completed spliceosome can then be exported from the nucleus and serves as a template for protein translation at the ribosome.

5.2 Post-translational modification of proteins

Translation describes the process of synthesis of new proteins in all living cells. After transcription of DNA into mRNA, the latter one is exported from the nucleus into the cytosol. The translation of mRNA into the encoded amino acid chains of the newly synthesized proteins takes place at the ribosomes. After translation, the polypeptide chain folds into the secondary structure consisting of e.g. alpha-helices or beta-sheets. These secondary structure elements together with torsion angles define the tertiary (3D) structure of the polypeptide chain. If a protein consists of several polypeptide chains, these subunits assemble to form the quaternary structure. However, after their biosynthesis, the resulting proteins are further modified by so-called post-translational modifications (PTMs). These modifications occur in form of a chemical modification in the polypeptide chain of the protein and are carried out by various enzymes (Uversky, 2013). Post-translational modifications can be both, reversible and irreversible, and over 400 different modifications are known (Khoury et al., 2011, Aebersold et al., 2018). Of the 20 known canonical amino acids, 15 can be modified (Walsh et al., 2005). The most common modifications are phosphorylation (-PO₃H₃), acetylation (-COCH₃), glycosylation (e.g. glucose), amidation (-NH₂), hydroxylation (-OH), methylation (-CH₃), and ubiquitylation (ubiquitin) (Khoury et al., 2011).

5.2.1 Protein phosphorylation

Phosphorylation of proteins is the most frequent PTM (Khoury et al., 2011, Aebersold et al., 2018). The Modification was studied in more detail in the 1950s, but was first mentioned in 1906, making it the oldest known PTM (Burnett and Kennedy, 1954, Ramazi and Zahiri, 2021). During phosphorylation, the gamma phosphate of ATP is transferred to serines, threonines, or tyrosines in the peptide chain of the protein (Adams, 2001). This reaction is catalyzed by tyrosine kinases or serine/threonine kinases whereas serine is phosphorylated most frequently. The ratio of serine, threonine, and tyrosine phosphorylation is approximately (pSer:pThr:pTyr) 1800:200:1 (Mann et al., 2002). Phosphorylations can be removed by phosphatases, which is why phosphorylations belong to the reversible PTMs (Walsh et al.,

2005). It is assumed that about one-third of all proteins are phosphorylated in the cell (Mann et al., 2002). Therefore, phosphorylations play a role in numerous cellular processes such as RNA splicing (Grimmler et al., 2005), autophagy (Wesselborg and Stork, 2015), or cell cycle regulation and cell signaling (Ardito et al., 2017).

During RNA splicing, numerous proteins are regulated by phosphorylation. For example, phosphorylation of SMN and Gemin 3, two components of the SMN complex, is important for the correct localization of these proteins and a successful assembly of U snRNPs (Grimmler et al., 2005, Husedzinovic et al., 2014). Also, pICln, an assembly chaperon during U snRNP biosynthesis, is highly phosphorylated (Sanchez-Olea et al., 1998, Grimmler et al., 2005). However, no kinase has yet been identified that catalyzes this phosphorylation event (Gruss et al., 2017).

In autophagy, important kinases are the mechanistic target of rapamycin (mTOR), the AMP-activated protein kinase (AMPK), and the Uncoordinated [unc-51] Like Kinase 1 (ULK1). An interplay of these three kinases controls autophagy in the cell through inhibitory as well as activating phosphorylation events (Alers et al., 2012). mTOR is the major component of mTOR complex 1 (mTORC1) consisting of mTOR, Raptor (regulatory-associated protein of mTOR), Deptor (DEP-domain-containing mTOR-interacting protein), PRAS40 (proline-rich AKT substrate 40 kDa), the Tti1/Tel2 complex, and mLST8 (mammalian lethal with sec-13 protein 8) (Laplante and Sabatini, 2012). mTORC1 is a nutrient sensor of the cell and is activated when there is a sufficient supply. Growth factors, amino acids, or ATP lead to the activation of mTOR, which in turn activates anabolic processes and inhibits catabolic processes, e.g. autophagy (Laplante and Sabatini, 2012, Shimobayashi and Hall, 2014). It interacts with the AMP-activated protein kinase (AMPK), an important energy sensor that measures the concentrations of ADP, AMP, and ATP in the cell and maintains the energy homeostasis (Hardie et al., 2012). Under starvation conditions, AMPK directly phosphorylates ULK1, thereby activating ULK1 and inducing autophagy (Kim et al., 2011, Egan et al., 2011). Furthermore, AMPK inhibits mTORC1 by phosphorylation of Raptor (Gwinn et al., 2008) and TSC2 (Inoki et al., 2003). Under nutrient-rich conditions, mTORC1 inhibits the ULK1 complex, which consist of ULK1, FIP200, ATG13, and ATG101, by phosphorylating ULK1 and ATG13 (Hosokawa et al., 2009, Ganley et al., 2009, Jung et al., 2009). As a result of the inhibition by AMPK, mTORC1 is no longer able to suppress ULK1 by phosphorylation, leading to the induction of autophagy by activated ULK1 (Shimobayashi and Hall, 2014, Hosokawa et al., 2009, Jung et al., 2009, Ganley et al., 2009). During autophagy activation and inhibition, the phosphorylation pattern of ULK1 changes. ULK1 loses phosphorylation by the mTORC1 complex at Ser757 and is in turn phosphorylated by AMPK at Ser317, Ser777, Ser467, Ser555,

Thr574, and Ser637 (Kim et al., 2011, Egan et al., 2011, Alers et al., 2012). The phosphorylation pattern of ULK1, therefore, plays an important role in regulating the functions of ULK1 in the cell.

5.2.2 Protein arginine methylation

To date, more than 5,500 methylated human proteins have been identified but research on protein methylation already began in the late 1950s and early 1960s with the discovery of methylations in bacteria (Ambler and Rees, 1959, Murn and Shi, 2017). Ambler and Rees found an ϵ -N-methyl-lysine in the protein flagellin in 1959, which was the first detection of a methylation event in proteins so far (Ambler and Rees, 1959). The first methylation in mammals was later

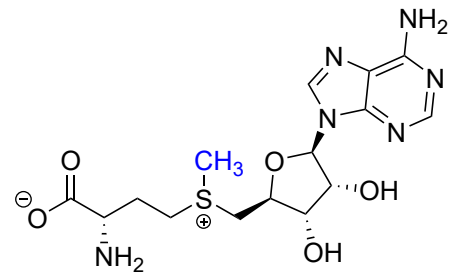


Figure 2: S-Adenosyl methionine (SAM). Substrate and methyl donor of protein arginine methyltransferases. The transferred methyl group is marked in blue.

discovered in 1964 and observed in histones (Murray, 1964). In 1965 Kim and Paik discovered the donor substrate of the methyl group, the S-adenosyl-L-methionine (SAM) (Figure 2) (Kim and Paik, 1965). Up to this point, only methylated lysines had been discovered. This changed three years later with the discovery of arginine as another methylatable amino acid (Paik and Kim, 1968). L-Arginine is a non-essential amino acid and contains a guanidinium group in the side chain. This group has some particular chemical properties: With a pKa value of 13.8, it acts as a strong base and is protonated under almost all physiological conditions (Fitch et al., 2015). The positive charge is thereby delocalized between the

three nitrogen atoms of the group (Figure 3). In addition, the guanidinium group can form five potential hydrogen bonds, making arginine one of the most common hydrogen bond donors (Luscombe et al., 2001, Bedford and Clarke, 2009). The guanidinium group is also the target of post-translational modifications. Two nitrogen atoms of the guanidinium group can be methylated. In this process, $-\text{CH}_3$ groups are transferred from SAM to arginine resulting in three different forms of arginine methylation (Figure 4): Arginine monomethylation (MMA), asymmetric arginine dimethylation (ADMA), and symmetric arginine dimethylation (SDMA). In monomethylation, only one of the two nitrogens is methylated, resulting in an N^G -monomethylarginine. Arginine dimethylation is divided into a

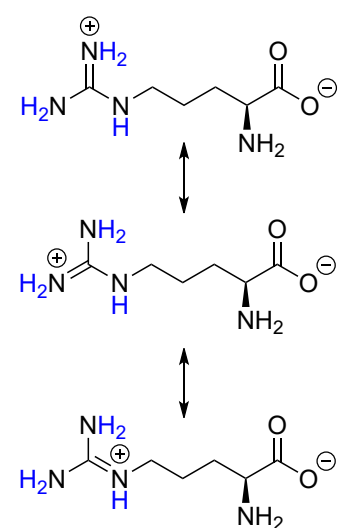


Figure 3: Delocalized positive charge in the guanidinium group of arginine. The five hydrogens involved in hydrogen bond formation are highlighted in blue.

symmetric form in which both nitrogens are monomethylated, resulting in an N^G, N^G-dimethylarginine, and an asymmetric form in which one nitrogen is doubly methylated, resulting in an N^G, N^G-dimethylarginine. The methylation pattern of the guanidinium group has a direct influence on the ability of arginine to form hydrogen bonds. They play a particularly important role in binding nucleic acids and the formation of protein-nucleic acid complexes, as hydrogen bonds interact with the phosphate backbone of the nucleic acids, in the case of arginine preferably with guanine (Luscombe et al., 2001). However, each methylation event blocks an opportunity for hydrogen bond formation, while the charge of the group is not affected (Evich et al., 2016). Through the methylation of arginine, binding to other biomolecules such as nucleic acids or proteins can thus be regulated. This plays an important role in histone development, RNA splicing, regulation of transcription and translation, nuclear export of proteins, protein-protein interactions, and cell signaling (Khoury et al., 2011, Murn and Shi, 2017, Blanc and Richard, 2017) highlighting the central function of this post-translational modification.

5.2.3 The protein arginine methyltransferases (PRMTs)

The enzyme family of protein arginine methyltransferases (PRMTs) catalyzes the different forms of arginine methylation by transferring the methyl group of SAM to the guanidinium group in the side chain of arginine in their respective substrates (Figure 4). This leads to the formation of a methylarginine and an S-adenosyl-L-homocysteine (SAH) (Tewary et al., 2019). PRMTs are conserved in all eukaryotes from yeast to humans (Bachand, 2007) and nine different enzymes are known in humans to date. These nine PRMTs are divided into three types depending on the catalyzed methylation reaction (Blanc and Richard, 2017, Hwang et al., 2021). Type I PRMTs catalyze mono methylations and asymmetric dimethylations and are known as PRMT1, 2, 3, 4, 6, and 8. Type II PRMTs catalyze mono methylations and symmetric dimethylations and consist of PRMT5 and PRMT9 (Branscombe et al., 2001, Cook et al., 2006). PRMT7 catalyzes only MMA and is currently the only member of type III PRMTs (Miranda et al., 2004, Zurita-Lopez et al., 2012, Feng et al., 2013). Based on sequence similarities with PRMT5 and PRMT1, it has been discussed whether PRMT7 is also capable of catalyzing SDMA (Miranda et al., 2004). Studies then showed SDMA activity for PMRT7 and described PRMT7 as a type II PRMT (Lee et al., 2005, Gonsalvez et al., 2007). Meanwhile, PRMT7 has been shown to produce only ω -MMA and thus belongs to a new class of type III methyltransferases (Zurita-Lopez et al., 2012). The confusion concerning PRMT7 resulted from a general design problem of PRMT studies. FLAG-tagged PRMTs were commonly purified with anti-FLAG M2-agarose, which was shown to also bind PRMT5 unspecifically (Nishioka and Reinberg, 2003) and

therefore contaminated purifications. This resulted in symmetric dimethylation properties being observed for FLAG-purified enzymes such as PRMT7 (Zurita-Lopez et al., 2012). Similar confusion was observed for PRMT9. Falsely, the F-box protein FBXO11 was termed and described as PRMT9 due to SDMA activity of FLAG-tagged FBXO11 purifications (Cook et al., 2006). However, in other studies, no methylation activity could be observed for FBXO11 (Fielenbach et al., 2007). Later another protein on chromosome 4q31 was characterized as type II methyltransferase and termed PRMT9 (Yang et al., 2015). Therefore, contrary to some mentions of PRMT7 and FBXO11 in the literature, the only methyltransferases known to date to catalyze symmetric dimethylations on arginines are PRMT5 and PRMT9. The contribution of the respective methyltransferases to symmetric dimethylations in the cell was demonstrated by a PRMT5 knockout leading to a nearly complete loss of SDMA in the cell (Hadjikyriacou et al., 2015). Likewise, it was shown that there is no redundancy between the two methyltransferases, as they do not methylate each other's substrates (Hadjikyriacou et al., 2015), clearly making PRMT5 the dominant and major SDMA methyltransferase in the cell.

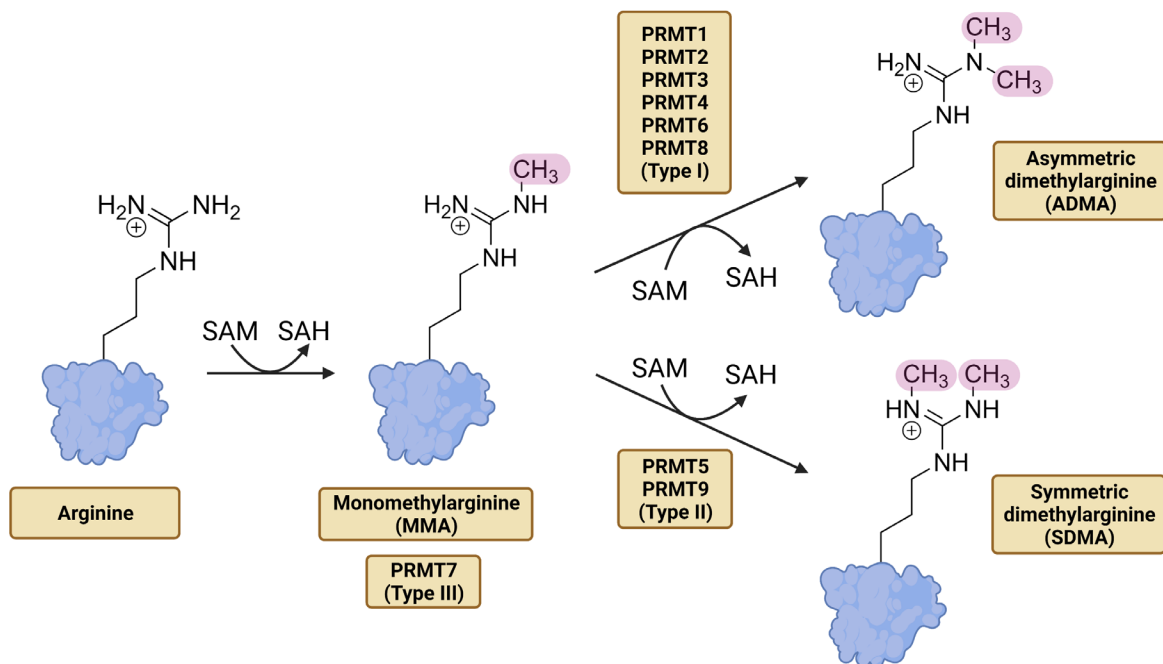


Figure 4: Different types of protein arginine methylation catalyzed by PRMTs. One of the two nitrogens in the guanidinium group of arginine is first methylated (MMA). Methyltransferases that catalyze only MMA are assigned to type III. Type I PRMTs then catalyze the methylation of the already singly methylated nitrogen, resulting in an asymmetrically dimethylated arginine (ADMA). Type II PRMTs catalyze the methylation of the opposite nitrogen, resulting in a symmetrically dimethylated arginine (SDMA).

5.3 Composition of the PRMT5 complex

5.3.1 PRMT5 and WD45 form the core complex

In the literature, PRMT5 is known by various names. In 1998, searching for the function of pICln, the interaction with PRMT5 was observed and PRMT5 was named 72 kDa ICln-binding protein (IBP72) (Krapivinsky et al., 1998). PRMT5 was also shown to be an interaction partner of Jak2 and is therefore known as Janus kinase binding protein 1 (Pollack et al., 1999). Based on sequence homologies with yeast methyltransferases, it was suggested that PRMT5 also exhibits methyltransferase activity (Pollack et al., 1999). The first symmetrically dimethylated protein discovered in the 1970s was the myelin basic protein, but the origin of methylation remained unclear (Baldwin and Carnegie, 1971b, Baldwin and Carnegie, 1971a, Brostoff and Eylar, 1971, Ghosh et al., 1988). This function was later assigned to PRMT5, which was identified as a symmetrically dimethylating type II methyltransferase (Pollack et al., 1999, Branscombe et al., 2001).

PRMT5 has a two-domain structure in which the N-terminal domain forms a TIM barrel and the C-terminal domain forms the catalytic methyltransferase domain (Sun et al., 2011, Antonysamy et al., 2012). The catalytic domain contains the SAM binding pocket, a Rossmann fold, and a β -barrel domain which is involved in substrate binding (Sun et al., 2011). The interaction between two PRMT5 monomers occurs between the N-terminal TIM barrel structure of one protein and the C-terminal catalytic domain of the other. In this process, four PRMT5 molecules form a tetramer with WD45 proteins attached on the outside (Sun et al., 2011, Antonysamy et al., 2012). WD45 interacts tightly with the N-terminal TIM barrel structure of PRMT5 and is important for PRMT5 activity. It enhances the methylation activity of PRMT5 by increasing its affinity for SAM and for substrates (Antonysamy et al., 2012). This results in an active basic hetero-octameric core complex consisting of four PRMT5 and four WD45 proteins with a molecular weight of ~450 kDa (Antonysamy et al., 2012). A special aspect of symmetric dimethylations is that two different nitrogens must be methylated. The nitrogen of the guanidinium group bound in the substrate-binding pocket cannot remain there after monomethylation and be dimethylated (Antonysamy et al., 2012). This is only possible with type I methyltransferases since the same nitrogen is methylated twice and can be rotated in the active site of the enzyme. For type II methyltransferases, rotation in the active site is sterically not possible. The monomethylated substrate must first leave the catalytic center and then rebind to the catalytic center with the second arginine (Antonysamy et al., 2012). An inhibitor often used to study PRMT5 is adenosine dialdehyde (Adox). Adox is an irreversible inhibitor of the S-adenosyl-L-homocysteine hydrolase that completely blocks methylation *in*

in vivo (Patel-Thombre and Borchardt, 1985, Borchardt et al., 1982). The inhibited hydrolase no longer catalyzes the reaction of S-adenosyl-L-homocystein (SAH) to adenosine and homocysteine, leading to accumulation of SAH, which in turn is a universal inhibitor of methyltransferases (Hoffman, 1980, Cantoni G.L., 1980, Chen et al., 2004). Through this mechanism, Adox indirectly prevents the methylation of all newly translated proteins (Hoffman, 1980, Cantoni G.L., 1980, Chen et al., 2004).

5.3.2 pICln and RioK1 – the adapter proteins of PRMT5

The PRMT5 core complex can be extended by the three known adapter proteins pICln, RioK1, and COPR5 (Krapivinsky et al., 1998, Guderian et al., 2011, Lacroix et al., 2008). The different complex composition of PRMT5 and its adapter proteins allows PRMT5 to recruit various substrates and influence different cellular functions (Figure 5): The PRMT5-WD45 complex methylates the histones H4R3, H2AR3, H3R8, and H3R2 directly without the use of an additional adapter protein (Pollack et al., 1999, Branscombe et al., 2001, Pal et al., 2004, Migliori et al., 2012). The PRMT5 substrates SmB, SmD1, and SmD3 (Brahms et al., 2001, Brahms et al., 2000) are recruited through the adapter protein pICln and play a role in U snRNP biogenesis (see chapter 5.1) (Pu et al., 1999, Meister et al., 2001b, Friesen et al., 2001b). Through the adapter protein RioK1, nucleolin is recruited (Guderian et al., 2011). Within the PRMT5-WD45 complex, the adapter proteins pICln and RioK1 compete for the same binding site (Guderian et al., 2011) at the TIM-barrel domain of PRMT5 (Antonysamy et al., 2012, Krzyzanowski et al., 2021). The interaction site with PRMT5 is located in the N-terminus of RioK1 (Guderian et al., 2011) and the C-terminal region of pICln (Krzyzanowski et al., 2021).

pICln is a protein with a molecular weight of 26 kDa (Uniprot, P54105). It is important for cellular processes demonstrated by the early lethality of mouse embryos carrying a knockout of the *ICln* gene (Pu et al., 2000). Likewise, embryonic stem cells without the *ICln* gene are not viable (Pu et al., 2000). pICln was initially incorrectly described as a chloride ion channel protein (Paulmichl et al., 1992, Pu et al., 1999). pICln was then discovered to be an adapter protein of PRMT5 (Krapivinsky et al., 1998) that recruits Sm proteins B, D1, and D3 to the methyltransferase for symmetrical dimethylation (Friesen et al., 2001b, Meister et al., 2001b). In snRNP biosynthesis, pICln functions as an assembly chaperone by first binding the Sm proteins SmD1 and SmD2 and recruiting them to the 6S complex and second by binding the Sm proteins SmB and D3 and transferring them to the SMN complex (Chari et al., 2008). The 6S complex consists of pICln, SmD1, SmD2, SmE, SmF, and SmG and forms an energetically stable ring structure. As long as the Sm proteins are bound to pICln, they are unable to bind

snRNA (Chari et al., 2008). Until now, it is not understood how this ring can be broken up since it is energetically more stable than its opened form (Chari et al., 2008).

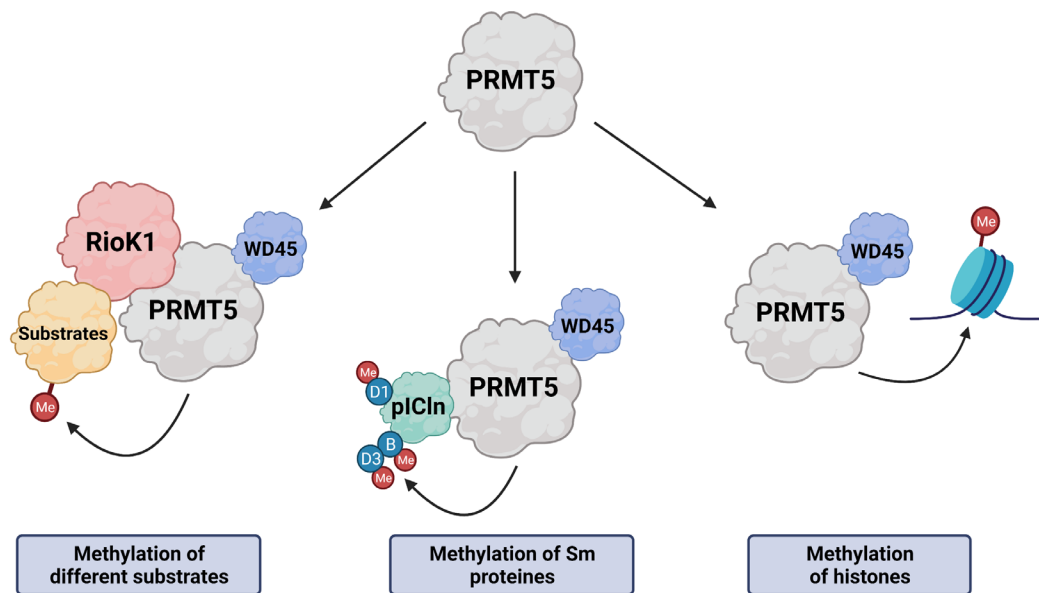


Figure 5: Known functions and composition of the PRMT5 complex. PRMT5 forms a functional complex with WD45. This complex directly methylates histones without an adapter protein. The adapter protein pICln transports the Sm proteins B, D1, and D2 to the PRMT5 complex where they are methylated. RioK1 acts as an adapter protein for different substrates and thus increases the substrate diversity of the PRMT5 complex.

RioK1 has a molecular weight of 66 kDa (Uniprot, Q9BRS2) and is located exclusively in the cytoplasm (Guderian et al., 2011). It belongs to the RIO (right open reading frame) family of atypical protein kinases. Three members of this family are known in humans: RioK1, RioK2, and RioK3 (LaRonde-LeBlanc and Wlodawer, 2005). RioK1 and RioK2 like proteins have been detected in all organisms from archaea to humans. RioK3 has so far only been detected in eukaryotes (LaRonde-LeBlanc and Wlodawer, 2005). Rio kinases are classified as atypical protein kinases because they contain a kinase motif but otherwise lack sequence similarity to eukaryotic protein kinases (LaRonde-LeBlanc and Wlodawer, 2005). Moreover, the only *in-vitro* kinase activity of RioK1 could be detected on typical kinase substrates such as MBP. *In-vivo*, no substrates are known to date (Laronde-Leblanc et al., 2005). Of the three members of the family, only RioK1 is known to interact with PRMT5. It acts as an adapter protein in the PRMT5 complex and recruits new substrates such as nucleolin to the methyltransferase (Guderian et al., 2011). RioK1 is also known for its role in ribosome biosynthesis. It is involved in the maturation of the 40S ribosomal subunit (Widmann et al., 2012). RioK1 binds the subunit via its C-terminus (Ameismeier et al., 2018), which is also responsible for substrate recruitment in the function of RioK1 as an adapter protein of PRMT5 (Guderian et al., 2011).

5.3.3 NF90 – the new methylation target

In the literature, there is a historical confusion around NF90 related to the discovery of the protein. NF90, along with NF45, was first described in 1994 (Kao et al., 1994, Corthesy and Kao, 1994). At that time, the IL2 gene was a model for studying T cell activation and numerous nuclear factors that bind to the IL2 promoter were discovered. A nuclear factor was sought with the properties of being T-cell specific, which was therefore named Nuclear Factor of Activated T cells (NFAT) (Corthesy and Kao, 1994, Shaw et al., 1988). Corthesy and Kao purified two proteins of 45 and 90 kDa from the NFAT binding site in the human IL2 promoter and postulated that these were two of the searched NFAT complex proteins (Corthesy and Kao, 1994, Kao et al., 1994). They named the proteins nuclear factor 45 (NF45) and nuclear factor 90 (NF90). However, it later turns out that NF45 and NF90 bind to the NFAT site but do not belong to the NFAT proteins (Jain et al., 1995). To date, the nuclear factor of activated T-cells proteins are: NFAT1, NFAT2, NFAT3, NFAT4, NFAT5 (Macian, 2005).

NF90 is a splice variant of the interleukin enhancer-binding factor 3 gene (*ILF3*) and represents isoform 2 (Uniprot Q12906-2). Other names are NFAR-1, DRBP76, TCP80, and MPP4. Another splice variant of *ILF3* not discussed in this work but often referred to in the literature is the isoform 1, known as NF110 (Duchange et al., 2000, Saunders et al., 2001). NF90 contains a bipartite nuclear localization signal (NLS) between residues 371-389 with the sequence “KRPMEEDGEEKSPSKKKK”. This corresponds to the common sequence motif “KRP....KKKK” of NLS (Robbins et al., 1991). Removal of this signal disturbs the transport of NF90 into the nucleus (Reichman et al., 2002). In addition, two double-stranded RNA-binding motifs were identified between AA398-467 and AA524-590 (Liao et al., 1998, Patel et al., 1999). NF90 was furthermore described to have dsRNA and DNA binding activity (Satoh et al., 1999). Typical for PRMT target proteins, NF90 contains prominent RG sites in the C-terminus between AA610-656 as potential methylation targets (Lischwe et al., 1985a, Lapeyre et al., 1986). This is similar to the already known PRMT5 substrate nucleolin (Guderian et al., 2011) (Figure 6). Between amino acids 640 and 656, there are seven arginines in an RG-rich region that could be potential targets of PRMT5 (Figure 6). The different names of NF90 show the

Nucleolin, (P19338)	660	670	680	690	700
	GGFGGRGGGR	GGFGGRGGGR	GGRGGFGGRG	RGGFGRGGGF	RGGRGGGGDH
NF90, (Q12906-2)	640	650	660		
	NEVPPPPNLR	GRGRGGSIRG	RGRGRGFGGA		

Figure 6: RG-rich sites in the amino acid sequence of the known PRMT5 substrate nucleolin (Uniprot, P19338) compared with NF90 (Uniprot, Q12906-2).

multiple functions of the protein in the cell. DNA binding activity of NF90 was observed as NF90 binds to the promoter of interleukin 2 as a transcription factor (Corthesy and Kao, 1994). As well, NF90 has been shown to interact with RNA. It binds double-stranded RNA and regulates RNA stability (Patel et al., 1999, Shim et al., 2002). NF90 also plays a role in virus replication where it interacts with RNA (Isken et al., 2003, Liao et al., 1998). The important role of NF90 for the cell is revealed by a knockout in mice, after which the animals suffer from neuromuscular respiratory failure and die 12 h after birth (Shi et al., 2005).

6 Aims

The aim of this thesis was to investigate the composition of the PRMT5 complex, the major symmetric dimethylating methyltransferase in the cell. The PRMT5 complex consist of PRMT5-WD45 and the adapter proteins pICln or RioK1. These adapter proteins recruit new substrates to the PRMT5 complex, thereby increasing the substrate diversity.

The PRMT5-WD45-pICln complex is known to play a role in the biosynthesis of U snRNPs. It methylates the Sm proteins SmB, SmD1, and SmD3, which are recruited to PRMT5 by pICln. pICln is also involved in the assembly of a hexameric precursor ring structure, the 6S-complex, consisting of SmD1, SmD2, SmE, SmF, and SmG during U snRNP formation. Until now, however, it was unknown how the kinetic trap of the energetically stable 6S ring could be overcome. It was known that pICln is the target of several phosphorylation events, but the responsible kinase has not yet been identified. In the first part of this work, the function of ULK1 in U snRNP biosynthesis is investigated and the role of ULK1 as part of the PRMT5-WD45-pICln complex is examined.

The second part of this thesis focuses on RioK1 as the second adapter protein of the PRMT5-WD45 complex. RioK1 competes as an adapter protein for the same binding site as pICln. So far, RioK1 is known to recruit nucleolin to the PRMT5 complex, where it is methylated. This led to the assumption that RioK1 not only recruits nucleolin but also serves as a more general adapter protein. The second part focuses on the PRMT5-WD45-RioK1 complex and the identification of a new PRMT5 substrate. The aim was the characterization of the methylation of the new substrate and the new interaction with PRMT5. Screening for new targets and their role in cellular processes will allow a better understanding of the PRMT5 complex and protein methylations and their role in cellular processes.

7 Publications

Chapter 1:

An essential role of the autophagy activating kinase ULK1 in snRNP biogenesis

Katharina Schmitz*, **Jan Cox***, Lea Marie Esser*, Martin Voss, Katja Sander, Antje Löffler, Frank Hillebrand, Steffen Erkelenz, Heiner Schaal, Thilo Kähne, Stefan Klinker, Tao Zhang, Luitgard Nagel-Steger, Dieter Willbold, Sabine Seggewiß, David Schlütermann, Björn Stork, Matthias Grimmmler, Sebastian Wesselborg and Christoph Peter

*These authors contributed equally to the work

Nucleic Acids Research, 49, 11, 2021, 6437-6455 DOI: 10.1093/nar/gkab452 (Schmitz et al., 2021)

Chapter 2:

NF90 – A new interaction partner of the PRMT5-WD45-RioK1 complex is highly methylated in the cell

Jan Cox, Lea Marie Esser, Katharina Schmitz, Kaja Reiffert, Matthias Grimmmler, Björn Stork, Sebastian Wesselborg, Christoph Peter

Manuscript in preparation

The author contributed to other publications outside the focus of this dissertation:

The Autophagy-Initiating Kinase ULK1 Controls RIPK1-Mediated Cell Death

Wenxian Wu, Xiaojing Wang, Niklas Berleth, Jana Deitersen, Nora Wallot-Hieke, Philip Böhler, David Schlütermann, Fabian Stuhldreier, **Jan Cox**, Katharina Schmitz, Sabine Seggewiß, Christoph Peter, Gary Kasof, Anja Stefanski, Kai Stühler, Astrid Tschapek, Axel Gödecke, Björn Stork

Cell Rep, 2020, 31, 107547 DOI: 10.1016/j.celrep.2020.107547 (Wu et al., 2020)

TNF-induced necroptosis initiates early autophagy events via RIPK3-dependent AMPK activation, but inhibits late autophagy

Wenxian Wu, Xiaojing Wang, Yadong Sun, Niklas Berleth, Jana Deitersen, David Schlütermann, Fabian Stuhldreier, Nora Wallot-Hieke, María José Mendiburo, **Jan Cox**, Christoph Peter, Ann Kathrin Bergmann, Björn Stork

Autophagy, 2021, 1-18 DOI: 10.1080/15548627.2021.1899667 (Wu et al., 2021)

7.1 Chapter 1 - An essential role of the autophagy activating kinase ULK1 in snRNP biogenesis

Title:	An essential role of the autophagy activating kinase ULK1 in snRNP biogenesis
Authors:	Katharina Schmitz*, Jan Cox*, Lea Marie Esser*, Martin Voss, Katja Sander, Antje Löffler, Frank Hillebrand, Steffen Erkelenz, Heiner Schaal, Thilo Kähne, Stefan Klinker, Tao Zhang, Luitgard Nagel-Steger, Dieter Willbold, Sabine Seggewiß, David Schlütermann, Björn Stork, Matthias Grimmmler, Sebastian Wesselborg and Christoph Peter *These authors contributed equally to the work
Published in:	<i>Nucleic Acids Research</i> Volume 49, Issue 11, 21 June 2021, Pages 6437-6455 https://doi.org/10.1093/nar/gkab452
Impact factor:	16,97
Proportional work on this manuscript:	20% Cloning of constructs Protein purification <i>In-vitro</i> kinase assays <i>In-vitro</i> methylation assays <i>In-vitro</i> translations and interaction assays Preparation of figures Contributing in writing the manuscript

An essential role of the autophagy activating kinase ULK1 in snRNP biogenesis

Katharina Schmitz^{1,10}, Jan Cox^{1,10}, Lea Marie Esser^{1,10}, Martin Voss^{1,2}, Katja Sander¹, Antje Löffler¹, Frank Hillebrand³, Steffen Erkelenz^{3,4}, Heiner Schaal³, Thilo Kähne⁵, Stefan Klinker⁶, Tao Zhang^{6,7}, Luitgard Nagel-Steger^{6,7}, Dieter Willbold^{6,7}, Sabine Seggewiß¹, David Schlütermann¹, Björn Stork¹, Matthias Grimmer^{8,9}, Sebastian Wesselborg¹ and Christoph Peter^{1*}

¹Institute of Molecular Medicine I, Medical Faculty, Heinrich Heine University Düsseldorf, Düsseldorf, Germany, ²Institute of Biochemistry, University of Cologne, Cologne, Germany, ³Institute of Virology, University Hospital Düsseldorf, Düsseldorf, Germany, ⁴Institute for Genetics and Cologne Excellence Cluster on Cellular Stress Responses in Aging-Associated Diseases (CECAD), University of Cologne, Cologne, Germany, ⁵Institute of Experimental Internal Medicine, Otto von Guericke University, Magdeburg, Germany, ⁶Institut für Physikalische Biologie, Heinrich-Heine-Universität Düsseldorf, Germany, ⁷Institute of Biological Information Processing (Structural Biochemistry: IBI-7), Forschungszentrum Jülich, Jülich, Germany, ⁸Hochschule Fresenius, Idstein, Germany, ⁹DiaSys Diagnostic Systems GmbH, Alte Strasse 9, 65558 Holzheim, Germany

* To whom correspondence should be addressed. Tel: +49 (0) 211 81-12196; Email: christoph.peter@uni-duesseldorf.de

¹⁰ The authors wish it to be known that, in their opinion, the first three authors should be regarded as joint First Authors

ABSTRACT

The biogenesis of small uridine-rich nuclear ribonucleoproteins (UsnRNPs) depends on the methylation of Sm proteins catalyzed by the methylosome and the subsequent action of the SMN complex, which assembles the heptameric Sm protein ring onto small nuclear RNAs (snRNAs). In this sophisticated process, the methylosome subunit pICln (chloride conductance regulatory protein) is attributed to an exceptional key position as an “assembly chaperone” by building up a stable precursor Sm protein ring structure. Here, we show that – apart from its autophagic role – the Ser/Thr kinase ULK1 (Uncoordinated [unc-51] Like Kinase 1) functions as a novel key regulator in UsnRNP biogenesis by phosphorylation of the C-terminus of pICln. As a consequence, phosphorylated pICln is no longer capable to hold up the precursor Sm ring structure. Consequently, inhibition of ULK1 results in a reduction of efficient UsnRNP core assembly. Thus ULK1, depending on its complex formation, exerts different functions in autophagy or snRNP biosynthesis.

INTRODUCTION

Splicing of mRNA precursors is essential for the maintenance and function of the cellular proteome. This ubiquitous process is mediated by RNA-protein complexes termed spliceosomal U-rich small nuclear ribonucleoprotein particles (UsnRNPs), which are composed of one specific small nuclear RNA (snRNA) and a heptameric ring of the seven common (Sm) proteins B, D1, D2, D3, E, F and G (1-3). The assembly of the UsnRNPs is a sophisticated and stepwise process regulated by the protein arginine methyltransferase 5 (PRMT5), also known as methylosome, and the survival motor neuron (SMN) complex (4-11).

In this segmented process, the methylosome subunit pICln is attributed to an exceptional key position as an “assembly chaperone” (1,12,13). During this assembly reaction pICln functions as a kinetic trap by building up a stable heterohexameric precursor ring structure together with the Sm proteins D1, D2, E, F, and G (13). For the consecutive assembly reaction of the UsnRNP core, it is essential that catalytic snRNA is transferred onto this ring structure with the help of the SMN complex. *In vitro* as well as by *in vivo* experimental systems / cellular extracts the completion of UsnRNP assembly strongly depends on metabolic energy by ATP hydrolysis (8,14). However, the involved regulating elements and the detailed structural and molecular mechanism of ATP-dependent UsnRNP core assembly have remained elusive to date.

Here, we identify the autophagy activating Ser/Thr Unc-51-like kinase (ULK1) as a novel key regulator in this process. We demonstrate that pICln is a specific new substrate of ULK1 and that the newly identified phosphorylation sites in the C-terminus of pICln are responsible for breaking up the Sm ring structure at the newly identified SmG-pICln contact surface. We demonstrate that phosphorylation of pICln by ULK1 is an essential regulatory step to promote efficient biogenesis of the UsnRNP. Thus, we show that ULK1 comprises a crucial key function in two distinct cellular processes: autophagy as well as UsnRNP biogenesis, a process which is known to be highly dependent on protein methylation and phosphorylation events (7,15,16).

MATERIALS AND METHODS

Antibodies

The following primary antibodies were used for immunoblotting and immunofluorescence: α -Actin (A5316, Sigma Aldrich), α -ATG3 (3415, CST), α -ATG101 (SAB4200175, Sigma-Aldrich), α -ATG13 (M183-3, MBL; SAB4200100, Sigma-Aldrich), α -ATG14 (PD026, MBL),

α -ATG14 pS29 (92340, CST), α -Coilin (PA5-29531, Invitrogen), α -FIP200 (A301-574A, Bethyl), α -GAPDH (ab8245, Abcam), α -GFP (3H9, Chromotek), α -LC3B (2775, CST), α -p62 (GP62-C, PROGEN), α -pICln (sc-393525, Santa Cruz), α -PRMT5 (2252, CST), α -SmB (S0698, Sigma-Aldrich), α -SmD1 (ab79977, Abcam), α -SmD2 (SAB2102257, Sigma-Aldrich), α -SmE (NBP2-43792, Novus), α -SmF (SAB2102258, Sigma-Aldrich), α -SmG (HPA064152, Sigma-Aldrich), α -SMN (clone 2B1, 05-1532, Merck Millipore), α -SNRNPB (Y12, MA5-13449, Invitrogen), α -Tubulin (clone B512, T5168, Sigma Aldrich), α -ULK1 (8054; CST), α -ULK2 (ab97695, Abcam), α -WD45 (2823, CST). The detection of proteins was carried out with the following fluorescent secondary antibodies: IRDye 680LT goat α -rabbit, IRDye 680LT goat α -mouse, IRDye 800CW donkey α -rabbit, IRDye 800CW donkey α -mouse, IRDye 800CW goat α -rat. For the detection of proteins *in vivo* via IF the following secondary antibodies were used: Alexa Fluor 568 donkey anti-mouse (A10037, Invitrogen) and Alexa Fluor 647 donkey anti-rabbit (A31573, Invitrogen).

Plasmids and proteins

For *in vitro* assays and pulldown experiments plasmids encoding full-length cDNAs of pICln (X91788.1), SmB (X17567.1), SmD3 (U15009.1), and SmG (X85373.1) were cloned from HEK293T, HeLa, or Jurkat cDNA (High Capacity cDNA Reverse Transcription Kit, Applied Biosystems) into pET-28a (69864-3, EMD Biosciences) or pGEX-6P-1 (27-4597-01, Amersham) with the following primers:

pICln, 5'-GGATCCATGAGCTTCCTCAAAGTTTCCC-3' and

5'-GTCTCGAGTCAGTGATCAACATCTGCATCC-3';

SmB, 5'-ATGAATTCATGACGGTGGGCAAGAGC-3' and

5'ATGCGGCCGCTCAAAGAAGGCCTCGCATC-3';

SmD3, 5'ATGAATTCATGTCTATTGGTGTGCCG-3' and

5'-ATCTCGAGTTATCTTCGCTTTTGAAAGATG-3';

SmG, 5'-ATGGAATTCATGAGCAAAGCTCACCCCT-3'

And 5'ATGCTCGAGTTATCGTTCCAAGGCTT-3'.

For cloning the pICln phosphorylation mutants the Pfu DNA Polymerase (Promega) and the following primers were used:

S193, 195, 197A,

5'-GATTAGAAGGAATGCTTGCTCAGGCTGTGGCCAGCCAGTATAATATG-3' and

5'-CATATTATACTGGCTGGCCACAGCCTGAGCAAGCATTCTTCTAATC-3';

S193, 195, 197D,

5'-GATTAGAAGGAATGCTTGATCAGGATGTGGACAGCCAGTATAATATG-3' and

5'-CATATTATACTGGCTGTCCACATCCTGATCAAGCATTTCCTTCTAATC-3';
 S193A, 5'-ATGCTTGCTCAGTCTGTGAGCAGCCAGTATAATATGGCTG-3' and
 5'-CAGACTGAGCAAGCATTTCCTTCTAATCTCTCCAGTGTGG-3';
 S195A, 5'-TTCTCAGGCTGTGAGCAGCCAGTATAATATGGCTGGGGTC-3' and
 5'-GCTCACAGCCTGAGAAAGCATTTCCTTCTAATCTCTCCAG-3';
 S197A, 5'-CAGTCTGTGGCCAGCCAGTATAATATGGCTGGGGTCAGG-3' and
 5'-GGCTGGCCACAGACTGAGAAAGCATTTCCTTCTAATCTC-3';
 S193D, 5'-ATGCTTGATCAGTCTGTGAGCAGCCAGTATAATATGGCTG-3' and
 5'-CAGACTGATCAAGCATTTCCTTCTAATCTCTCCAGTGTGG-3';
 S195D, 5'-TTCTCAGGATGTGAGCAGCCAGTATAATATGGCTGGGGTC-3' and
 5'-GCTCACATCCTGAGAAAGCATTTCCTTCTAATCTCTCCAG-3';
 S197D 5'-CAGTCTGTGGACAGCCAGTATAATATGGCTGGGGTCAGG-3' and
 5'-GGCTGTCCACAGACTGAGAAAGCATTTCCTTCTAATCTC-3';.

Generation of pGEX6P-1-PRMT5; -WD45 (17); -SmD1; pET28a-SmD1 (18); pcDNA-FRT-TO-GFP; -GFP-ULK1; -GFP-ULK1kd; -GFP-ULK1/ Δ CTD (19) and pMSCVbsd/GFP-ULK1 plasmids have been described previously (20). pET100/D-TOPO-SmE; -SmF; -SmD2 and pcDNA5-FRT-TO-GFP-ULK1 C-terminal domain (AA828-1050) and ULK1-GABARAP domain (AA287-416) were synthesized by GeneArt (Thermo Fisher Scientific).

For interaction studies, pMSCVbsd/GFP and pMSCVbsd/GFP-ULK1 kinase domain plasmids were generated by using pMSCVbsd/GFP-ULK1 and the following primers:

5'-CATGGACGAGCTGTACAAGTGAGGACTCGGATCCCTGGAG-3' (GFP) and
 5'-GTTTTTTCATCACCCCTTCTAACTCGATGCCAGCCCC-3' (ULK1 kinase domain).

For purification of GST-tagged proteins and pulldown assays glutathione sepharose 4B from GE Healthcare was used. For HIS-tagged proteins HisPur™ Ni-NTA Resin from Thermo Fischer was used. For pulldown assays, recombinant proteins were pre-incubated 1,5 h at 4 °C. Subsequently, sepharose was added and further incubated for one hour. After washing, analysis of the respective immobilized proteins per SDS-PAGE and western blotting with specific antibodies was performed.

Recombinant active ULK1, ULK2, and PRMT5 were purchased from Sigma-Aldrich (SRP5096, SRP5097, SRP0145). ULK1/2 inhibitor MRT67307 was obtained through the MRC PPU Reagents and Services facility (MRC PPU, College of Life Sciences, University of Dundee, Scotland, mrcpureagents.dundee.ac.uk).

Cell lines and cell culture

Generation of inducible Flp-In T-REx 293 cells system expressing GFP, GFP-ULK1, GFP-ULK1kd, GFP-ULK1/ Δ CTD, and GFP-pICln were carried out according to the manufacturer's instructions (Invitrogen, Thermo Fisher Scientific) and has been described previously (19). For induction of GFP, GFP-ULK1, GFP-ULK1kd, and GFP-ULK1/ Δ CTD expression, Flp-In T-REx 293 cell lines were stimulated with 0.1 μ g/ml Doxycycline (Clontech) for 18 h. For starvation treatment, cells were incubated in Earle's Balanced Salt Solution (EBSS; Gibco, Thermo Fisher Scientific) for 1 h. For ULK1 knockdown HEK293T cells were transfected using DharmaFECT1 (GE Dharmacon) with 50 nM ULK1 siRNA (L-005049-00-0010, SMARTpool, ON-TARGETplus, GE Dharmacon), 50 nM ULK2 siRNA (L-005396-00-0005, SMARTpool, ON-TARGETplus), and 50 nM of the control siRNA (D-0018-10-1020, SMARTpool, On target plus non-targeting pool) for 48 h.

For interaction studies, HEK293T was transiently transfected with pcDNA5-FRT-TO-GFP-ULK1 GABARAP domain and -ULK1 C-terminal domain constructs using Lipofectamine 3000 (Invitrogen, L3000-015). The cells were harvested 24 h after transfection. Additionally, HEK293T cells stably expressing the GFP-ULK1 kinase domain and GFP were generated. Therefore Plat-E cells were used as packaging cell line and transfected with the retroviral pMSCVbsd expression vectors using FuGENE6 (Promega, E2692). HEK293T cells were incubated with the retroviral supernatant containing 3 mg/ml Polybrene (Sigma-Aldrich, H9268-106) and selected with Blasticidin.

All cell lines were cultured in DMEM (4.5 g/l D-glucose; Gibco, Thermo Fisher Scientific) supplemented with 10% (v/v) FCS (Biochrom, Merck), 100 U/ml Penicillin, and 100 μ g/ml Streptomycin (Gibco, Thermo Fisher Scientific) in a 5% CO₂ humidified atmosphere at 37 °C. For the retroviral transduction Mouse Embryonic Fibroblast (MEF) cells lacking ULK1/2 first Plat E cells were transfected with pMSCV- based expression vectors with FuGENE6 to reconstitute the cells with ULK1 (human) or ULK2 (mouse) for 48 h at 37 °C and 5% CO₂. In a second step, the retroviral supernatant was added to the MEF ULK1/2 DKO cells for reconstitution for 72 h and afterward selected in DMEM high glucose media with 5 μ g/ml Puromycin.

Protein expression and purification

Proteins were overexpressed in BL21 competent *E. coli* for 4 h at RT after induction with 1 mM IPTG. Cells were lysed in 300 mM NaCl, 50 mM Tris/HCl pH 7.5, 5 mM EDTA, 5 mM EGTA,

0.01% (v/v) Igepal, protease inhibitors (cOmplete, EDTA-free protease inhibitor cocktail tablets, Roche), 50 mg/ml Lysozyme (Serva) and by sonication. After centrifugation at 10,000 g for 30 min. the lysate was incubated with glutathione sepharose 4B (GE Healthcare) for 1.5 h at 4 °C and subsequently washed 3 times with lysis buffer.

Immunoblotting and immunopurification

Protein amounts of cleared S100 cytoplasm extract were determined by the Bradford method. Samples were separated by Tris/Tricine or Tris/Glycine SDS gel electrophoresis (21) and transferred to PVDF membranes (Immobilon-FL, Merck Millipore). The immunoblot analysis was performed using the indicated antibodies and signals were detected with an Odyssey LICOR Imaging System. For GFP immunopurification S100 extracts were incubated with GFP-Trap_A beads (ChromoTek) at 4 °C for at least 1.5 h with rotation. Purified proteins were washed 3 times with washing buffer (lysis buffer without Triton X-100 and protease inhibitors), eluted in sample buffer [375 mM Tris pH 7.5; 25.8% (w/v) glycerol; 12.3% (w/v) SDS; 0.06% (w/v) Bromophenol blue; 6% (v/v) β -mercaptoethanol; pH 6.8] and analyzed by immunoblotting. For endogenous immunopurification protein-G-sepharose (GE Healthcare) was washed 3x with HBSS and in following coated with 1 μ g ULK1 antibody. Size exclusion fractions were incubated with the coated sepharose at 4 °C overnight with rotation. Coated sepharose was washed three times with washing buffer (see above) and analyzed by immunoblotting. To generate cleared cellular lysates, cells were lysed in lysis buffer (50 mM Tris-HCl, pH 7.5, 150 mM NaCl, 1 mM EDTA, 1 mM Na_3VO_4 , 50 mM NaF, 5 mM $\text{Na}_4\text{P}_2\text{O}_7$, 1% [v/v] Triton X-100, and protease inhibitor cocktail (Sigma-Aldrich, #P2714) for 30 minutes on ice. Lysates were cleared by centrifugation at 18,000 rpm and 4 °C for 15 min.

Immunofluorescence microscopy

HEK293T and Flp-In T-REx 293 cells were seeded on coverslips in DMEM high glucose media (4,5g/L D-glucose) with 10% (v/v) FCS (Biochrom, Merck), 100 U/ml Penicillin, and 100 μ g/ml Streptomycin (Gibco, Thermo Fisher Scientific) one day before staining. On the next day after washing the cells once with Dulbecco's phosphate-buffered saline (DPBS), fixing was performed with 4% paraformaldehyde for 10 min. Cells were permeabilized with 0.2% Triton X-100/PBS for 10 min. and blocked with 5% BSA for 30 minutes. Proteins were detected with anti-SMN clone 2B1 (1:1000) and anti-Coilin antibody (1:1000), incubation time 2 h. As a secondary antibody, Alexa Fluor 568 (1:200; shown in green) and Alexa Fluor 647 (1:200; shown in red) were used. Analysis of the staining was performed with the ZEISS Apotome.2

and a 40x oil immersion objective. For each counted cell a z-stack with every five pictures per cell, one stack every 0.2 μm , was analyzed.

Cytoplasm extraction (S100) and size exclusion chromatography

HEK293T cells were incubated with Roeder A buffer (22) in an appropriate amount for 10 min at room temperature, dounced 10 times, and adjusted to 150 mM NaCl. After centrifugation at 17,000 g for 30 min the supernatants (S100 extracts) were filtrated with Millex-HA, 0.45 μm filter unit (Merck Millipore) and applied to a Superdex 200 HiLoad 16/600 or Superdex 200 increase 10/300 GL column (GE Healthcare). 2 ml respectively 0.5 ml fractions were collected in running buffer (150 mM NaCl, 50 mM Tris/HCl pH 7.5) and analyzed by immunoblotting. The columns were calibrated with thyroglobulin (669 kDa), ferritin (440 kDa), catalase (232 kDa), aldolase (158 kDa), albumin (67 kDa), ovalbumin (43 kDa), and RNase (14 kDa) (GE Healthcare).

***In vitro* phosphorylation**

GST-PRMT5, -WD45, and -pICln were purified from *E. coli*, GFP-ULK1, and GFP-ULK1kd from Flp-In T-REx 293 cells. GST-ULK1 (1-649) and GST-ULK2 (1-631) were used from Sigma-Aldrich. Recombinant active GST-ULK1/2 or purified GFP-ULK1 and GST substrate in appropriate amounts were incubated in 2 μM ATP, 10 μCi [32P]-ATP (Hartmann Analytic), 2.5 mM Tris/HCl pH 7.5, 5 μM EGTA, 50 μM DTT and 3.75 mM $\text{Mg}(\text{CH}_3\text{COO})_2$ for 45 min at 30 °C. Gel filtration fractions were incubated 1:1 with kinase buffer (50 mM NaCl, 25 mM Tris/HCl pH 7.5, 10 mM MgCl_2 , 2 mM CaCl_2), GST-pICln and 10 μCi [32P]-ATP for 45 min at 30 °C and washed 3 times with kinase washing buffer (300 mM NaCl, 50 mM Tris/HCl pH 7.5, 5 mM EGTA, 5 mM EDTA, 0.01% (v/v) Igepal). The reaction was terminated by adding sample buffer, samples were subjected to SDS-PAGE, and after coomassie staining autoradiography was performed.

***In vitro* translation and interaction assay**

[35S]methionine-labelled (Hartmann Analytic) proteins were made using the TNT Quick Coupled Transcription/Translation System (Promega). For binding assay *in vitro* translated proteins were incubated with GST fusion proteins bounded on glutathione sepharose 4B (GE Healthcare) in interaction buffer (300 mM NaCl, 50 mM Tris/HCl pH 7.5, 1 mM EGTA, 1 mM EDTA, 1 mM DTT and 0.01% (v/v) Igepal) for 1.5 h at 4 °C under rotation. After washing 2 times with interaction buffer bounded proteins were eluted by adding sample buffer, separated by SDS-PAGE, and analyzed by coomassie staining and autoradiography.

***In vitro* methylation**

Target proteins were purified from *E. coli*, GFP-ULK1 from Flp-In T-REx 293 cells. Active PRMT5 (Active Motif/Sigma-Aldrich) and an appropriate amount of target proteins were incubated in 1 μ Ci Adenosyl-L-Methionine, S-[methyl- 3 H] (Perkin Elmer/Hartmann-Analytic), 50 mM Tris/HCl pH 7.5, 1 mM EGTA and 1 mM EDTA for 1-1.5 h at 37 °C. The reaction was terminated by adding sample buffer, samples were subjected to SDS-PAGE. After coomassie staining or western blotting and subsequent amido black staining, autoradiography was performed.

***In vitro* transcription and assembly of UsnRNPs**

The U1 snRNA was *in vitro* transcribed and labelled with 10 μ Ci [32P]-UTP (Hartmann Analytic). For the analysis of the UsnRNP assembly *in vitro*, a GFP-pICln immunoprecipitation was performed with 1 mg cytoplasmic extract (S100). The efficiency of the UsnRNP biogenesis of this immunoprecipitation was analyzed by adding U1 snRNA to the immunoprecipitation in the presence/absence of ATP and active ULK1, or ULK2 kinase. The assembly of UsnRNPs in S100 extracts was performed with 50 μ g of S100 extract. The reactions were incubated at 35 °C for 45 min with 800 counts [32P]-UTP labelled, U1 snRNA, 2 μ g t-RNA, 5 mM ATP and 1 μ l RNAsin in a final volume of 20 μ l PBS. The assembly reactions were analyzed by a native RNA gel electrophoresis and subsequent autoradiography.

Analysis of ULK1 mediated pICln phosphorylation by LC-MS/MS

Samples were separated by SDS-PAGE after *in vitro* kinase assay. Gel areas containing GST-pICln were excised and subjected to in-gel digestion in an adapted manner according (23). NanoLC-MS/MS analysis was performed on a hybrid dual-pressure linear ion trap/orbitrap mass spectrometer (LTQ Orbitrap Velos Pro, Thermo Fisher Scientific) equipped with a U3000 nano-flow HPLC (Thermo Fisher Scientific) as described (24). The procedure in brief: Samples were separated on a 75 μ m I.D., 25 cm PepMap C18-column (Dionex Thermo Fisher Scientific) applying a gradient from 2% (v/v) ACN to 35% (v/v) ACN in 0.1% (v/v) formic acid over 95 min at 300 nl/min. The LTQ Orbitrap Velos Pro MS used exclusively CID-fragmentation with wideband activation (pseudo-MS3 for neutral losses of phosphate residues) when acquiring MS/MS spectra. The spectra acquisition consisted of an orbitrap full MS scan (FTMS; resolution 60,000; m/z range 400-2000) followed by up to 15 LTQ MS/MS experiments (Linear Trap; minimum signal threshold: 500; wideband isolation; dynamic exclusion time setting: 30 s; singly-charged ions were excluded from selection, normalized collision energy: 35%; activation time: 10 ms). Raw data processing, protein identification, and

phosphopeptide assignment of the high-resolution orbitrap data were performed by PEAKS Studio 7.0 (Bioinformatics Solutions Inc.). The false discovery rate (FDR) was set to < 1%. Phosphorylation sites were accepted as confident for $P < 0.005$ (modified t-test, included in PEAKS Studio 7.0) and PhosphoRS score > 90 (25).

Analysis of pICln complex formation by quantitative LC-MS/MS

5 μg of GST-pICln wt and mutants were incubated with 1 mg HEK293T S100 extract overnight at 4 °C. After the addition of 30 μl glutathione sepharose 4B (GE Healthcare) and further incubation at 4 °C for 4 h, purified proteins were washed 3 times with washing buffer (see above) and 3 times with PBS. Then GST-pICln bound to GSH-beads were subjected to “on beads digestion” as described earlier (26). The procedure in brief: GST-pICln bound to beads were resuspended in 50 mM ammonium bicarbonate. Cysteines were reduced by adding 2 mM dithiothreitol (DTT) for 30 min at room temperature and subsequently β -methylthiolated by addition of 10 mM methylmethanethiosulfonate (MMTS). Digestion was performed by the addition of 0.5 μg trypsin (Promega) and incubation overnight at 37 °C. Peptides were extracted by pooling the primary supernatant and the supernatant of a subsequent washing step using 0.1% (v/v) trifluoroacetic acid (TFA). Peptides were purified with reversed-phase C18 ZipTip nano-columns (EMD Millipore), eluted with 0.1% (v/v) TFA/70% (v/v) ACN, and dried. Protein identification was performed by high-resolution mass spectrometry on a hybrid dual-pressure linear ion trap/orbitrap mass spectrometer as described above. Relative protein quantification was achieved using Skyline analysis platform (27) for MS-peak integration on extracted ion chromatograms of the following selected peptides: sp|P54105|ICLN_HUMAN: K.GLGTGTLIAESR.L [30, 42], K.FEESKEPVADEEEEDSDDDVEPITEFR.F [85, 112], R.LEGMLSQSVSSQYNMAGVR.T [187, 205]; sp|P62308|RUXG_HUMAN: R.GNSIIMLEALER.V [63, 74], R.GNSIIMLEALER.V [63, 74]; sp|P62306|RUXF_HUMAN: R.CNNVLYIR.G [65, 72], sp|P62304|RUXE_HUMAN: K.VMVQPINLIFR.Y [12, 22], K.GDNITLLQSVSN.- [80, 91]; sp|P62314|SMD1_HUMAN: K.LSHETVTIELK.N [9, 19], K.NREPVQLETLSIR.G [48, 60], R.YFILPDSLPLDTLLVDVEPK.V [66, 85]; sp|P62316|SMD2_HUMAN: K.NNTQVLINCR.N [37, 46], R.GDSVIVVLR.N [102, 110]; sp|P62318|SMD3_HUMAN: R.VAQLQVYIR.G [54, 63], R.FLILPDMLK.N [69, 77]; sp|P14678|RSMB_HUMAN: R.VLGLVLLR.G [65, 72], R.GENLVSMTVEGPPPK.D [73, 87]. pICln peptides have been used for internal normalization.

Surface plasmon resonance

The affinity dissociation constants (K_d) of pICln wt and pICln aspartate mutant for SmG were determined by surface plasmon resonance (SPR) using a T200 device (Biacore, GE Healthcare). The immobilization of the ligand was performed under mild acidic condition by dissolving the respective protein stock solution (50 mM HEPES, 150 mM NaCl, 1 mM EDTA, pH 7.0) in 10 mM sodium acetate buffer pH 5.0 and injection onto the N-hydroxysuccinimide (NHS) / 1-ethyl-3-(3 dimethylaminopropyl)carbodiimide (EDC) activated series S CM5 sensor chip (Biacore, GE Healthcare) surface. By sequential injection of several μl of ligand solvent, the target immobilization level of 400 RU for the 51 kDa ligand GST-pICln was reached. The remaining activated surface of the ligand flow cell, as well as the activated reference flow cell, was blocked by the injection of 1 M ethanolamine pH 8.5 for 7 min. Affinity measurements were performed in running buffer (300 mM NaCl, 50 mM Tris/HCl pH 7.5, 1 mM EDTA and 1 mM EGTA). The analytes were stored in purification buffer and freshly dissolved in sample buffer (300 mM NaCl, 50 mM Tris/HCl pH 7.5, 1 mM EDTA, 1 mM EGTA, 1 mg/ml BSA, 1 mM DTT and 0.01% (v/v) Igepal) before analysis. During measurement analyte samples were sealed against evaporation and stored at 10 °C until injection. For affinity determination of the analytes, multi-cycle kinetic experiments were applied at 20 °C and 10 $\mu\text{l min}^{-1}$ flow rate. In between each cycle, a regeneration command (200 s injection of 10 mM glycine pH 10 at 30 $\mu\text{l min}^{-1}$, followed by a stabilization period of 500 s with running buffer) was executed if dissociation phase time was not sufficient to dissociate the formed complex of ligand and analyte. Association and dissociation phase of 100 s and 600 s for GST-pICln – SmG analysis was chosen. As a quality control for the activity of the used analyte batch, wild type, and respective mutants were run sequentially on the same sensor chip. The reference flow cell and buffer cycles were used for double referencing of the sensorgrams. For evaluation, the sensorgrams were fitted applying the steady-state fit model of the Biacore T200 Evaluation Software 2.0 (GE Healthcare) and the offset was constantly set to zero.

Sedimentation velocity analysis

Sedimentation velocity analytical ultracentrifugation (SV-AUC) was carried out using a ProteomLab XL-A ultracentrifuge (Beckman Coulter, Brea, CA, USA) equipped with a fluorescence detection system (Aviv Biomedical inc., Lakewood, NJ, USA). Samples were filled into 3-mm double-sector titanium cells (Nanolytics, Potsdam, Germany) with a volume of 100 μl , respectively. Quartz windows were used for all cell assemblies. Radial fluorescence scans were collected continuously at 40,000 rpm using a 488 nm laser for excitation and a 520 nm cut-off emission filter using a constant photomultiplier voltage. A radial resolution of 20 μm

was used for data acquisition. The gains for all samples were adjusted for optimum signal-to-noise ratios. All samples were thermally equilibrated to 20 °C for about 1.5 hours before starting the measurement. The experiments were performed at 40,000 rpm (equivalent to $129,024\times g$) at 20 °C for 5 h. All SV data was then analyzed with continuous distribution $c(s)$ Lamm equation model with maximum entropy regularization, which is implemented in the software package SEDFIT (version 15.01b, <http://www.analyticalultracentrifugation.com/>) (28). The fitting parameters, including the partial specific volumes (\bar{v}), buffer density (ρ), and viscosity (η) were calculated based on the protein sequences and buffer composition, respectively, by applying SEDNTERP (version 20130813 BETA, http://bitcwiki.sr.unh.edu/index.php/Main_Page). The size distributions as well as the sedimentation profiles were presented by GUSI (version 1.2.1) (29). The final sedimentation coefficients were normalized to the s -values at 20 °C in pure water solvent ($s_{20, w}$).

RESULTS

ULK1 is a new interaction partner of the PRMT5 complex

To identify new interaction partners of ULK1 we established an inducible expression system of GFP-ULK1 in Flp-In T-REx 293 cells. Utilizing this system, we identified and characterized new substrates of ULK1 by subsequent co-immunopurification and mass spectrometry like the AMP-activated protein kinase (α , β , and γ AMPK) (19). This survey also revealed a putative association of ULK1 with the Protein arginine N-methyltransferase 5 (PRMT5) as well as its binding partners the methylosome protein 50 (MEP50/WD45) and the chloride conductance regulatory protein (pICln).

To validate our mass spectrometry results we performed immunoblot analysis from Flp-In T-REx 293 cells expressing inducible GFP-ULK1 or a GFP control. Only immunopurification of GFP-ULK1 but not GFP alone revealed an interaction with PRMT5, WD45, and pICln (Fig. 1A). Furthermore, the interaction of the methylosome with ULK1 seems to be independent of autophagy induction since PRMT5 and its binding partners were co-immunopurified to the same extent upon incubation with starvation medium for induction of autophagy (Fig. 1A, B). During autophagy, ULK1 is associated with ATG13, ATG101, and RB1CC1/FIP200 in a high molecular weight complex of 2 MDa (30). The formation of this autophagy-inducing complex requires the C-terminal domain (CTD) of ULK1 (31). When we used Flp-In T-REx 293 cells inducibly expressing a mutant lacking the CTD of ULK1 (GFP-ULK1/ Δ CTD) we still can co-immunopurify comparable amounts of PRMT5, WD45, and pICln (Fig. 1C). In contrast ATG13, ATG101 and FIP200 could only be co-immunopurified with full-length ULK1 (Fig. 1C) or with

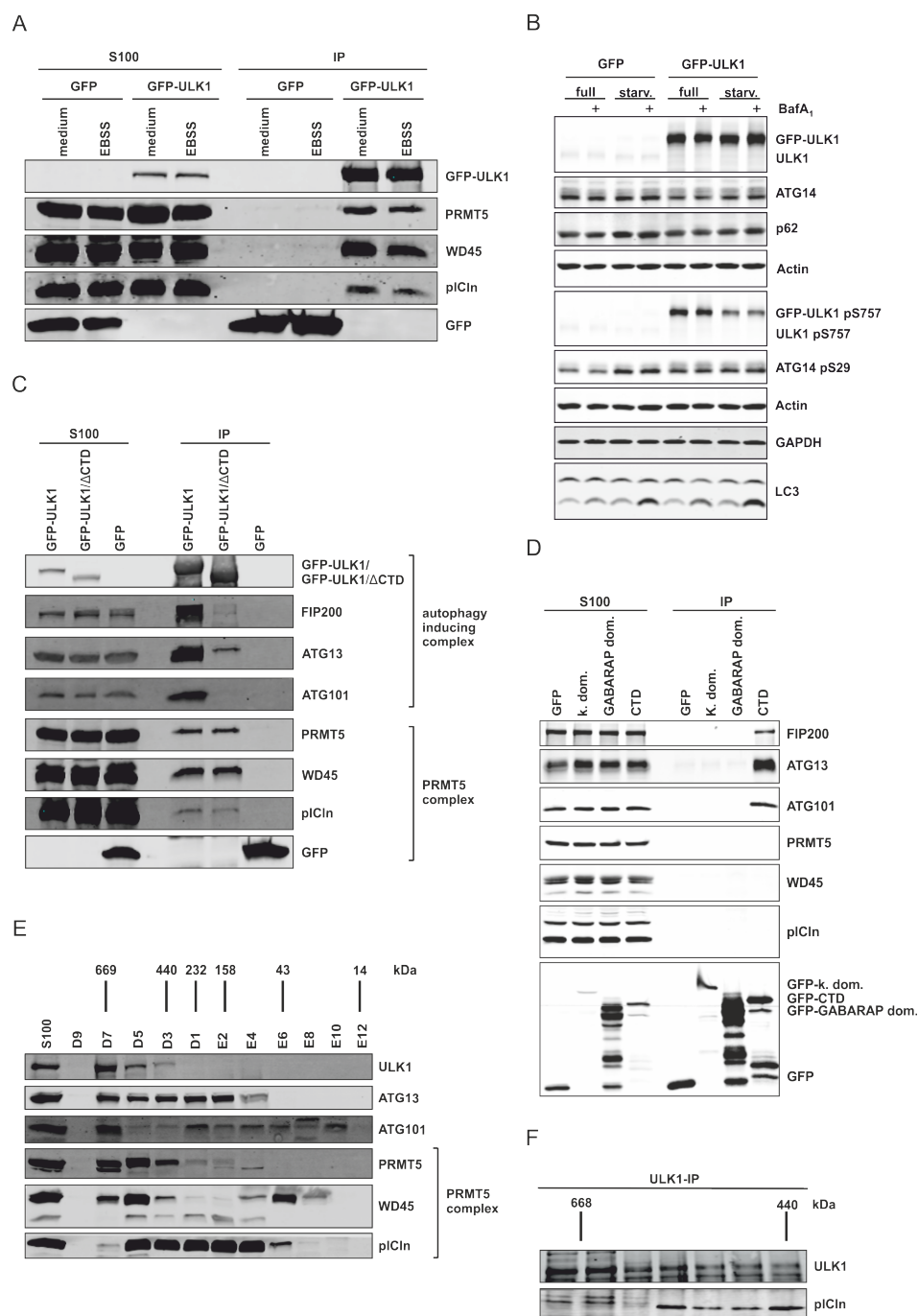


Figure 1. ULK1 interacts directly with the PRMT5 complex independent of its role in autophagy. (A) Flp-In T-REx 293-GFP-ULK1 and Flp-In T-REx 293-GFP cells were stimulated with 0.1 μ g/ml doxycycline for 18 h, followed by 1 h of starvation treatment with EBSS. After cytoplasm extraction (S100) GFP-IP was performed and analyzed by Tris/Glycine-SDS-PAGE and western blotting using antibodies against GFP, PRMT5, WD45, and pICln. (B) Flp-In T-REx 293-GFP-ULK1 and Flp-In T-REx 293-GFP cells were stimulated with 0.1 μ g/ml doxycycline for 18 h, followed by treatment with full or starvation medium (EBSS) in the absence or presence of bafilomycin A1 (BafA1; 10 nM) for 1 h. Afterward, cells were harvested, lysed, and cleared cellular lysates were subjected to Tris/Glycine-SDS-PAGE and immunoblotting for GFP, ULK1 pS757, ATG14, ATG14 pS29, p62, LC3, GAPDH, and Actin. (C) Flp-In T-REx 293-GFP-ULK1, -GFP-ULK1/ Δ CTD, and -GFP cells were stimulated with 0.1 μ g/ml doxycycline for 18 h. After cytoplasm extraction (S100) GFP-IP was performed and analyzed by Tris/Glycine-SDS-PAGE and western blotting using antibodies against FIP200, GFP, PRMT5, ATG13, WD45, pICln, and ATG101. (D) HEK293T cells were stably transfected with pMSCVbsd-GFP-ULK1 kinase domain (k. dom.) and pMSCVbsd-GFP constructs. Additionally, HEK293T cells were transiently transfected with pcDNA5-FRT-TO-GFP-ULK1 GABARAP domain (GABARAP dom.) and -ULK1 C-terminal domain (CTD) constructs. After cytoplasm extraction (S100) GFP-IP was performed and analyzed by Tris/Glycine-SDS-PAGE and western blotting using antibodies against GFP, FIP200, ATG13, ATG101, PRMT5, WD45, and pICln. (E) S100 extract was generated of HEK293T cells and applied to a Superdex 200 increase column. Fractions were analyzed by Tris/Glycine-SDS-PAGE and immunoblotting using antibodies against ULK1, ATG13, ATG101, PRMT5, WD45, and pICln. (F) S100 extract of HEK293T cells was applied to a Superdex 200 increase column and subsequent immunoprecipitation of endogenous was performed with antibody against ULK1. Immunoprecipitation was analyzed by Tris/Glycine-SDS-PAGE using antibodies against ULK1 and pICln.

the C-terminal domain of ULK1 (Fig. 1D). Thus, the interaction of ULK1 with the methylosome is independent of the C-terminal domain of ULK1 and additionally independent of its kinase and GABARAP domain (Fig. 1D). In addition, recombinant co-purified ULK1 and pICln confirmed these results and showed that ULK1 directly interacts with pICln (SD Fig. 1A). This intriguing observation suggests that apart from its central role in autophagy, ULK1 may also play a crucial part in UsnRNP biogenesis and activity.

Furthermore to the established and well-characterized autophagy-inducing complex with a size of >2000 kDa (30), overexpressed ULK1 can be detected in a smaller population in a CTD-independent manner with a molecular mass of 400 to 500 kDa (31). Since the PRMT5 complex also has a molecular size of 400 to 600 kDa (4,5), we used Superdex 200 increase column size exclusion chromatography to analyze the co-migration of ULK1 with the PRMT5 complex. Consistent with the results from Chan and coworkers (31) we detected endogenous ULK1 from HEK293T cells in a size range of 400 to 600 kDa (Fig. 1E). We could identify the co-migration of ULK1 with the endogenous PRMT5 complex in these fractions (Fig. 1E). Additionally, we also could co-immunopurify endogenous pICln along with endogenous ULK1 after size-exclusion chromatography in the corresponding fractions of ULK1 / pICln co-migration (Fig. 1F).

These results posed the question of whether ULK1 is a new substrate of the methylosome. Subsequent radioactive *in vitro* methylation assays with active PRMT5 could not provide evidence for this, whereas the Sm protein D1, a known substrate of PRMT5 (5), was efficiently methylated (SD Fig. 1B).

The methylosome subunit pICln is a new substrate of the autophagy initiating kinase ULK1

Recent studies have shown that besides methylation UsnRNP biogenesis crucially depends on ATP levels (8,14-16). Moreover, the PRMT5 complex subunit pICln is highly phosphorylated *in vitro* and *in vivo* (15,32).

To test if the methylosome is a substrate of ULK1, we performed *in vitro* kinase assays using recombinant purified GST fusion proteins of PRMT5, WD45, and pICln as substrates and active GST-ULK1 purified from Sf9 insect cells. Surprisingly, among all used substrates only pICln showed strong ³²P incorporation upon incubation with active GST-ULK1 (Fig. 2A), indicating that pICln represents a new substrate of ULK1. To prove if the observed phosphorylation of pICln is ULK1 specific, we conducted the kinase assay with a kinase-dead

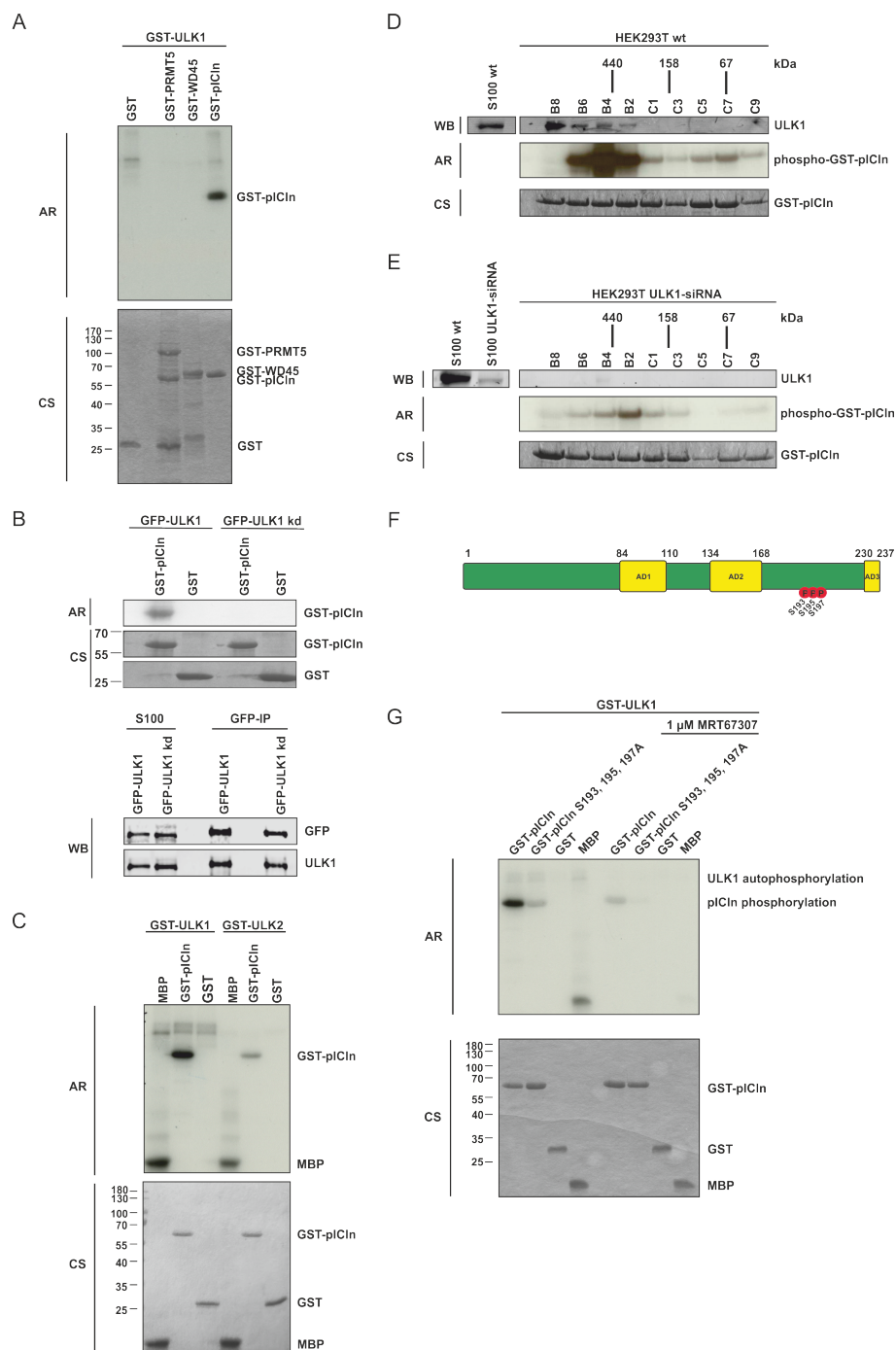


Figure 2. ULK1 phosphorylates pICln in the C-terminal region on residues S193, S195, and S197. **(A)** In vitro kinase assay using recombinant active GST-ULK1 expressed in Sf9 insect cells and GST-PRMT5, -WD45, and -pICln purified from *E. coli* as substrate proteins were incubated with 10 μ Ci [32 P]-ATP for 45 min. at 30 $^{\circ}$ C. Samples were separated by Tris/Glycine-SDS-PAGE and analyzed by autoradiography. **(B)** In vitro kinase assay with purified GFP-ULK1 or GFP-ULK1 kinase-dead mutant (GFP-ULK1kd) overexpressed in Flp-In T-REx 293 cells and GST-pICln was executed as described in **(A)**. Amounts of the GFP precipitation from GFP-ULK1 and GFP-ULK1 kinase-dead were directly compared by Tris/Glycine-SDS-PAGE and Western-Blot analysis using antibodies against ULK1 and GFP. **(C)** In vitro kinase assay using recombinant active GST-ULK1 or -ULK2 expressed in Sf9 cells and GST-pICln was executed as described in **(A)**. **(D; E)** Gel filtration was performed with HEK293T wild type **(D)** and HEK293T ULK1-siRNA knockdown **(E)** S100 extracts fractionated by a Superdex 200 column and evaluated by western blotting. Appropriate fractions were used for in vitro kinase assay using exogenous GST-pICln substrate protein and 10 μ Ci [32 P]-ATP for 45 min. at 30 $^{\circ}$ C and analyzed by autoradiography (Exposure time of 30 minutes for **(D)** and **(E)**). **(F)** Schematic view of pICln protein with its three acidic domains (AD1-3) and the ULK1-dependent phosphorylation sites. In vitro kinase assay was performed with recombinant active GST-ULK1 from Sf9 cells and GST-pICln as described in **(A)**. After Tris/Glycine-SDS-PAGE and coomassie blue staining, the pICln band was excised and phosphorylation status was analyzed by mass spectrometry (LC-MS/MS). Three phosphosites were detected: S193 ($p=3.05E-05$, 94.5%), S195 ($p=2.3E-07$, 100%), S197 ($p=2.8E-06$, 100%). **(G)** Recombinant active GST-ULK1 from Sf9 insect cells was incubated with 1 μ M ULK inhibitor MRT67307 for 30 min. at 30 $^{\circ}$ C. In vitro kinase assay with inhibitor-treated and non-treated GST-ULK1 was performed using substrate proteins GST-pICln wild type and alanine mutant purified from *E. coli* as described in **(A)**. AR: autoradiography, CS: coomassie blue staining, WB: western blotting. See also Supplementary Figure SD2.

mutant of ULK1 (GFP-ULK1kd) (Fig. 2B) (19). Consistent with the previous results, only immunopurified active GFP-ULK1 was able to phosphorylate pICln. In contrast, pICln incubated with the kinase-dead mutant GFP-ULK1kd did not exhibit ^{32}P incorporation at all, although expressed and purified in the same amount as ULK1wt (Fig. 2B).

Since ULK2 is known to compensate for the activity of ULK1 in the regulation of autophagic processes (33), we investigated whether ULK2 can also phosphorylate pICln. In contrast to ULK1, ULK2 was not proficient to phosphorylate pICln with comparable efficiency (Fig. 2C). To evaluate whether ULK1 represents the pICln-associated kinase in cellular extracts we incubated the fractions of a size exclusion chromatography experiment of HEK293T cells with recombinant purified GST-pICln and ^{32}P γ -ATP. Autoradiographic analysis of these particular fractions showed strongly phosphorylated GST-pICln in fractions B2, B4, and B6 (Fig. 2D). Interestingly, predominant phosphorylation of pICln was observed in fraction B4 that corresponds to the entire PRMT5 complex of ~440 kDa consisting of all components (PRMT5, WD45, pICln, and ULK1) (SD Fig. 2A).

To further confirm the specificity of ULK1 dependent phosphorylation of pICln *in vivo*, we performed siRNA knockdown experiments of ULK1 in HEK293T followed by size exclusion chromatography and subsequent assessment of pICln phosphorylation status by kinase assays using recombinant purified GST-pICln as substrate and ^{32}P γ -ATP. By these means, we observed an almost complete reduction in phosphorylation of pICln (Fig. 2E), whereas the composition of the PRMT5 complex was not affected (SD Fig. 2B). Remarkably, the whole PRMT5 complex migrates in a lower size range if ULK1 is absent (SD Fig. 2A, B).

To identify the respective ULK1 phosphorylation sites of pICln, we performed *in vitro* kinase assays following SDS-PAGE, in-gel digestion, and NanoLC-MS/MS analysis. Thereby we identified three novel phosphorylation sites in the C-terminal region of pICln on serine residues 193, 195, and 197 (Fig. 2F).

The substitution of all three serines by alanine residues prevented the phosphorylation of pICln by active ULK1 (Fig. 2G). Also, pharmacological inhibition of active ULK1 with the ULK1/ULK2 specific inhibitor MRT67307 (34) significantly reduces phosphorylation of pICln (Fig. 2G). MS analyses of phosphorylation of pICln by ULK1 showed exclusive phosphorylation of the C-terminal domain. In this region, serines 193, 195, and 197 appeared well ahead of other putative phosphorylation sites with approximately equal signal strength.

Many ULK1 substrates have multiple ULK-specific phosphorylation sites of serines, such as ATG13, FIP200, Beclin1, and AMBRA (35). This prompted us to investigate the ULK-specific phosphorylation of pICln at individual serine residues 193, 195, and 197. However, no preference was detected in *in vitro* phosphorylation experiments in which these residues were replaced individually (SD Fig. 2C, D). Random single phosphorylation or patch phosphorylation appears to be the more favorable model in the case of pICln with respect to known ULK1 substrates. Taken together, we demonstrated by amino acid exchange within pICln as well as ULK1 specific inhibition, ULK1 siRNA, and ULK1 kinase-dead mutant that ULK1 binds and phosphorylates pICln on newly identified sites within its C-terminal region.

ULK1 dependent phosphorylation of pICln regulated binding of pICln towards SmG

pICln is part of the methylosome complex (5,7). For this, we investigate to what extent phosphorylation of pICln does affect PRMT5-mediated methylation of Sm proteins. Hence, we performed *in vitro* methylation assays using the substrate proteins SmB, D1, and D3 with or without the presence of pICln wildtype and phosphomutants thereof. For the methylation of SmB and D3, the presence of pICln does not seem to be necessary, confirming so far findings by Neuenkirchen and colleagues (36). This is in clear contrast to SmD1, as SmD1 is only methylated in the presence of pICln. However, comparing the methylation efficiency of Sm proteins, we see no difference using pICln wildtype or the phosphomutants thereof (SD Fig. 3A-B). To this end methylation of SmD1 is pICln-dependent but independent of the phosphostatus of pICln (SD Fig. 3B).

Extensive and conclusive analysis by A. Chari and coworkers revealed the function of pICln as an assembly chaperone in the biogenesis of UsnRNPs (13). In this function, pICln forms two subcomplexes: One consisting of pICln, the Sm proteins B and D3 (SmB/D3) and the other subcomplex consists of pICln and the Sm proteins D1, D2, E, F, and G (SmD1/D2/E/F/G), see also Fig. 8). In the latter case pICln directly binds to SmD1 and G and builds a highly stable hexameric ring structure, also known as the 6S complex (5,13,37). Consequently, we investigated to which extent the phosphorylation status of pICln affects its binding to the Sm proteins B, D3, D1, and G. To this end, we used GST-tagged recombinant pICln and phosphomutants thereof to analyze the interaction with *in vitro* translated ³⁵S-labelled SmB, SmD3, SmD1 and SmG (Fig. 3A-D). Neither the phospho-inactivating serine-to-alanine nor the phospho-mimicking serine-to-aspartate substitutions at positions 193, 195, and 197 affected the binding capacity of pICln to the Sm proteins B, D3, and D1 (Fig. 3A-C). In striking contrast,

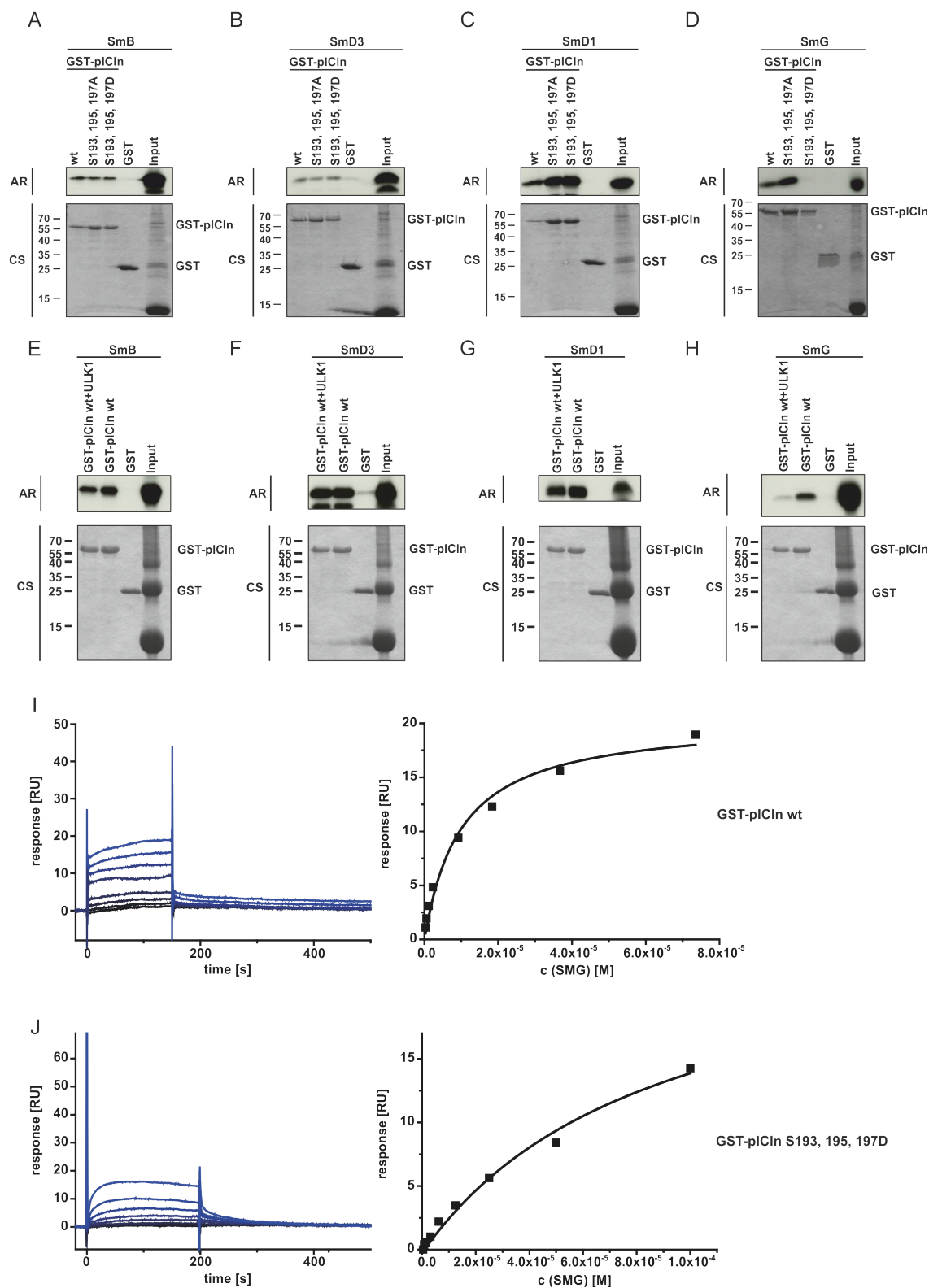


Figure 3. ULK1 dependent phosphorylation of pICln regulated binding of pICln towards SmG. (A-D) In vitro translated L-[³⁵S]-Methionine labelled Sm Proteins D1, D3, B, and G were applied to an interaction assay with GST-pICln wt and phosphomutants purified from *E. coli*. After incubation for 1.5 h at 4 °C and two times washing, purified proteins were separated by Tris/Glycine-SDS-PAGE and analyzed by autoradiography. (E-H) In vitro translated L-[³⁵S]-Methionine labelled Sm Proteins D1, D3, B, and G were applied to an interaction assay with GST-pICln wt and GST-pICln pre-phosphorylated by ULK1. Pre-phosphorylation of pICln was performed for 1.5 h with 100 ng of active ULK1. After incubation for 1.5 h at 4 °C with translated Sm Proteins and two times washing, purified proteins were separated by Tris/Glycine-SDS-PAGE and analyzed by autoradiography. (I; J) SmG (analyte), and GST-pICln (ligand) wild type, and aspartate mutant were purified from *E. coli*. Affinity dissociation constants were analyzed by steady-state analysis (SmG - GST-pICln wt, K_d $11.5 \pm 1.5 \mu\text{M}$; SmG - GST-pICln S193,195,197D, K_d $84.7 \pm 14.7 \mu\text{M}$; $n = 3$). AR: autoradiography, CS: coomassie blue staining.

the phospho-mimicking aspartate mutations of pICln displayed no interaction with SmG, whereas the phospho-inactivating alanine mutations of pICln exhibited increased binding to SmG (Fig. 3D).

In addition to these results binding of GST-pICln wildtype, phosphorylated by ULK1 does not affect association to the Sm proteins B, D3, and D1 (Fig. 3E-G). In contrast, pICln, phosphorylated by ULK1 shows dramatically reduced interaction with SmG compared to unphosphorylated pICln (Fig. 3H).

These results were further corroborated by surface plasmon resonance measurement. The affinity of wild-type pICln for SmG yielded a dissociation constant (K_d) of $11.5 \pm 1.5 \mu\text{M}$ (Fig. 3I). The introduction of phospho-mimicking aspartate mutations (S193, 195, 197D) within pICln reduced the affinity for SmG by almost one order of magnitude to a K_d of $84.7 \pm 14.7 \mu\text{M}$ (Fig. 3J).

Summarizing results so far, we see that phosphorylation of pICln in its C-terminal part by ULK1 does not alter binding properties to SmD1 but does block its binding towards SmG.

Phosphorylation of pICln by ULK1 alters the structure of the 6S complex

These findings are in line with Grimm and colleagues, who proposed the pICln-SmG contact surface as a “mobility hotspot” of the 6S structure by *in silico* prediction (38). From their comprehensive work, the authors concluded that the 6S ring structure has to be transiently opened on the pICln-SmG interface to be able to load Sm proteins onto the SMN complex. To evaluate if phosphorylation of pICln within the 6S complex also alters its composition or structure *in vivo* we used analytical ultracentrifugation (AUC). AUC analysis is an absolute method to determine the size and shape of macromolecules in solution. The sedimentation of macromolecules in a centrifugal force field depends on molecular mass, as well as shape according to the Svedberg equation (SV) (39). SV analysis was applied to detect potential differences in the conformations of wild-type pICln complex and pICln complex with S193, S195, S197D mutations. The used GFP tagged phosphomutants of pICln can interact with its well-known binding partners PRMT5, WD45, and SMN to the same extent as wildtype pICln does (SD Fig. 3A). Also, no differences in interaction with Sm proteins or methylation efficiency could be detected (SD Fig. 3A; B), ensuring the functionality of used mutated constructs. A closed ring structure is expected to sediment faster than an elongated open ring structure of the same mass because of less friction. For this experiment, a GFP variant of pICln

was used. This specific labelling allowed tracing of pICln in its diverse states during ultracentrifugation, using SV-AUC equipped with a fluorescence detection system, in the presence of cytoplasm extract. Other non-fluorescing proteins or macromolecules also present in the S100 extract are invisible. As shown in Figure 4A, the SV analysis of the wild-type complex revealed a major species with a weight averaged s_{app} -value of 4.7 S and a minor species at 16.1 S. For the mutated complex, however, only one species with a weight averaged s_{app} -value of 3.5 S was detected. Concomitantly, the weight average frictional ratio (f/f_0), which is informative on the hydrodynamic shape of a molecule in solution, was higher in the $c(s)$ analysis for the serine-to-aspartate mutant pICln complex. Assuming that the molar mass of the complex stays constant during centrifugation, the SV analysis suggests that the mutant form of the complex has a different, more elongated conformation than the wild-type complex. Since the density and viscosity of the cytoplasm extract were unknown only the relative differences between wild type and mutant complex can be reported as apparent sedimentation coefficients s_{app} . These results are in agreement with our model of a closed ring conformation for the wild type and an open ring structure for the serine-to-aspartate mutant pICln-complex (for the model also see Fig. 8).

To examine whether the phosphorylation of pICln leads to a conformational change of the 6S complex and thus to a reduced sedimentation velocity, we purified the 6S complex containing GFP-pICln by size exclusion chromatography (pooled fractions B12 and B13, SD Fig. 3C) and incubated it with active GST-ULK1 and ATP. As a control, we included the active kinase ULK1 but no additional ATP to demonstrate that the observed effects are not due to the presence of the kinase only but require phosphorylation of pICln. As can be seen from Figure 4B the wild-type pICln complex displayed a heterogeneous distribution pattern in our experiment, with a major peak at 4.5 S and a shoulder peak at about 6.3 S. A very similar distribution was observed in the pICln complex incubated with ULK1 (Fig. 4C). However, the addition of ATP to pICln complex with ULK1 significantly reduced the fraction of the species at ~6.3 S, as depicted in Fig. 4D, suggesting that the closed-ring structures have been converted to open-ring structures in the presence of ULK1 and ATP.

The measured s -value of the complex in the present study is in agreement with the literature for the 6S ring-shaped complexes (38). The SV analysis demonstrated that the phospho-mimicking pICln complex is indeed more elongated than the wild-type complex (Fig. 4A). Additionally, we could show that phosphorylation of pICln within the wild type 6S complex by ULK1 favors the formation of open ring structures (Fig. 4B-E).

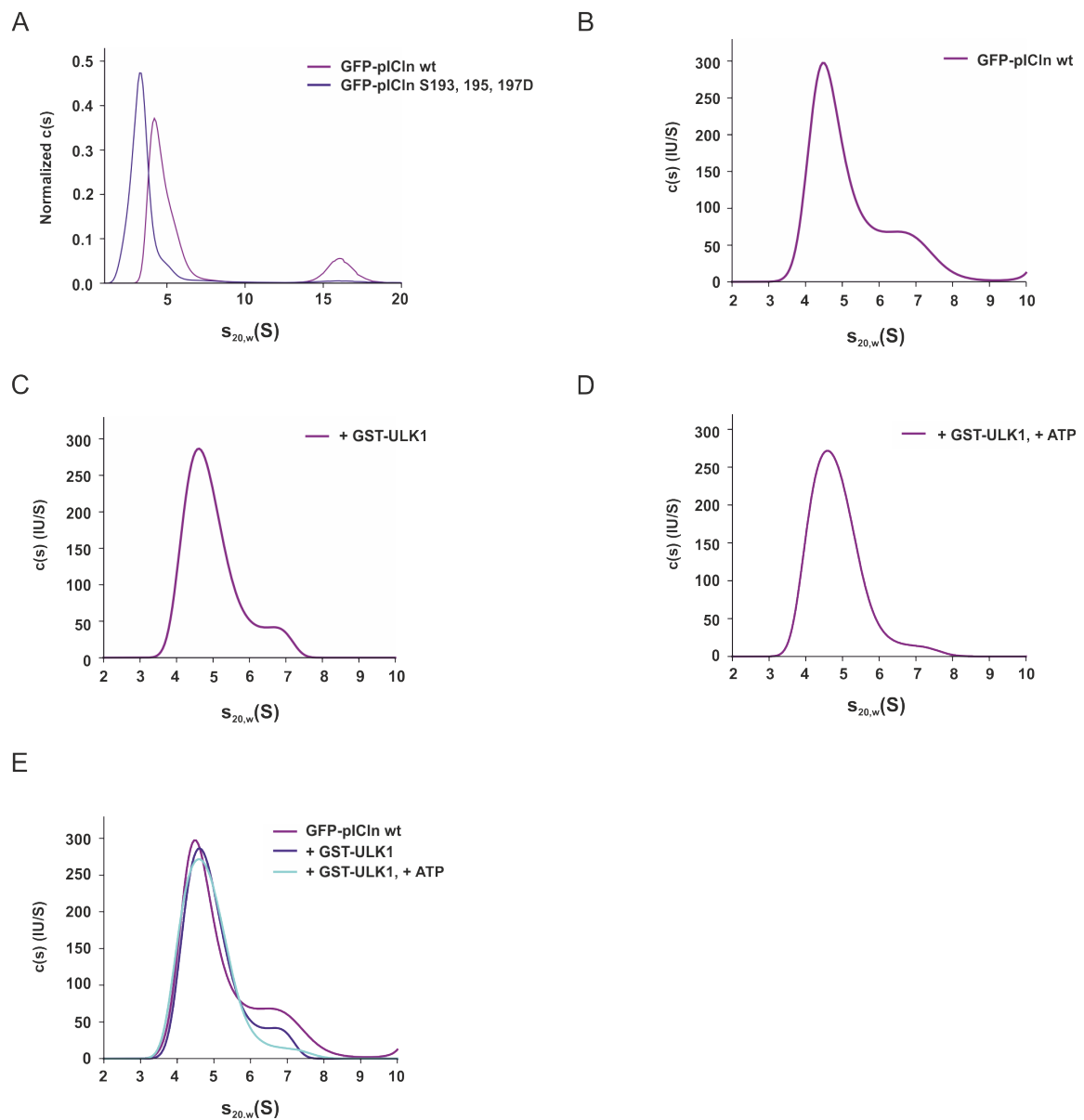


Figure 4. Phosphorylation of pICln by ULK1 alters the structure of the 6S complex. (A) Sedimentation velocity (SV) analysis of GFP-pICln wild type and aspartate mutant in S100 extracts. The $c(s)$ distributions for wild type pICln complex (magenta curve) and pICln complex with S193, S195, S197D mutations (blue curve) obtained from SV analysis at 40,000 rpm at 20 °C for 5 h are shown. For better comparability normalization according to the area under the curve was done. (B-E), Size exclusion chromatography of Flp-In T-REx 293-GFP-pICln S100 extract using a Superdex 200 increase column was performed following a sedimentation velocity analysis (B) for GFP-pICln wild type of the 6S fractions B13 and B12. (C) Sedimentation coefficient distribution for wild-type pICln complex incubated with recombinant active GST-ULK1. (D) Sedimentation coefficient distribution for wild-type pICln complex incubated with recombinant active GST-ULK1 and ATP. (E) Overlay of $c(s)$ distributions for all three samples acquired under the same conditions. All measurements were performed at 40,000 rpm at 20 °C for 5 h. See also Supplementary Figure SD3.

Phosphorylated pICln is not able to build the 6S complex and to promote the subsequent Sm protein transfer onto the SMN complex

To prove whether the phospho-dependent interaction between pICln and SmG is crucial for the biogenesis of the 6S complex *in vivo*, we performed pulldown assays with recombinant GST-tagged wild type, phospho-mimicking (S193, 195, 197D) and -inactivating (S193, 195, 197A) pICln proteins in HEK293T derived cytosolic extracts. Pulldowns were followed by protein identification and relative protein quantification by mass spectrometry analysis (for details see materials and methods section). Thus both, the phospho-mimicking and -inactivating pICln mutants pulled down the same amount of the SmB/D3 subcomplex normalized to pICln wild type (Fig. 5A). In contrast, all components of the 6S complex (SmD1/D2/E/F/G) displayed a substantial reduction in binding to phospho-mimicking pICln mutant whereas the binding capacity of the phospho-inactivating pICln mutant was only slightly affected (Fig. 5A). These data underscore that the phosphorylation status of pICln represents a crucial event in the assembly of the 6S complex: phosphorylated pICln is not able to bind SmD1/D2/E/F/G to the same extent as non-phosphorylated pICln.

Neuenkirchen et al. postulate a model in which pICln binds first to SmD1 and D2 and recruits it for methylation by PRMT5/WD45. After methylation of SmD1 pICln further recruits the subcomplex of SmE/F/G to assemble the final 6S complex that stays associated with the PRMT5 complex (36). Beyond that, we could now show that ULK1 interacts with the PRMT5/6S complex and phosphorylates the C-terminus of pICln. To test the influence of ULK1 mediated pICln phosphorylation towards the biogenesis of the 6S complex, we executed direct binding studies. For this, we used GST-tagged recombinant pICln and phosphomutants thereof to investigate the interaction with *in vitro* translated ³⁵S-labelled preformed Sm protein subcomplexes D1/D2 and E/F/G (Fig. 5B-C). Neither the serine-to-alanine nor the phospho-mimicking serine-to-aspartate substitutions at positions 193, 195, and 197 affected the binding capacity of pICln to the SmD1/D2 subcore (Fig. 5B). In contrast, the phospho-mimicking aspartate mutant of pICln did not interact with the SmE/F/G subcore in comparison to the serine-to-alanine mutant and the wild-type protein (Fig. 5B). Next, we reconstituted the entire 6S complex in a stepwise process, using *in vitro* translated ³⁵S-labelled Sm proteins. In a first step, we incubated GST-tagged recombinant pICln or phosphomutants with *in vitro* translated ³⁵S-labelled subcomplex SmD1/D2. In a subsequent step and after intensive washing, we added *in vitro* translated ³⁵S-labelled subcomplex SmE/F/G. Consistent with our previous data Sm proteins E/F/G only bind to the pICln-SmD1/D2 subcomplex with the wild-type protein and the serine-to-alanine mutant of pICln, but not to the pICln-SmD1/D2 subcomplex

with the serine-to-aspartate mutant (Fig. 5C). We also observed that the binding of the SmE/F/G subcomplex to pICln wt and alanine mutant was increased after incubation with the SmD1/D2 subcomplex (Fig. 5B-C), supporting the model of a sequential binding of Sm protein subcomplexes during 6S assembly.

Our results demonstrate that binding of single Sm proteins, Sm-subcomplexes as well as the formation of a reconstituted entire 6S complex depend on the phosphorylation status of the C-terminus of pICln and its interaction with SmG.

Inhibition of ULK1 results in a decreased number of Cajal bodies

Since Cajal (CBs) bodies dynamically form as a self-organized system, i.e. whenever the concentration of important components or macro-complexes reaches a concentration threshold (40), inhibition of snRNP biosynthesis should lead to a reduction of CBs. Therefore we treated HEK293T cells with ULK1 and ULK2 siRNA followed by immunofluorescence using SMN and Coilin specific antibodies to visualize the quantity of Cajal bodies as a marker of snRNP assembly capability (40-42) (Fig. 6A, B). The number of CBs per nucleus (mean) was significantly decreased in ULK1 knockdown HEK cells (1.10) compared to HEK control cells (1.54) without cumulative effect by concurrent knockdown for ULK2 (1.10 compared to 1.06) (Fig. 6A, B). These results were confirmed by treatment of cells with the ULK1 inhibitor MRT67307 (SD Fig. 4A). The number of CBs per nucleus (mean) was significantly decreased in HEK293T cells after 3 h (0.78) and 5 h (0.6) upon inhibitor treatment compared to HEK cells without treatment (1.49) (SD Fig. 4B).

Comparable results were obtained when we investigated the number of CBs in HEK cells overexpressing phospho-mimicking (S193, 195, 197D) and -inactivating (S193, 195, 197A) pICln proteins (Fig. 6C, D). The mean of CBs in HEK Flp-In T-Rex cells overexpressing the pICln phosphomutants was decreased (1.22 for the alanine mutant and 1.26 for the aspartate mutant) compared to 1.64 in HEK Flp-In T-Rex cells overexpressing the wildtype protein (Fig. 6C, D). In summary, the immunostaining results clearly show an altered content of UsnRNPs upon ULK1-dependent phosphorylation of pICln in the cell.

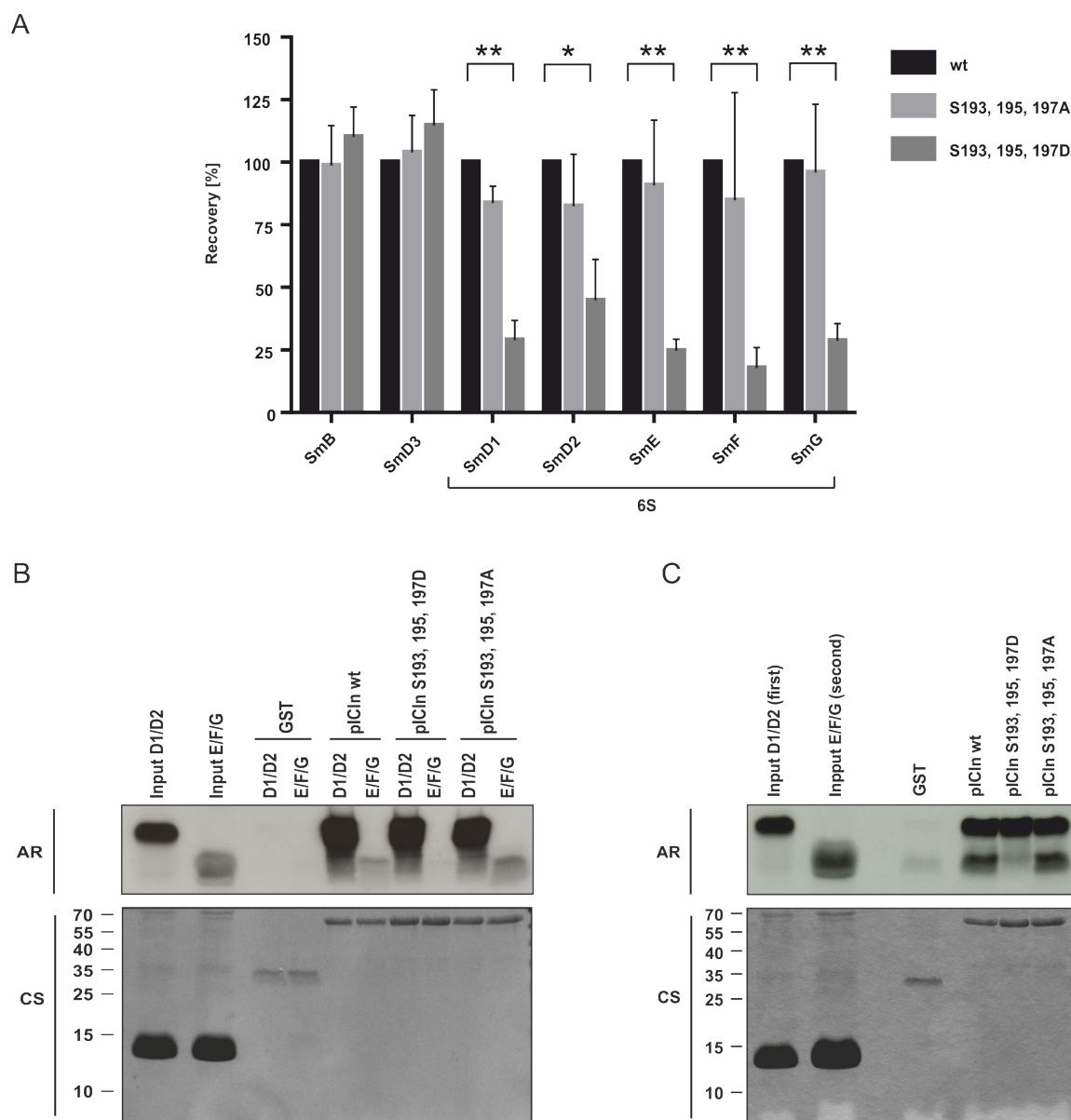


Figure 5. Phosphorylated pICln is not able to build the 6S complex and to promote the subsequent Sm protein transfer onto the SMN complex. **(A)** Pulldown experiments using GST-pICln wild type and phosphomutants were executed in HEK293T S100 extract overnight at 4 °C and co-purified Sm proteins were quantified by mass spectrometry and normalized to pICln wild type (LC-MS/MS; * $p < 0.05$; ** $p < 0.01$). **(B)** Sm proteins D1, D2, E, F, and G were in vitro translated and labelled with L-[³⁵S]-Methionine. D1/D2 and E/F/G were pre-incubated for 1 h at 30 °C and applied to an interaction assay with GST-pICln wt and phosphomutants purified from E. coli. Following incubation for 1.5 h at 4 °C and three times washing purified proteins were separated by Tris/Glycine-SDS-PAGE and analyzed by autoradiography. **(C)** Sm proteins D1, D2, E, F, and G were in vitro translated and labelled with L-[³⁵S]-Methionine. To form the 6S structure D1/D2 and E/F/G were pre-incubated for 1 h at 30 °C. To assess the influence of pICln as an “assembly chaperone” Sm protein complex D1/D2 was first incubated (1 h at 4 °C) using GST-pICln wt or phosphomutants purified from E. coli. After three times washing of the resulting pICln- SmD1/D2 complex, SmE/F/G complex was added to the mixture for a further 1 h at 4 °C. After 3 times washing purified proteins were separated by Tris/Glycine-SDS-PAGE and analyzed by autoradiography. AR: autoradiography, CS: coomassie blue staining.

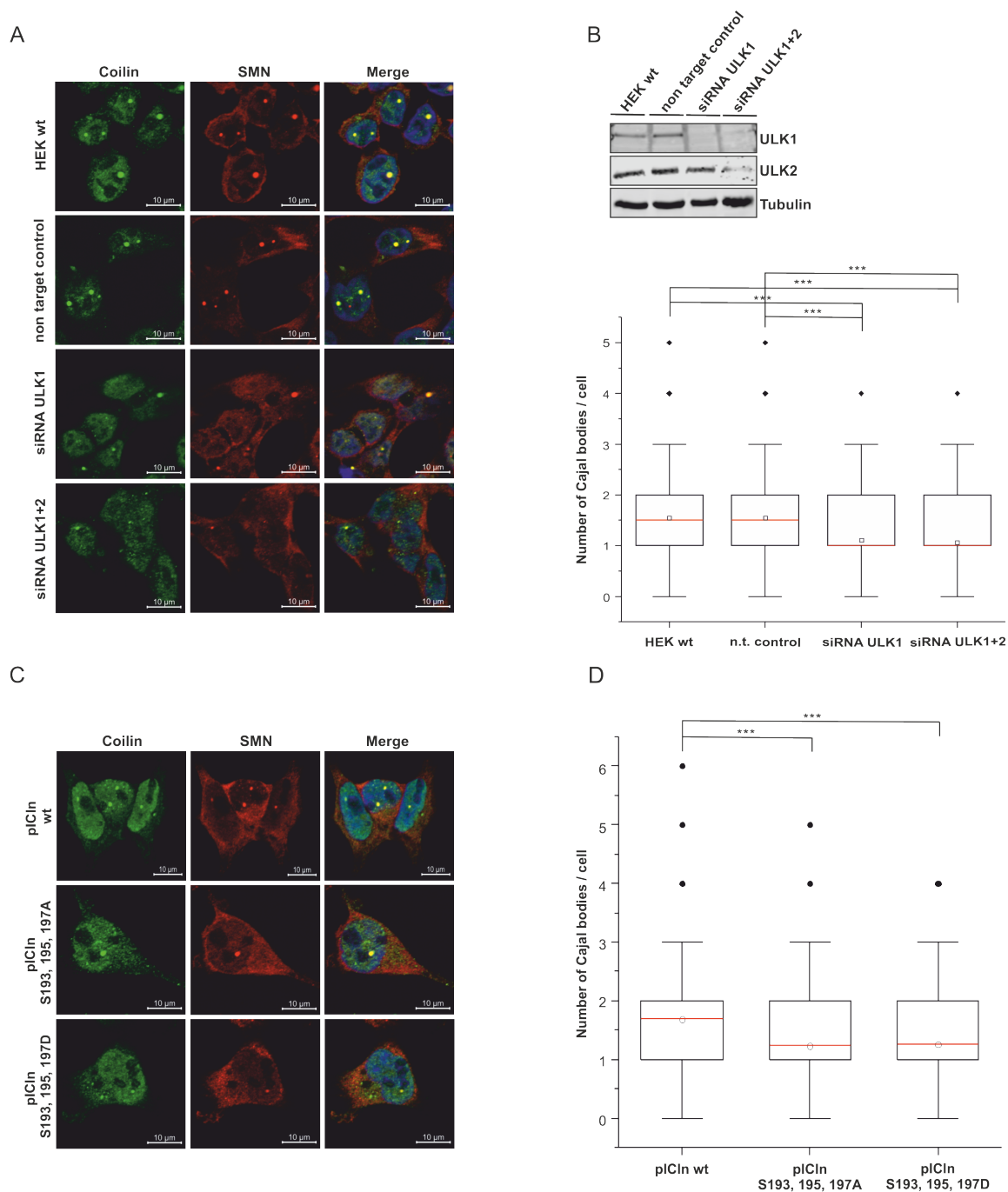


Figure 6. Decrease of endogenous ULK1 results in a decreased number of Cajal bodies. **(A; B)** HEK293T cells were treated with 50 nM ULK1,2 siRNA or non-targeting control for 48 h. **(A; C)** The cells were fixed and Cajal bodies were visualized with antibody staining against Coilin (green) and SMN (red). The DNA was stained with DAPI (blue). **(B)** Cell lysates of siRNA-treated cells were analyzed by Tris/Glycine-SDS-PAGE using antibodies against ULK1, ULK2, and Tubulin. The downregulation of ULK1 causes a reduction in the snRNP storage pool. In the boxplot diagram, the “box” represents 25-75% of all values and the mean (red), standard deviation, and out layers are visualized. HEK293T cells show an average of 1.54 (n=500) Cajal bodies. Treatment of cells with siRNA caused a 1. significant decrease in the number of Cajal bodies. **(C; D)** The phosphorylation status of pICln influences the number of Cajal bodies per cell. **(D)** Overexpression of pICln in Flp-In T-Rex cells causes an increase in the number of Cajal bodies, mean 1.69 (n = 502). Phosphomutants of pICln (S193, 195, 197A, or D), cause a decrease in the number of Cajal bodies per cell. The p-value was calculated with Origin using the Mann-Whitney U test. ***P < 0.005; scale bars: 10 μ m (A and C).

ULK1 regulates UsnRNP biogenesis

As the phosphorylation status of pICln influences the nuclear Cajal bodies, we asked whether ULK1 directly regulates the UsnRNP assembly activity. By using native polyacrylamide gel electrophoresis, we demonstrate that immobilized GFP-pICln derived from HEK Flp-In T-Rex cells can generate U1snRNP cores super-shifted by the anti-Sm antibody Y12 upon incubation with a human *in vitro* transcribed ³²P-labelled U1snRNA (Fig. 7A compare lanes 2 and 3). This assembly reaction is remarkably increasable by adding ATP (Fig. 7A compare lanes 3 and 5) confirming the ATP dependency of the UsnRNP biogenesis by previous studies (8,14,18). It also implies that the corresponding kinase is associated with the immunoprecipitated complex, capable of UsnRNP assembly. The addition of purified ULK1 to the immobilized GFP-pICln/U1 snRNA mixture without extra ATP does not affect the assembly efficiency (Fig. 7A compare lanes 3 and 7). In striking contrast, the simultaneous addition of ULK1 and ATP strongly increases the ability of U1 snRNP core biogenesis (Fig. 7A lane 9). UsnRNP assembly efficiency increases up to 2.6 fold upon the addition of ATP and active ULK1 (see enlarged part of Fig. 7A). On the contrary, the addition of active ULK2 has no stimulatory effect on the UsnRNP assembly efficiency (Fig. 7B).

Complementary to these results HEK cells treated with siRNA against ULK1 and ULK1/ULK2 shown reduced assembly UsnRNP assembly activity (Fig. 7C). A comparable reduction was observed in constitutive ULK1/ULK2-double knockout MEF cells (Fig. 7D). Only double-knockout cells reconstituted with ULK1 but not ULK2 alone can assemble snRNPs with comparable efficiency as MEF wild-type cells do (Fig. 7D).

This data demonstrates that an isolated, purified assembly complex directly is capable to increase UsnRNP biogenesis upon the addition of ATP. It further clearly shows that only ULK1 stimulates UsnRNP biogenesis by direct phosphorylation of pICln. To test whether the observed snRNP biogenesis effects are ULK1-dependent and not due to an overall autophagy-dependent effect we used ATG3 knockouts MEF cells (SD Fig. 5A). Autophagy is completely blocked in this cell line (43) (SDFig. 5A). However, we could detect any difference concerning snRNP assembly activity between normal or ATG3 knockout cells (SD Fig. 5B).

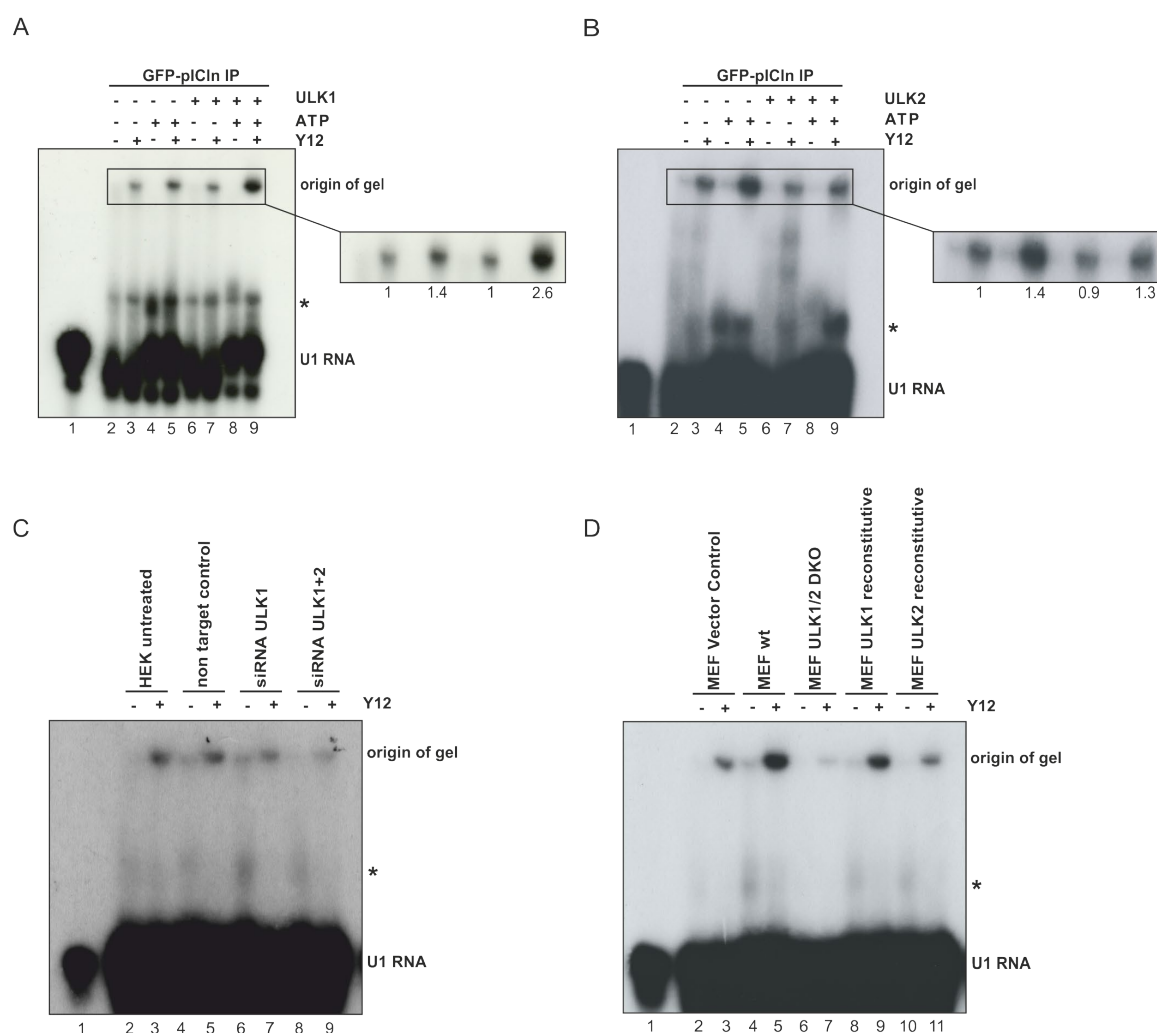


Figure 7. ULK1 phosphorylation of pICln regulates UsnRNP biogenesis. **(A; B)** GFP-pICln IP contains all proteins necessary for U1 snRNP core assembly. In vitro transcribed U1 snRNA labeled with 10 μ Ci [32 P]-UTP was incubated with GFP-pICln IP. After incubation samples were directly analyzed by native gel electrophoresis (2, 4, 6, 8), or the same samples were subjected to supershift analysis with the Y12 antibody to show the specific formation of snRNPs (3, 5, 7, 9). The formation of snRNPs was quantified with Image Studio to compare the efficiency of the snRNP biogenesis. Adding ATP to the GFP-pICln IP increases efficiency (1.4) while adding ATP and ULK1 (2.6) leads to the highest efficiency in snRNP formation compared to the GFP-pICln IP alone. Adding ULK2 and ATP to the GFP-pICln IP caused no effect at all (1.3). **(C)** In vitro transcribed U1 snRNA labelled with 10 μ Ci [32 P]-UTP was incubated with S100 extract from HEK293T cells treated with siRNA against ULK1, ULK 1+2, or a non-targeting control. After a native gel electrophoresis supershift analysis was performed using the Y12 antibody. **(D)** S100 extract from Mouse Embryonic Fibroblasts (MEFs) lacking ULK1/2, or reconstituted with vector control, ULK1 or ULK2 were incubated with [32 P] labelled U1 snRNA, after a native gel electrophoresis supershift analysis occurred.

DISCUSSION

Although the ATP dependency of the Sm core assembly and phosphorylation of some key components within the UsnRNP pathway has been known for many years (8,15,16,44), neither the responsible kinases nor the structural or mechanistic consequences of the modified residues were known so far. In our study, we identified the Ser/Thr kinase ULK1 as a functional component of the PRMT5 complex and as an essential key regulator of UsnRNP biogenesis by specific phosphorylation of pICln.

The identified phospho-serines 193, 195, and 197 are located in a region of pICln that, based on crystal structures, is not known for Sm protein binding so far, but match the previously reported consensus sequence for ULK1 phosphorylation (35). Certainly, the structure determination of pICln has only been executed with pICln of *D. melanogaster*, C-terminal deletions of pICln of *D. melanogaster* (13,38,45), or with the isolated N-terminus of canine pICln (46,47). Recent studies also have determined the C-terminus of canine pICln by NMR (48). The authors demonstrated that the C-terminus of pICln is highly conserved in vertebrates and natively unstructured with secondary structure elements. These unstructured regions often function as flexible linkers in the assembly of macromolecular systems regulated by post-translational modifications (49). The lack of essential elements of the intrinsic disorder region in initial experiments based on *D. melanogaster* pICln may explain why this region was not addressed for Sm protein binding in the human system so far (SD Fig. 6) (50). It also may explain the difficulties to solve the crystal structure of the human 6S intermediate complex, containing flexible unstructured regions (45). In the capacity of an assembly chaperone of Sm proteins (13), the conformational flexibility of pICln generated by the disordered C-terminus is an important property in the consecutive transfer of the Sm proteins onto the SMN complex. The work presented here specifically does focus on the exclusive use of human proteins and human snRNA to assess the status and mechanism of human Sm core assembly and UsnRNP biogenesis.

The newly identified ULK1-dependent phosphorylation sites within the C-terminus of pICln regulate the contact surface of pICln and SmG (Fig. 2F, 3D, H-J); consequently, they also influence binding properties towards the SmE/F/G subcomplex (Fig. 5B, C). Consistent with these are the results from the analytical ultracentrifugation analysis, demonstrating that the phosphorylation of purified cytoplasmic 6S complex by ULK1 favors the formation of an open ring structure (Fig. 4E). As the formation of 6S, along with UsnRNP assembly is a sophisticated process also involving the interaction of 6S with the PRMT5- and subsequently, also the interaction with the SMN complex, re-arrangements on PRMT5-6S-SMN cannot be excluded completely. Therefore, it would also be conceivable that the phosphorylation state of pICln impairs the transfer of Sm proteins to the SMN or from the PRMT5 complex. Direct structural data by Cryo-EM or NMR upon phosphorylation of pICln finally will cover the dynamics of this process on a molecular level in the future.

These results prove the pICln-SmG contact surface as a mobility hotspot of the 6S complex (38). Our data also provide information on the composition and conformation of the native human 6S complex and its functional regulation by phosphorylation of pICln.

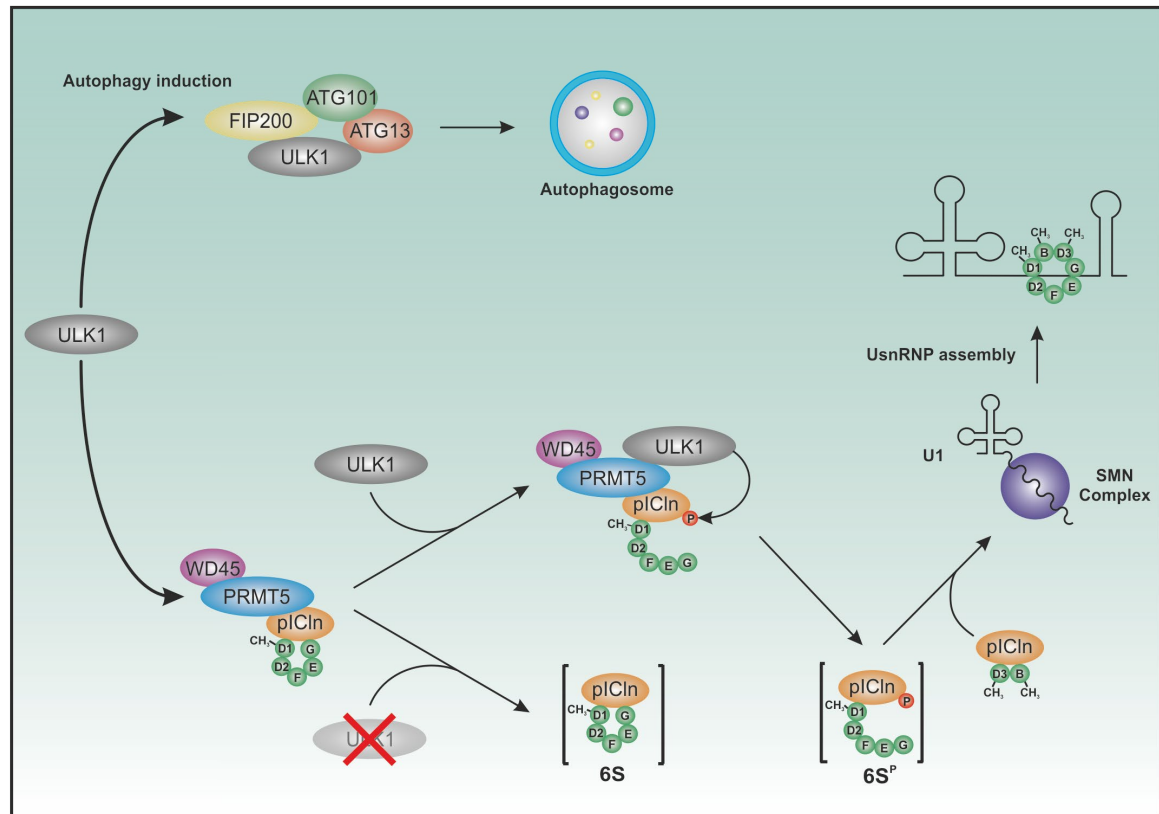


Figure 8. Schematic illustration summarizing the new role of ULK1 in the UsnRNP assembly as well as its well-known function in autophagy induction.

We further show that ULK1 dependent phosphorylation sites within the C-terminus of pICln affect the interaction between pICln and SmG. Recent studies convincingly demonstrated that the SMN subcomplex consisting of SMN and GEMIN2 can directly bind the Sm pentamer via GEMIN2 (9). The authors pointed out that there probably exist at least two sequential occurring mechanisms of Sm pentamer binding: A first step by binding to pICln, as a second sequential one by binding to GEMIN2. Future studies of pICln/phospho-pICln and the SMN/SMN subcomplexes are necessary to address the detailed mechanism of how phosphorylated pICln contributes to this step of UsnRNP assembly.

With the autophagy activating kinase ULK1 we identified an unknown player in this complex pathway. Although our data demonstrate a new regulatory function of ULK1 independent of autophagy, the latest studies were also able to link the autophagy pathway with UsnRNP biogenesis by providing evidence of an autophagosome mediated Sm protein degradation

pathway during the early phase of UsnRNP biosynthesis (51). The authors showed that only the Sm proteins D1, D2, D3, and B (but not Sm proteins E, F, and G) are degraded by autophagy to avoid toxic Sm protein aggregation in a scenario of pICln deficiency prohibiting disturbances in UsnRNP biogenesis. Our results now show that the autophagy activating Ser/Thr kinase ULK1 attributes an additional key regulatory function in UsnRNP biogenesis by direct phosphorylation of pICln. Phosphorylation of pICln by ULK1 and not by ULK2 results in an enhancement of UsnRNP biogenesis (Fig. 7A, B). Convenient to this, in cell lines deficient for ULK1 and ULK2, the UsnRNP biogenesis is dramatically reduced and could be reestablished by reconstitution of ULK1 only (Fig. 7D). If ULK1 dependent phosphorylation of pICln is blocked the Cajal bodies in the nucleus are altered (Fig. 6A-D). The observations from Prusty and colleagues (51) together with our results demonstrate that not only the amount of free available pICln but also the phosphorylation status of pICln is a critical parameter for the storage pool of Sm proteins and an efficient assembly reaction. It will be right of interesting to investigate in the future eg. by using ULK1 deficient cells lacking pICln phosphorylation, how the Sm protein balance is regulated, but even more of interest to answer the question of how the activity of ULK1 is regulated in this pathway. In this context, it is very much relevant to note, that recent studies already demonstrated a connection of the intracellular energy sensor mTOR to the spliceosomal proteins, especially to SmE (52) and to motor neuron development in context to SMA (53). Conversely, work by Cheng (54) and colleagues have shown that overexpression of U1snRNA leads to induction of autophagy. This suggests a cross-link of both pathways and it remains exciting to investigate how this occurs in detail.

The data presented in this work provide the molecular basis of how the transient opening of the 6S ring, catalyzed by ULK1, lowers the energy barrier during UsnRNP biogenesis. The provided data prove the contact area of pICln and SmG as the predetermined breaking point of the 6S ring to initiate the transfer of the open 6S entity onto the SMN complex *in vivo* and show that ULK1 mediated phosphorylation is a crucial regulatory and essential step of efficient UsnRNP biogenesis.

Our data also show that the PRMT5-ULK1-complex conjoins two distinct post-translational mechanisms of regulation in one complex: Symmetrical dimethylation and phosphorylation of the 6S complex to allow for the efficient and highly ordered assembly of UsnRNPs.

Core assembly of UsnRNPs and splicing are ubiquitous processes to regulate translation and differential gene expression in eukaryotic cells. A highly ordered and efficient assembly reaction is a prerequisite to keep the responsive gene to protein balance by mRNA transcription of a cell. Mutations or metabolic disorders within this spliceosomal process lead to a dramatic medical outcome like in amyotrophic lateral sclerosis (ALS), *Retinitis pigmentosa*, or spinal muscular atrophy (SMA) in humans. The evolutionary conserved Unc-51-like kinase (ULK1) was first identified in *C. elegans* as the main factor in early neuronal differentiation and axonal elongation (55). The new mechanism of phosphorylation of pICln by ULK1 may help to explain and address specific neuronal aspects associated with inefficient or reduced UsnRNP assembly in this kind of neuronal human diseases. Intensive work will be necessary to understand in more detail the molecular impact of ULK1 within neuronal disorders and the regulation of ULK1 activity in this context.

DATA AVAILABILITY

All data and constructs are available upon request to christoph.peter@uni-duesseldorf.de.

SUPPLEMENTARY DATA

Supplementary Data are available at NAR online.

ACKNOWLEDGEMENTS

We thank Alexander Lang for technical help and critical discussion on the manuscript. We also thank our colleagues Maria Jose Mendiburo, Niklas Berleth, Philip Böhler, and Wenxian Wu for comments on the manuscript. Furthermore, we thank Alexander K. Büll and Nicola Vettore for their technical support.

FUNDING

Stefan Klinker and Dieter Willbold received funding from the Deutsche Forschungsgemeinschaft (DFG) via the SFB974 and Dieter Willbold received funding from the DFG via the SFB1208. Financial support of Luitgard Nagel-Steger was provided by “Portfolio Technology and Medicine”, the Helmholtz-Validierungsfonds of the Impuls and Vernetzungsfonds der Helmholtzgemeinschaft. Funding for open access charge: University of Düsseldorf.

CONFLICT OF INTEREST

The authors declare that they have no conflict of interest.

REFERENCES

1. Matera, A.G. and Wang, Z. (2014) A day in the life of the spliceosome. *Nat Rev Mol Cell Biol*, **15**, 108-121.
2. Kambach, C., Walke, S., Young, R., Avis, J.M., de la Fortelle, E., Raker, V.A., Luhrmann, R., Li, J. and Nagai, K. (1999) Crystal structures of two Sm protein complexes and their implications for the assembly of the spliceosomal snRNPs. *Cell*, **96**, 375-387.
3. Newman, A.J. and Nagai, K. (2010) Structural studies of the spliceosome: blind men and an elephant. *Curr Opin Struct Biol*, **20**, 82-89.
4. Friesen, W.J., Wyce, A., Paushkin, S., Abel, L., Rappsilber, J., Mann, M. and Dreyfuss, G. (2002) A novel WD repeat protein component of the methylosome binds Sm proteins. *J Biol Chem*, **277**, 8243-8247.
5. Friesen, W.J., Paushkin, S., Wyce, A., Massenet, S., Pesiridis, G.S., Van Duyne, G., Rappsilber, J., Mann, M. and Dreyfuss, G. (2001) The methylosome, a 20S complex containing JBP1 and pICln, produces dimethylarginine-modified Sm proteins. *Mol Cell Biol*, **21**, 8289-8300.
6. Meister, G. and Fischer, U. (2002) Assisted RNP assembly: SMN and PRMT5 complexes cooperate in the formation of spliceosomal UsnRNPs. *EMBO J*, **21**, 5853-5863.
7. Meister, G., Eggert, C., Buhler, D., Brahms, H., Kambach, C. and Fischer, U. (2001) Methylation of Sm proteins by a complex containing PRMT5 and the putative U snRNP assembly factor pICln. *Curr Biol*, **11**, 1990-1994.
8. Meister, G., Buhler, D., Pillai, R., Lottspeich, F. and Fischer, U. (2001) A multiprotein complex mediates the ATP-dependent assembly of spliceosomal U snRNPs. *Nat Cell Biol*, **3**, 945-949.
9. Zhang, R., So, B.R., Li, P., Yong, J., Glisovic, T., Wan, L. and Dreyfuss, G. (2011) Structure of a key intermediate of the SMN complex reveals Gemin2's crucial function in snRNP assembly. *Cell*, **146**, 384-395.
10. Liu, Q., Fischer, U., Wang, F. and Dreyfuss, G. (1997) The spinal muscular atrophy disease gene product, SMN, and its associated protein SIP1 are in a complex with spliceosomal snRNP proteins. *Cell*, **90**, 1013-1021.
11. Fischer, U., Liu, Q. and Dreyfuss, G. (1997) The SMN-SIP1 complex has an essential role in spliceosomal snRNP biogenesis. *Cell*, **90**, 1023-1029.
12. Chari, A. and Fischer, U. (2010) Cellular strategies for the assembly of molecular machines. *Trends Biochem Sci*, **35**, 676-683.
13. Chari, A., Golas, M.M., Klingenhager, M., Neuenkirchen, N., Sander, B., Englbrecht, C., Sickmann, A., Stark, H. and Fischer, U. (2008) An assembly chaperone collaborates with the SMN complex to generate spliceosomal SnRNPs. *Cell*, **135**, 497-509.
14. Pellizzoni, L., Yong, J. and Dreyfuss, G. (2002) Essential role for the SMN complex in the specificity of snRNP assembly. *Science*, **298**, 1775-1779.
15. Grimmler, M., Bauer, L., Nousiainen, M., Korner, R., Meister, G. and Fischer, U. (2005) Phosphorylation regulates the activity of the SMN complex during assembly of spliceosomal U snRNPs. *EMBO Rep*, **6**, 70-76.
16. Husedzinovic, A., Oppermann, F., Draeger-Meurer, S., Chari, A., Fischer, U., Daub, H. and Gruss, O.J. (2014) Phosphoregulation of the human SMN complex. *Eur J Cell Biol*, **93**, 106-117.
17. Guderian, G., Peter, C., Wiesner, J., Sickmann, A., Schulze-Osthoff, K., Fischer, U. and Grimmler, M. (2011) RioK1, a new interactor of protein arginine methyltransferase 5 (PRMT5), competes with pICln for binding and modulates PRMT5 complex composition and substrate specificity. *J Biol Chem*, **286**, 1976-1986.
18. Grimmler, M., Otter, S., Peter, C., Muller, F., Chari, A. and Fischer, U. (2005) Unrip, a factor implicated in cap-independent translation, associates with the cytosolic SMN complex and influences its intracellular localization. *Hum Mol Genet*, **14**, 3099-3111.

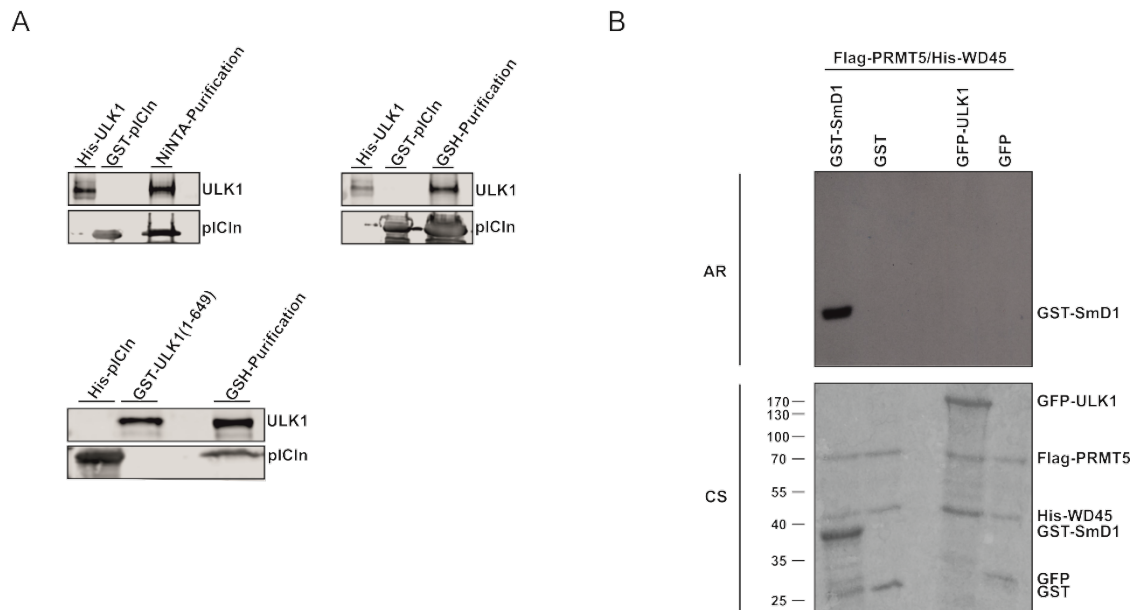
19. Loffler, A.S., Alers, S., Dieterle, A.M., Keppeler, H., Franz-Wachtel, M., Kundu, M., Campbell, D.G., Wesselborg, S., Alessi, D.R. and Stork, B. (2011) Ulk1-mediated phosphorylation of AMPK constitutes a negative regulatory feedback loop. *Autophagy*, **7**, 696-706.
20. Hieke, N., Loffler, A.S., Kaizuka, T., Berleth, N., Bohler, P., Driessen, S., Stuhldreier, F., Friesen, O., Assani, K., Schmitz, K. *et al.* (2015) Expression of a ULK1/2 binding-deficient ATG13 variant can partially restore autophagic activity in ATG13-deficient cells. *Autophagy*, **11**, 1471-1483.
21. Laemmli, U.K. (1970) Cleavage of structural proteins during the assembly of the head of bacteriophage T4. *Nature*, **227**, 680-685.
22. Dignam, J.D., Lebovitz, R.M. and Roeder, R.G. (1983) Accurate transcription initiation by RNA polymerase II in a soluble extract from isolated mammalian nuclei. *Nucleic Acids Res*, **11**, 1475-1489.
23. Shevchenko, A., Wilm, M., Vorm, O. and Mann, M. (1996) Mass spectrometric sequencing of proteins silver-stained polyacrylamide gels. *Anal Chem*, **68**, 850-858.
24. Niewalda, T., Michels, B., Jungnickel, R., Diegelmann, S., Kleber, J., Kahne, T. and Gerber, B. (2015) Synapsin determines memory strength after punishment- and relief-learning. *J Neurosci*, **35**, 7487-7502.
25. Taus, T., Kocher, T., Pichler, P., Paschke, C., Schmidt, A., Henrich, C. and Mechtler, K. (2011) Universal and confident phosphorylation site localization using phosphoRS. *J Proteome Res*, **10**, 5354-5362.
26. Dubiel, D., Bintig, W., Kahne, T., Dubiel, W. and Naumann, M. (2017) Cul3 neddylation is crucial for gradual lipid droplet formation during adipogenesis. *Biochim Biophys Acta*, **1864**, 1405-1412.
27. MacLean, B., Tomazela, D.M., Shulman, N., Chambers, M., Finney, G.L., Frewen, B., Kern, R., Tabb, D.L., Liebler, D.C. and MacCoss, M.J. (2010) Skyline: an open source document editor for creating and analyzing targeted proteomics experiments. *Bioinformatics*, **26**, 966-968.
28. Schuck, P. (2000) Size-distribution analysis of macromolecules by sedimentation velocity ultracentrifugation and lamm equation modeling. *Biophys J*, **78**, 1606-1619.
29. Brautigam, C.A. (2015) Calculations and Publication-Quality Illustrations for Analytical Ultracentrifugation Data. *Methods Enzymol*, **562**, 109-133.
30. Hosokawa, N., Hara, T., Kaizuka, T., Kishi, C., Takamura, A., Miura, Y., Iemura, S., Natsume, T., Takehana, K., Yamada, N. *et al.* (2009) Nutrient-dependent mTORC1 association with the ULK1-Atg13-FIP200 complex required for autophagy. *Mol Biol Cell*, **20**, 1981-1991.
31. Chan, E.Y., Longatti, A., McKnight, N.C. and Tooze, S.A. (2009) Kinase-inactivated ULK proteins inhibit autophagy via their conserved C-terminal domains using an Atg13-independent mechanism. *Mol Cell Biol*, **29**, 157-171.
32. Sanchez-Olea, R., Emma, F., Coghlan, M. and Strange, K. (1998) Characterization of pICln phosphorylation state and a pICln-associated protein kinase. *Biochim Biophys Acta*, **1381**, 49-60.
33. Lee, E.J. and Tournier, C. (2011) The requirement of uncoordinated 51-like kinase 1 (ULK1) and ULK2 in the regulation of autophagy. *Autophagy*, **7**, 689-695.
34. Petherick, K.J., Conway, O.J., Mpamhanga, C., Osborne, S.A., Kamal, A., Saxty, B. and Ganley, I.G. (2015) Pharmacological inhibition of ULK1 kinase blocks mammalian target of rapamycin (mTOR)-dependent autophagy. *J Biol Chem*, **290**, 11376-11383.
35. Egan, D.F., Chun, M.G., Vamos, M., Zou, H., Rong, J., Miller, C.J., Lou, H.J., Raveendra-Panickar, D., Yang, C.C., Sheffler, D.J. *et al.* (2015) Small Molecule Inhibition of the Autophagy Kinase ULK1 and Identification of ULK1 Substrates. *Mol Cell*, **59**, 285-297.

36. Neuenkirchen, N., Englbrecht, C., Ohmer, J., Ziegenhals, T., Chari, A. and Fischer, U. (2015) Reconstitution of the human U snRNP assembly machinery reveals stepwise Sm protein organization. *EMBO J*, **34**, 1925-1941.
37. Fisher, D.E., Conner, G.E., Reeves, W.H., Wisniewolski, R. and Blobel, G. (1985) Small nuclear ribonucleoprotein particle assembly in vivo: demonstration of a 6S RNA-free core precursor and posttranslational modification. *Cell*, **42**, 751-758.
38. Grimm, C., Chari, A., Pelz, J.P., Kuper, J., Kisker, C., Diederichs, K., Stark, H., Schindelin, H. and Fischer, U. (2013) Structural basis of assembly chaperone-mediated snRNP formation. *Mol Cell*, **49**, 692-703.
39. Chaturvedi, S.K., Ma, J., Zhao, H. and Schuck, P. (2017) Use of fluorescence-detected sedimentation velocity to study high-affinity protein interactions. *Nat Protoc*, **12**, 1777-1791.
40. Nizami, Z., Deryusheva, S. and Gall, J.G. (2010) The Cajal body and histone locus body. *Cold Spring Harb Perspect Biol*, **2**, a000653.
41. Strzelecka, M., Trowitzsch, S., Weber, G., Luhrmann, R., Oates, A.C. and Neugebauer, K.M. (2010) Coilin-dependent snRNP assembly is essential for zebrafish embryogenesis. *Nat Struct Mol Biol*, **17**, 403-409.
42. Mao, Y.S., Zhang, B. and Spector, D.L. (2011) Biogenesis and function of nuclear bodies. *Trends Genet*, **27**, 295-306.
43. Sou, Y.S., Waguri, S., Iwata, J., Ueno, T., Fujimura, T., Hara, T., Sawada, N., Yamada, A., Mizushima, N., Uchiyama, Y. *et al.* (2008) The Atg8 conjugation system is indispensable for proper development of autophagic isolation membranes in mice. *Mol Biol Cell*, **19**, 4762-4775.
44. Husedzinovic, A., Neumann, B., Reymann, J., Draeger-Meurer, S., Chari, A., Erfle, H., Fischer, U. and Gruss, O.J. (2015) The catalytically inactive tyrosine phosphatase HD-PTP/PTPN23 is a novel regulator of SMN complex localization. *Mol Biol Cell*, **26**, 161-171.
45. Pelz, J.P., Schindelin, H., van Pee, K., Kuper, J., Kisker, C., Diederichs, K., Fischer, U. and Grimm, C. (2015) Crystallizing the 6S and 8S spliceosomal assembly intermediates: a complex project. *Acta Crystallogr D Biol Crystallogr*, **71**, 2040-2053.
46. Schedlbauer, A., Kontaxis, G., Konig, M., Furst, J., Jakab, M., Ritter, M., Garavaglia, L., Botta, G., Meyer, G., Paulmichl, M. *et al.* (2003) Sequence-specific resonance assignments of ICl_n, an ion channel cloned from epithelial cells. *J Biomol NMR*, **27**, 399-400.
47. Furst, J., Schedlbauer, A., Gandini, R., Garavaglia, M.L., Saino, S., Gschwentner, M., Sarg, B., Lindner, H., Jakab, M., Ritter, M. *et al.* (2005) ICl_n159 folds into a pleckstrin homology domain-like structure. Interaction with kinases and the splicing factor LSm4. *J Biol Chem*, **280**, 31276-31282.
48. Schedlbauer, A., Gandini, R., Kontaxis, G., Paulmichl, M., Furst, J. and Konrat, R. (2011) The C-terminus of ICl_n is natively disordered but displays local structural preformation. *Cell Physiol Biochem*, **28**, 1203-1210.
49. Dyson, H.J. and Wright, P.E. (2005) Intrinsically unstructured proteins and their functions. *Nat Rev Mol Cell Biol*, **6**, 197-208.
50. Corpet, F. (1988) Multiple sequence alignment with hierarchical clustering. *Nucleic Acids Res*, **16**, 10881-10890.
51. Prusty, A.B., Meduri, R., Prusty, B.K., Vanselow, J., Schlosser, A. and Fischer, U. (2017) Impaired spliceosomal UsnRNP assembly leads to Sm mRNA down-regulation and Sm protein degradation. *J Cell Biol*, **216**, 2391-2407.
52. Quidville, V., Alsafadi, S., Goubar, A., Commo, F., Scott, V., Pioche-Durieu, C., Girault, I., Baconnais, S., Le Cam, E., Lazar, V. *et al.* (2013) Targeting the deregulated spliceosome core machinery in cancer cells triggers mTOR blockade and autophagy. *Cancer Res*, **73**, 2247-2258.

-
53. Piras, A., Schiaffino, L., Boido, M., Valsecchi, V., Guglielmotto, M., De Amicis, E., Puyal, J., Garcera, A., Tamagno, E., Soler, R.M. *et al.* (2017) Inhibition of autophagy delays motoneuron degeneration and extends lifespan in a mouse model of spinal muscular atrophy. *Cell Death Dis*, **8**, 3223.
 54. Cheng, Z., Du, Z., Zhai, B., Yang, Z. and Zhang, T. (2018) U1 small nuclear RNA overexpression implicates autophagic-lysosomal system associated with AD. *Neurosci Res*, **136**, 48-55.
 55. Ogura, K., Wicky, C., Magnenat, L., Tobler, H., Mori, I., Muller, F. and Ohshima, Y. (1994) *Caenorhabditis elegans* unc-51 gene required for axonal elongation encodes a novel serine/threonine kinase. *Genes Dev*, **8**, 2389-2400.

SUPPLEMENTARY DATA

SD Figure 1

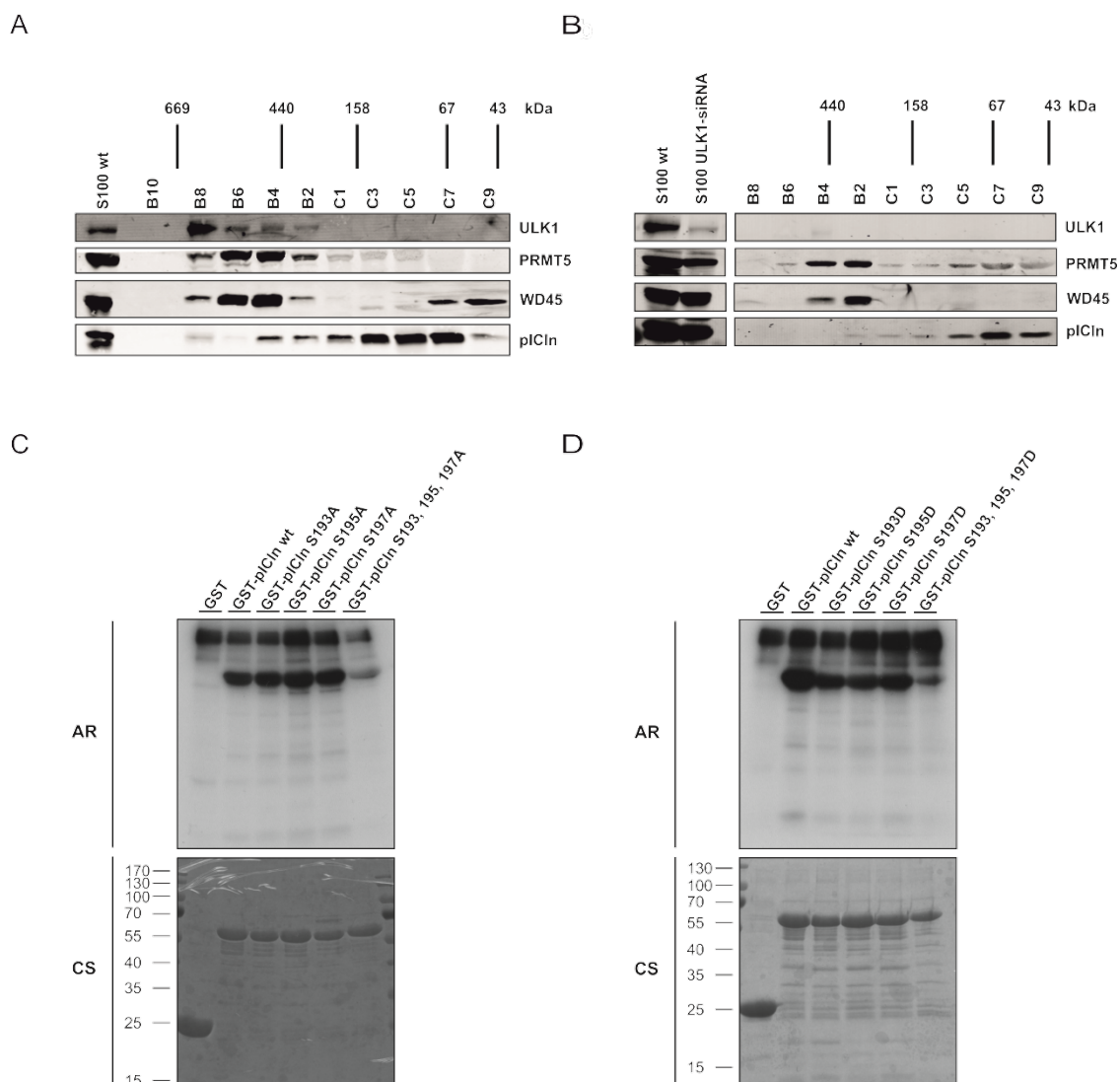


Supplementary Data Figure 1

rULK1 interacts directly with rpICln *in vitro*

A, Recombinant His-ULK1, GST-pICln, GST-ULK1(1-649) or His-pICln were purified by GSH-beads or NiNTA, respectively. Purified rULK1 and rpICln were incubated together for 1,5 h at 4 °C. Subsequently they were re-purified by GSH-beads or NiNTA for 1 h at 4 °C. Respective protein co-binding was analyzed by Tris/Glycine-SDS-PAGE and western blotting using antibodies against ULK1 and pICln. B, 1 µg recombinant active Flag-PRMT5/His-WD45 was incubated with GFP-ULK1 or GST-SmD1 (positive control) and 1 µCi [³H]-SAM for 1 h at 37 °C. Samples were separated by Tris/Glycine-SDS-PAGE and analyzed by autoradiography. AR: autoradiography, CS: coomassie blue staining.

SD Figure 2

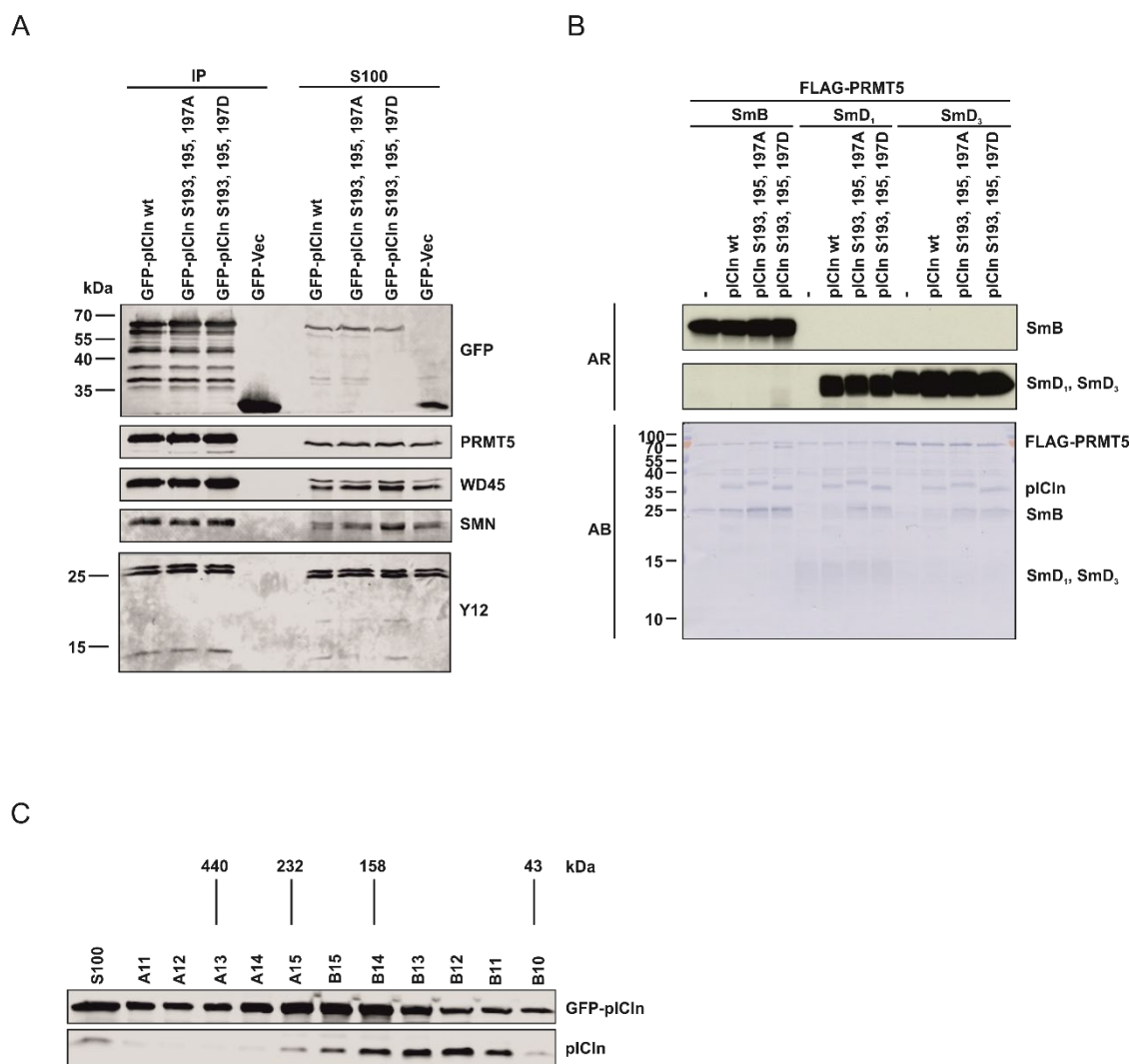


Supplementary Data Figure 2

Western Blot of size exclusion chromatography of wild type HEK293T and HEK293T ULK1-siRNA knockdown S100 extracts

A; B, S100 extract of wild type HEK293T cells (wt) and HEK293T-ULK1-siRNA knockdown (ULK1-KD) cells was resolved by gel filtration, using a Superdex 200 column. Complexes were analyzed by Tris/Glycine-SDS-PAGE and western blotting using antibodies against ULK1, PRMT5, WD45 and pICln. C; D, ULK1 phosphorylates pICln in the C-terminal region on residues S193, S195, and S197. C, *In vitro* kinase assays using recombinant active GST-ULK1 expressed in Sf9 insect cells and GST-pICln wt, -pICln S193A, -pICln S195A, -pICln S197A, -pICln S193, 195, 197A and GST purified from *E. coli* as substrate proteins were incubated with 10 μ Ci [32 P]-ATP for 45 min. at 30 $^{\circ}$ C. Samples were separated by Tris/Glycine-SDS-PAGE and analyzed by autoradiography. D, *In vitro* kinase assays with GST-pICln wt, -pICln S193D, -pICln S195D, -pICln S197D, -pICln S193, 195, 197D and GST, purified from *E. coli* as substrate proteins, were performed as described in C.

SD Figure 3

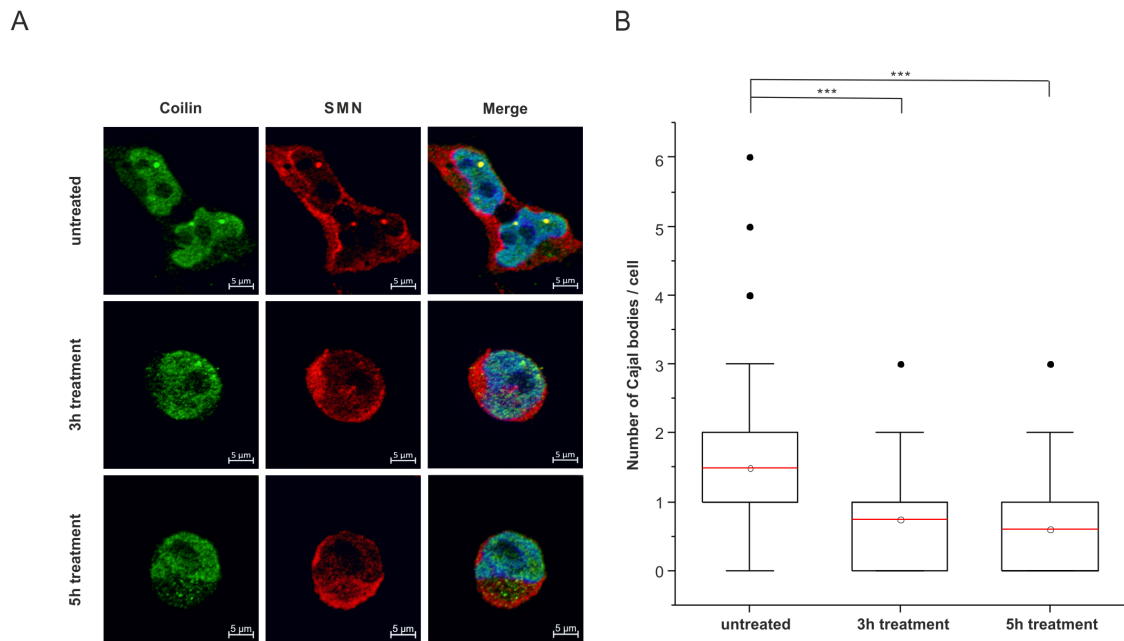


Supplementary Data Figure 3

Composition and activity of the PRMT5-complex with pICln phosphomutants in reference to pICln wt

A, GFP-IP was performed and analyzed by Tris/Glycine-SDS-PAGE and western blotting using antibodies against GFP, PRMT5, WD45, SMN and Y12. B, Radioactive methylation assay of SmB, SmD1 and SmD3 by PRMT5. 500 ng of Sm substrate proteins were pre-incubated with or without (-) pICln and the corresponding mutants for 30 min. Methylation assay was performed for 1.5 h at 37 °C with 150 ng of active PRMT5. C, For velocity analysis, gel filtration was performed with S100 extract of Flp-In T-REx 293-GFP-pICln cells, using a Superdex 200 increase column. Separation of GFP-pICln and endogenous pICln were analyzed by Tris/Glycine-SDS-PAGE and western blotting using antibodies against GFP and pICln.

SD Figure 4

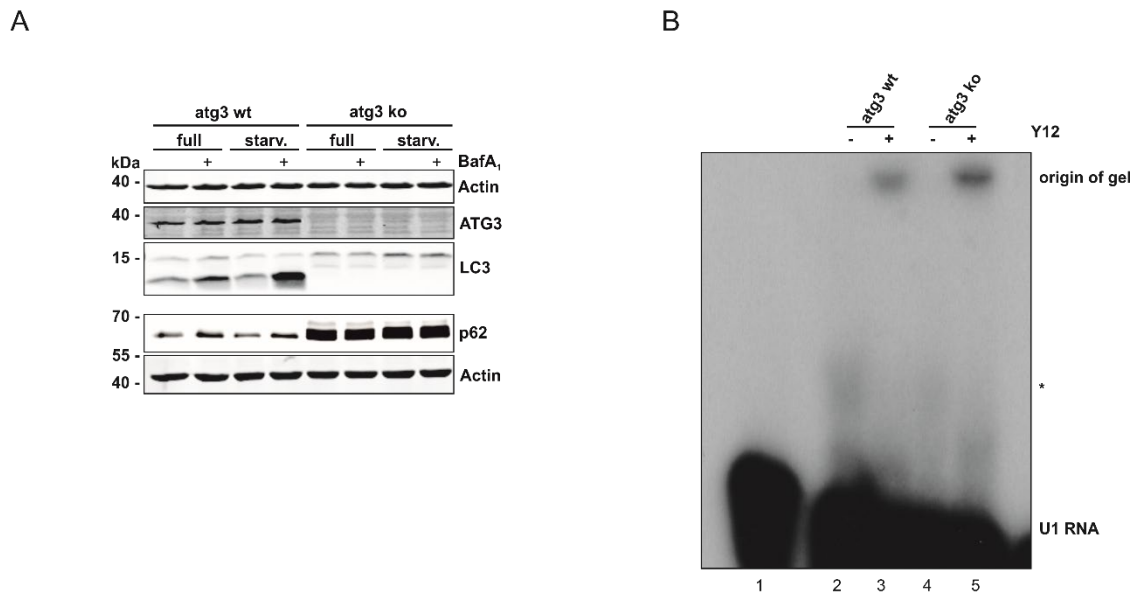


Supplementary Data Figure 4

Inhibition of ULK1 results in a decreased number of Cajal bodies

A; B, HEK293T cells were treated with 30 μ M ULK inhibitor MRT67307 for 3 and 5 h. A, The cells were fixed and Cajal bodies were visualized with antibody staining against Coilin (green) and SMN (red). DNA was stained with DAPI (blue). B, Inhibition of ULK causes a reduction in the snRNP storage pool. In the boxplot diagram the “box” represents 25-75% of all values and the mean (red), standard deviation and out layers are visualized. HEK293T cells show an average of 1.49 (n = 518) Cajal bodies. Treatment of cells with ULK inhibitor caused a significant decrease in the number of Cajal bodies. The p-value was calculated with Origin using the Mann-Whitney U test. *** $P < 0.005$; scale bars: 5 μ m (A).

SD Figure 5



Supplementary Data Figure 5

ATG3 deficient cells are capable for UsnRNP biogenesis

A, MEF cells, which express wild type atg3 or are deficient for ATG3, were treated with full or starvation medium (EBSS) in the absence or presence of bafilomycin A1 (BafA1; 10 nM) for 2 h. Afterwards, cells were harvested, lysed and cleared cellular lysates were subjected to SDS-PAGE and immunoblotting for ATG3, p62, LC3, and Actin. B, *In vitro* transcribed U1 snRNA labelled with 10 μ Ci [32 P]-UTP was incubated with S100 extracts from MEF cells either lacking ATG3 or cells reconstituted with ATG3 wt. After incubation samples were directly analyzed by native gel electrophoresis or the same samples were subjected to supershift analysis with the Y12 antibody to show the specific formation of snRNPs.

SD Figure 6

```

ICLN_HUMAN MSFLKSFPPPGPAEGLLRQQPDT EAVLNGKGLGTGTLTYAESRLSWLDGS 50
ICLN_DROME MVLIMRVSP--EHGLLYTANNIKLKLGDKVVGEGTVYIAQNTLSWQPTE 48

ICLN_HUMAN -GLGFSLEYPTISLHALSRDRSDCL-----GEHLYVMVNAK 85
ICLN_DROME LAEGISIEWKQVSLHGISSNPRKCLYFMLDHKVEWNGVYGDPPQQA VNGR 98

ICLN_HUMAN FEEESKEPVAD---EEEESDDDVPE-----ITEFRFVPSDKSALEA 124
ICLN_DROME NGGGSEAEVDEGNGSDEHDEDDNFEDAVDEQFGEVTECWLMPEDIHTVDT 148

ICLN_HUMAN MFTAMCECQALHPDPEDESDDDYDGEEDVVEAHEQGQGDIPTFYTYEEGL 174
ICLN_DROME MYSAMTTCQALHPDSANSDESDSDPMDAGGLEDEAMEEDDALTLGRNGV 198

ICLN_HUMAN SHLTAEGQATLERLEGMLSQSVSSQYNMAGVRTEDSIRDYEDGMEVDTPP 224
ICLN_DROME QNLSLDDDE--ERFEDA----- 215

ICLN_HUMAN TVAGQFEDADVDH 237
ICLN_DROME ----- 215

```

Supplementary Data Figure 6**Sequence alignment of human pICln**

Sequence alignment (multalin) of human pICln (P54105-1) and drosophila pICln (A1ZAW5-1). Black shade indicates identical amino acids whereas grey shade indicates similar amino acids. Sequence identity: 22.05%. Underlined serines indicate phosphorylation sites of ULK1 in human pICln at positions 193, 195 and 197. These phosphorylation sites are missing in drosophila pICln.

7.2 Chapter 2 - NF90 – A new interaction partner of the PRMT5-WD45-RioK1 complex is highly methylated in the cell

Title:	NF90 - A new interaction partner of the PRMT5-WD45-RioK1 complex is highly methylated in the cell
Authors:	Jan Cox, Lea Marie Esser, Katharina Schmitz, Kaja Reiffert, Matthias Grimmer, Björn Stork, Sebastian Wesselborg, Christoph Peter
Published in:	to be submitted
Proportional work on this manuscript:	70% Cloning of constructs Generation of stable cell lines Protein expression and purification Immunoprecipitation and immunoblotting <i>In-vitro</i> methylation assays Interaction studies Preparation of figures Writing the manuscript

NF90 – A new interaction partner of the PRMT5-WD45-RioK1 complex is highly methylated in the cell

Jan Cox¹, Lea Marie Esser¹, Katharina Schmitz¹, Kaja Reiffert¹, Matthias Grimm^{2,3}, Björn Stork¹, Sebastian Wesselborg¹, Christoph Peter^{1*}

¹Institute of Molecular Medicine I, Medical Faculty, Heinrich Heine University Düsseldorf, Düsseldorf, Germany; ²Hochschule Fresenius, Idstein, Germany; ³DiaSys Diagnostic Systems GmbH, Alte Strasse 9, 65558 Holzheim, Germany

* To whom correspondence should be addressed. Tel: +49 (0) 211 81-12196; Email: christoph.peter@uni-duesseldorf.de

ABSTRACT

Protein-arginine methylation is a common posttranslational modification and plays a crucial role in various cellular processes, such as protein-protein interactions or the binding of nucleic acids by proteins. The most important enzyme for symmetric protein arginine methylation is the protein arginine methyltransferase 5 (PRMT5). While the methylation reaction is well understood, recruitment and differentiation between substrates remain unclear. For PRMT5, the adapter proteins pICln and RioK1 were identified, which compete for the same binding site and regulate the substrate diversity of PRMT5. Since PRMT5 is upregulated in many cancer cells, it is also a promising target in cancer therapy. Several methyltransferase inhibitors are in development and the identification of new target proteins contributes to a better understanding of PRMT5. Here, we describe NF90 as a novel substrate, that interacts with the PRMT5-RioK1 complex. We show that NF90 is symmetrically dimethylated by PRMT5 and has no free methylation sites under intracellular conditions, resulting in a fully methylated protein. Within the RG-rich region in the C-terminus of NF90, we localized four arginines at positions 644, 649, 653, and 655 as preferentially methylated targets and identified the C-terminal region of NF90 as the interaction site with PRMT5.

INTRODUCTION

Posttranslational modifications are an important mechanism to regulate the functions of cellular proteins. The methylation of nitrogen in the side chain of arginine is one of the most common posttranslational modifications and plays an important role in nearly all cellular processes such as histone methylation, RNA splicing, transcription and translation regulation, nuclear export of proteins, protein-protein interactions, and cell signaling (Khoury et al., 2011, Murn and Shi, 2017, Blanc and Richard, 2017). To date, more than 5,500 human proteins have been detected to be methylated, highlighting the central function of this modification (Murn and Shi, 2017). Three different methylation patterns are known for the arginine residue in the amino acid side chain (Blanc and Richard, 2017). Methylation of one nitrogen leads to a N^G-monomethylarginine (MMA). If both nitrogen atoms are methylated, a distinction is made between symmetrical dimethylation (SDMA) and asymmetrical dimethylation (ADMA). In SDMA, both nitrogens are single methylated, resulting in a N^G, N'^G-dimethylarginine. In ADMA, one of the two nitrogens is double methylated, resulting in a N^G, N^G-dimethylarginine. Responsible for this modification is the family of protein arginine methyltransferases (PRMTs), which transfer the methyl group of S-adenosylmethionine (SAM) to the guanidine group in the side chain of arginine (Bedford and Clarke, 2009). The family consists of 9 different enzymes divided into three types according to the catalyzed methylation reaction (Blanc and Richard, 2017, Hwang et al., 2021). Type I PRMTs 1, 2, 3, 4, 6, and 8 catalyze MMA reactions and ADMA reactions (Blanc and Richard, 2017). Type II PRMTs 5 and 9 catalyze MMA reactions and SDMA reactions (Branscombe et al., 2001, Cook et al., 2006). PRMT7 catalyzes only MMA and is currently the only member of type III PRMTs (Miranda et al., 2004, Zurita-Lopez et al., 2012, Feng et al., 2013). The methyltransferases PRMT5 and PRMT9 are the only known methyltransferases that catalyze symmetric dimethylation on arginines (Yang et al., 2015). However, PRMT5 is the main methyltransferase, as loss of PRMT5 leads to nearly complete loss of SDMA (Hadjikyriacou et al., 2015). Also, no redundancy in protein methylation was observed upon loss of either methyltransferase (Hadjikyriacou et al., 2015, Yang et al., 2015). PRMT5 together with WD45 forms a hetero-octameric complex of ~450 kDa consisting of four PRMT5 and four WD45 monomers (Antonysamy et al., 2012). This structure forms the basic core complex and can be extended by the adapter proteins pICln and RioK1 (Krapivinsky et al., 1998, Guderian et al., 2011, Krzyzanowski et al., 2021)

These adapter proteins increase the substrate specificity of PRMT5 by recruiting new target proteins such as the Sm proteins, histone H4, or nucleolin (Meister et al., 2001, Friesen et al.,

2001b, Guderian et al., 2011). Overexpression of PRMT5 is directly associated with cancer and a poor therapeutic prognosis (Stopa et al., 2015). Because of its role as an oncogene, PRMT5 is extensively examined in cancer research and several PRMT5 inhibitors are in clinical trials (Siu et al., 2019, Watts et al., 2019) (NCT03614728, NCT02783300). The discovery of adapter proteins and their role in recruiting new methylation substrates to PRMT5 extended the focus on this protein as a potential target for anti-cancer therapies.

Here, we identified NF90 as a novel substrate of the PRMT5-WD45-RioK1 complex. NF90 was first discovered as NFAT and is also known as NFAR-1, NFAT-90, DRBP76, or TCP80 (Kao et al., 1994, Corthesy and Kao, 1994, Castella et al., 2015). It is together with NF110 (NFAR-2) a major splice variant of the ILF3 gene (Saunders et al., 2001, Duchange et al., 2000). This and the different names led to much confusion in the literature. The various names result from the independent discovery of NF90 in different functions. For example, NF90 has been described as a DNA binding protein and a transcription factor that binds to the promoter of interleukin 2 (Corthesy and Kao, 1994). NF90 is also able to bind double-stranded RNA and thereby regulate mRNA stability (Patel et al., 1999, Shim et al., 2002) and it is involved in virus replication where it also interacts with RNA (Isken et al., 2003, Liao et al., 1998). It could be shown that the knockout of NF90 is lethal highlighting the important role of NF90 (Shi et al., 2005). Knockout mice suffer from neuromuscular respiratory failure and die 12 h after birth (Shi et al., 2005). Strikingly, NF90 has RG-rich sequences in the C-terminus, representing potential methylation sites by PRMT5 but no methylation has yet been shown (Richard et al., 2005). Even though much is known about the actual mechanism of methylation and numerous substrates have been identified in recent years, a central question remains how methyltransferases recognize their substrates, differentiate between them and recruit them (Murn and Shi, 2017). In this work, we show that recruitment of NF90 as a novel substrate occurs via the PRMT5-RioK1 complex, demonstrating that adapter proteins are key players in gaining fundamental information on these questions.

MATERIAL AND METHODS

Cloning and Plasmids

NF90 DNA (CCDS12247.1) was amplified from HEK293 cells cDNA generated with High-Capacity cDNA Reverse Transcription Kit (4368814, Applied Biosystems) and cloned into pGEX-6P-1 (28954648, Cytiva) and pcDNA5-FRT-TO (V601020, Invitrogen) using Gibson

assembly technique (NEB HiFi DNA Assembly Master Mix, E2621S) or restriction enzyme-based cloning. For amplification, Phusion High-Fidelity DNA Polymerase (M0530, NEB) and the following primers (Sigma-Aldrich) were used:

pGEX-6P-1-NF90 wt, 5'-GTGAATTCATGCGTCCAATGCGAATT-3'

and 5'-GTGCGGCCGCCTAGGAAGACCCAAAATCATGAT-3';

pGEX-6P-1-NF90 AA1-639, 5'-CACAAGAGGAGCTGGAGGCAGTCCAGAACATGGTG-3'

and 5'-TCCAGCTCCTTGTGTTGGATAAACGGAAGAATG-3'

and 5'-AACCTTTAGGCGGCCGCATCGTGACTGACTG-3'

and 5'-CGGCCGCCTAAAGGTTGGGGGTGGGGGCAC-3';

pGEX-6P-1-NF90 AA1-479, 5'-GTGAATTCATGCGTCCAATGCGAATT-3'

and 5'-GTGCGGCCGCCCCCTTGCTCGAGTCC-3';

pGEX-6P-1-NF90 AA480-702, 5'-GTGAATTCGAGGACTCGGCTGAGGAG-3'

and 5'-GTGCGGCCGCCTAGGAAGACCCAAAATCATGAT-3';

pGEX-6P-1-NF90 AA1-391, 5'-GTGAATTCATGCGTCCAATGCGAATT-3'

and 5'-GTGCGGCCGCCTACTGAATCTTCTTCTTTTTGCTG-3';

pGEX-6P-1-NF90 AA392-702, 5'-GTGAATTCAGAAAGAGGAGAAGGCAGAG-3'

and 5'-GTGCGGCCGCCTAGGAAGACCCAAAATCATGAT-3';

pGEX-6P-1-NF90 AA609 R->K, 5'-AGCCCCAGTACCCGTCAAAGGGGGACC-3'

and 5'-GGTCCCCCTTTGACGGGTACTGGGGCT-3';

pGEX-6P-1-NF90 7x AA640, 642, 644, 649, 651, 653, 655 R->K (GeneArt Gene Synthesis, Invitrogen);

pGEX-6P-1-NF90 AA640 R->K, 5'-CCCCAACCTTAAAGGGCGGGGAAGAGGCGGGAG-3'

and 5'-CCCCGCCCTTAAAGGTTGGGGGGTGGGGGCAC-3';

pGEX-6P-1-NF90 AA642 R->K, 5'-TCGAGGGAAGGGAAGAGGCGGGAGCATCCGGGGAC-3'

and 5'-CCGCCTTCCCTTCCCTCGAAGGTTGGGGGGTGG-3';

pGEX-6P-1-NF90 AA644 R->K, 5'-TCGAGGGCGGGAAAAGGCGGGAGCATCCGGGGAC-3'

and 5'-CCGCCTTTTCCCCGCCCTCGAAGGTTGGGGGGTGG-3';

pGEX-6P-1-NF90 AA649 R->K, 5'-AGGCGGGAGCATCAAGGGACGAGGGCGCGGGCGAG-3'

and 5'-CGTCCCTTGATGCTCCCGCCTCTTCCCCGCCCTC-3';

pGEX-6P-1-NF90 AA651 R->K, 5'-ATCCGGGGAAAAGGGCGCGGGCGAGGATTTGG-3'

and 5'-CCC GCGCCCTTTTCCCCGGATGCTCCCGCCTC-3';

pGEX-6P-1-NF90 AA653 R->K, 5'-ACGAGGGAAGGGGCGAGGATTTGGTGGCGCCAAC-3'

and 5'-AATCTCGCCCTTCCCTCGTCCCGGATGCTCC-3';

pGEX-6P-1-NF90 AA655 R->K, 5'-GGGCGCGGGAAAGGATTTGGTGGCGCCAACCATGG-3'

and 5'-ACCAAATCCTTTCCCCGCGCCCTCGTCCCGGATG-3';

Plasmids used for generating stable cell lines:

pcDNA5-FRT-TO-NF90 wt, pcDNA5-FRT-TO-NF90 AA640, 642, 644, 649, 651, 653, 655 R->K (7x), 5'-ATGCGTCCAATGCGAATTTTTGTGAATGATGAC-3'

and 5'-TCGCATTGGACGCATGGATCCGAGCTCGGTACCAAGC-3'

and 5'-TTTGGGTCTTCTAGGCGGCCGCTCGAGTCTAGAGG-3'

and 5'-CTAGGAAGACCCAAAATCATGATAGCCGTAG-3';

pcDNA5-FRT-TO-eGFP-NF90 wt and pcDNA5-FRT-TO-eGFP-NF90 AA640, 642, 644, 649, 651, 653, 655 R->K (7x), 5'-ATCCATGCGTCCAATGCGAATTTTTGTGAATGATGAC-3'

and 5'-CATTGGACGCATGGATCCGAGTCCGGACTTGTACAG-3'

and 5'-TTTGGGTCTTCTAGGCGGCCGCTCGAGTCTAGAGG-3'

and 5'-CTAGGAAGACCCAAAATCATGATAGCCGTAG-3';

pcDNA5-FRT-TO-eGFP-PRMT5, 5'-GGATCCATGGCGGCGATGGCGGT-3'

and 5'-GCGGCCGCCTAGAGGCCAATGGTATAT-3';

pcDNA5-FRT-TO-eGFP-RioK1, 5'-GGATCCATGGACTACCGGCGGCTTC-3'

and 5'-GCGGCCGCCTATTGCCTTTTTTCGTCT-3';

pcDNA5-FRT-TO-eGFP-pICln, 5'-GGATCCATGAGCTTCTCAAAGTTTCCC-3'

and 5'-GTCTCGAGTCAGTGATCAACATCTGCATCC-3';

pcDNA5-FRT-TO-eGFP-WD45, 5'-GGATCCATGCGGAAGGAAACCCAC-3'

and 5'-GCGGCCGCCTACTCAGTAACAATTGCAGGTCC-3'.

Generation of pGEX-6P-1-PRMT5, pGEX-6P-1-WD45, pGEX-6P-1-RioK1 (Guderian et al., 2011), and pGEX-6P-1-pICln (Schmitz et al., 2021), and pcDNA5-FRT-TO-eGFP (Loffler et al., 2011) plasmids have been described previously.

Protein expression and purification

E. coli BL21 were transformed with described plasmids and grown overnight at 37 °C on LB agar selection plates (100 µg/ml ampicillin). 150 ml LB medium were inoculated and grown overnight at 37 °C shaking. 1 L SB media (35 g/L Tryptone, 20 g/L Yeast extract, 5 g/L NaCl) culture was adjusted to an OD₆₀₀ of 0.1 and grown to 0.8. Afterwards, protein expression was induced with 1 mM IPTG at 18 °C overnight. The bacteria were lysed in 300 mM NaCl, 50 mM Tris pH 7.5, 5 mM EDTA, 5 mM EGTA, 0.01% (v/v) Igepal, Protease inhibitors (cOmplete EDTA-free Protease Inhibitor Cocktail, 4693132001, Roche) and 50 mg/ml Lysozyme. After sonication, lysates were centrifuged for 30 min. at 10.000 g, incubated for 1.5 h at 4 °C with Glutathione-Sepharose 4B (Cytiva, 17075601), and washed three times with lysis buffer.

Purified proteins were used directly with or without GST-tag after cleavage with PreScission Protease (Cytiva, 27084301) overnight at 4 °C.

The recombinant active PRMT5-WD45 complex was purchased from Active Motif (31521). GFP-tagged proteins were expressed in HEK293 cells and purified by GFP-Trap Agarose (gta-20, Chromotek).

Antibodies

The following primary and secondary antibodies were used for immunoblotting and immunoprecipitation: α -NF90 (A303-651A, Bethyl Laboratories), α -PRMT5 (2252, CST), α -WD45 (2823, CST), α -RioK1 (NBP1-30103, Novus Biologicals), α -pICln (sc-393525, Santa Cruz), α -GFP (3H9, Chromotek). The detection of proteins was carried out with the following fluorescent secondary antibodies using LI-COR Odyssey Imaging System: IRDye 680LT goat α -rabbit, IRDye 680LT goat α -mouse, IRDye 800CW donkey α -rabbit, IRDye 800CW donkey α -mouse, IRDye 800CW goat α -rat (LI-COR Biosciences).

Cell culture and cell lines

HEK293 cells were cultured in high glucose DMEM (41965039, Gibco) supplemented with 10% (v/v) tetracycline-free FCS (10270106, Gibco) and 100 units/mL of Penicillin and 100 μ g/mL Streptomycin (15140122, Gibco) in a 5% CO₂ humidified atmosphere at 37 °C. Cells were washed with PBS (14190169, Gibco) and treated with Trypsin-EDTA (25300054, Gibco).

Inducible Flp-In T-REx 293 cell lines (R78007, Invitrogen) stably expressing NF90 wt, NF90 7x, GFP-NF90 wt, GFP-NF90 7x, GFP-PRMT5, GFP-WD45, GFP-pICln, and GFP-RioK1 were generated by co-transfecting 4.5 μ g pOG44 and 0.5 μ g pcDNA5 plasmids with FuGENE HD (E2311, Promega). Cells were selected with 200 μ g/ml Hygromycin B Gold (ant-hg-1, Invivogen) and 5 μ g/ml Blasticidin (ant-bl-05, Invivogen) for three weeks. GFP-pICln cells were generated as described in (Schmitz et al., 2021). Protein expression was induced with 0.1 μ g/ml Doxycycline and cells were harvested after 24 h. For methylation experiments, cells were treated with 20 μ M of S-adenosylhomocysteine hydrolase inhibitor Adenosine Dialdehyde (Adox) (Cay15644, Cayman Chemical) for 24 h followed by immunoprecipitation of NF90 or GFP-NF90 as described.

Immunoprecipitation and immunoblotting

Cell lysates of HEK293 cells were generated using lysis buffer with 50 mM Tris pH 7.5, 150 mM NaCl, 1 mM EDTA, 1 mM EGTA, 1% Triton X-100 and 1x Protease inhibitor cocktail (P2714, Sigma-Aldrich). Protein concentration was measured by Bradford assay (5000006, Bio-Rad).

500 µg cell lysate was used for immunoprecipitation studies together with 1 µg of previously described antibodies and Protein G Sepharose (17061801, Cytiva) at 4 °C for 1.5 h with rotation. GFP-tagged proteins were purified by GFP-Trap Agarose (gta-20, Chromotek) at 4 °C for 1.5 h with rotation. Samples were washed three times with washing buffer (lysis buffer without Triton X-100 and protease inhibitors) and eluted in sample buffer (375 mM Tris pH 7.5, 25.8% (w/v) Glycerol, 12.3% (w/v) SDS, 0.06% (w/v) Bromophenol blue, 6% (v/v) β-Mercaptoethanol, pH 6.8). Subsequently, samples were separated by Tris/Glycine-SDS-PAGE and transferred to a PVDF membrane (Immobilon-FL, Merck Millipore). The immunoblot detection was carried out using the indicated primary and fluorescent-labeled secondary antibodies and the LI-COR Odyssey Imaging System.

***In vitro* methylation**

Target proteins were incubated with 150 ng of active Flag-PRMT5-WD45 complex from Sf9 insect cells (Active Motif, 31521) and 1 µCi Adenosyl-L-Methionine, S-[methyl-³H] (Hartmann-Analytic, ART0288) in 50 mM Tris pH 7.5, 1 mM EGTA and 1 mM EDTA for 1.5 h at 37 °C. The reaction was stopped by adding sample buffer. Samples were separated by Tris/Glycine-SDS-PAGE and, after blotting and amido black staining (40% Methanol (v/v), 10% Acetic acid (v/v), 0.1% Amido black 10B (w/v)), analyzed by autoradiography with Amersham Hyperfilm MP (28906844, Cytiva) and BioMax TranScreen LE (1622034, Carestream).

Microscale thermophoresis

A Monolith NT 115 device (NanoTemper Technologies) was used for microscale thermophoresis binding studies. Purified recombinant proteins GST-PRMT5, RioK1 or NF90 were labeled with AlexaFluor488-NHS (A20000, Invitrogen) in 50 mM HEPES, 300 mM NaCl, pH 7.5. 50 nM of labeled proteins and 4-14 µM of unlabeled proteins were used for interaction studies. Recombinant proteins were measured as triplicates with 50% MST power and 50% LED power in premium or hydrophobic capillaries.

RESULTS

NF90 interacts with the PRMT5-WD45-RioK1 complex

In our previous work, we identified NF90 as a new potential interaction partner of the PRMT5-WD45-RioK1 complex by mass spectrometry (Guderian et al., 2011). In this follow up study, we performed in-depth analyses of the PRMT5-WD45-RioK1 complex and present NF90 as a new substrate. To investigate the complex, its composition, and the recruitment of NF90, we

generated Flp-In T-Rex HEK293 cell lines stably overexpressing PRMT5, WD45, and RioK1 as GFP fusion proteins. In immunoprecipitation studies, we observed co-immunoprecipitation of NF90 with GFP-PRMT5, GFP-WD45, and GFP-RioK1, whereas we could not precipitate NF90 with GFP-pICln (Fig. 1A). Our preceding data showed that the substrate specificity and recruitment of new substrates of PRMT5 are controlled by its interaction partners RioK1 and pICln (Guderian et al., 2011). NF90, purified by GFP-RioK1, supports this model of regulating the substrate specificity of PRMT5 via its adapter proteins pICln and RioK1. In pull-down experiments with heterologous expressed GST fusion proteins from *E. coli*, we obtained identical results. Endogenous NF90 from HEK293 lysates binds to GST-RioK1 and GST-PRMT5 but not to GST-pICln or GST-WD45 (Fig. 1B).

Interaction with the PRMT5-WD45-RioK1 complex occurs via the C-terminus of NF90

NF90 is a multi-domain protein consisting of two double-stranded RNA-binding motifs (DRBM), a domain associated with zinc fingers (DZF), a bipartite nuclear localization signal (NLS), and an RG-motif. Due to the multi-domain structure of NF90, we generated truncated forms of NF90 (Fig. 2C) and examined the interaction region with the proteins of the PRMT5-WD45-RioK1 complex (Fig. 1C). We divided NF90 between the two DRBMs (NF90 AA1-479 and NF90 AA480-702) and between the DZF domain and both DRBMs (NF90 AA1-391 and NF90 AA392-702) (Fig. 2C). Another truncated form represents NF90 without the RG-motif in the C-terminal region (NF90 AA1-639) (Fig. 2C). The experiments with these forms revealed an interaction of the PRMT5-WD45-RioK1 complex with the C-terminal region of NF90 from amino acid 391 to 702 (Fig. 1C). Interestingly, the truncated form AA1-639, which represents almost the entire protein except for the RG-motif, showed only weak interaction. This indicates that the interaction occurs in the RG-rich region at the C-terminus of NF90 (Fig. 1C and Fig. 2C). To determine the affinities within the PRMT5 complex and between NF90 and the complex, microscale thermophoresis experiments were performed. GST-PRMT5 was labeled with Alexa fluor 488 fluorescent dye and first measured against the known interaction partners of the complex, RioK1 and WD45. PRMT5 showed a strong affinity for RioK1 with a K_D of 100 nM and still a strong attachment to WD45 with a K_D of 622 nM (Fig. 1D, SD Fig. 1). Afterward, the affinity of NF90 as a potential substrate of the methyltransferase PRMT5 was determined with a high affinity of 57 nM (Fig. 1D, SD Fig. 1). Only weak changes in the affinity could be observed if we added WD45 or WD45 and RioK1, which leads to the assumption that NF90 is a strong substrate of PRMT5.

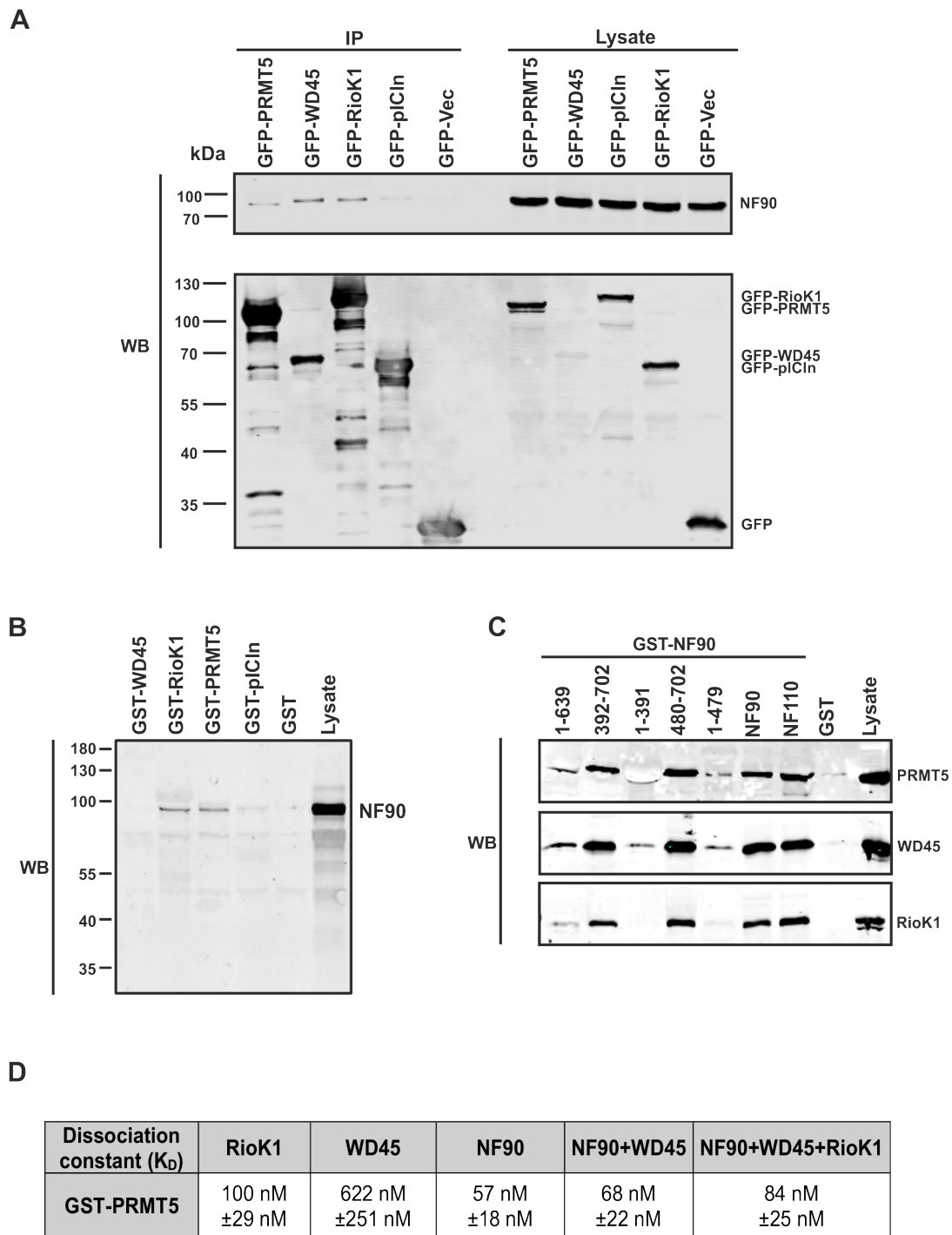


Figure 1: NF90 interacts with the PRMT5-WD45-RioK1 complex. (A) Immunoprecipitation from GFP-PRMT5, -WD45, -RioK1, -pICln, and GFP overexpressing cells. Protein expression was induced with 0.1 $\mu\text{g}/\text{ml}$ doxycycline for 24 h. After cell lysis, GFP-IP was performed and analyzed by Tris/Glycine-SDS-PAGE and western blotting using antibodies against GFP and NF90. NF90 was co-immunoprecipitated with GFP-PRMT5, GFP-WD45 and GFP-RioK1. (B) Pull-down assays with recombinant GST-PRMT5, -WD45, -pICln, -RioK1, and GST purified from *E. Coli* were executed in HEK293 lysate overnight at 4 °C. Co-precipitation of NF90 was analyzed using NF90 antibody and was detectable for GST-RioK1 and GST-PRMT5. (C) Pull-down assay as described above with different truncated forms of GST-NF90 purified from *E. Coli*. Detection of co-precipitated proteins was performed with RioK1, WD45, and PRMT5 antibodies. Only the C-terminus of NF90 interacts with RioK1, WD45, and PRMT5. (D) Interaction studies using microscale thermophoresis measurements (MST). GST-PRMT5 was labeled with AlexaFluor488 fluorescent dye and measured against the interaction partners RioK1, WD45, and NF90. GST-PRMT5 showed a high affinity to its substrate NF90 with 57 nM. WB: western blotting.

NF90 is a new substrate of PRMT5

Based on this strong *in vitro* interaction, we performed radioactive *in vitro* methylation assays with recombinant NF90 and active PRMT5 to test whether NF90 is methylated by PRMT5. We observed a transfer of the radioactive methyl group from [³H]-SAM to GST-NF90 (Fig. 2A). No radioactive incorporation was detected after EPZ015666 treatment, a specific PRMT5 inhibitor that binds in the substrate-binding pocket and the substrate arginine side chain binding site of PRMT5 (Chan-Penebre et al., 2015). This proves that NF90 is symmetrically methylated by PRMT5 *in vitro* (Fig. 2A).

To get an idea of how fast the methylation reaction is, we performed kinetic studies. For this and to exclude a disturbing influence of the GST-tag on the reaction rate, we first cleaved it from NF90 and subsequently performed a methylation reaction. Long-term kinetics up to 1 hour showed that NF90 was completely methylated after 15 minutes and no further increase was observed (Fig. 2B). For a more detailed analysis of methylation, the time window was reduced and shorter kinetics in 2 min steps up to 24 minutes were carried out. Again, no increase in methylation could be observed after 15 minutes (Fig. 2B). According to the measured dissociation constant (K_D) of 57 nM between NF90 and PRMT5, the methylation reaction proceeds very fast (Fig. 2B). After studying the methylation of the full-length wild-type, we determined the methylation sites within the NF90 protein by analyzing truncated forms and methylation site mutants. The protein contains several putative methylations sites in form of arginine-glycine-repeats in its sequence. A prominent site is present in form of an RG-motif in the C-terminus between the amino acids 609 to 656. We identified eight arginines as potential targets in this region (highlighted in Fig. 2C). The previously described truncated forms (Fig. 1C) were subjected to methylation assays and we observed radioactive incorporation for the C-terminal forms NF90 AA392-702 and NF90 AA480-702 and the wild-type (Fig. 2D). In contrast, no methylation was observed for the N-terminal forms NF90 AA1-391, NF90 AA1-479, and NF90-AA1-639 (Fig. 2D). These results clearly show methylation of NF90 by PRMT5 exclusively in the C-terminal region from amino acid 640 to 702. This is consistent with the RG-rich sequence described, which ranges from amino acid 640 to 658.

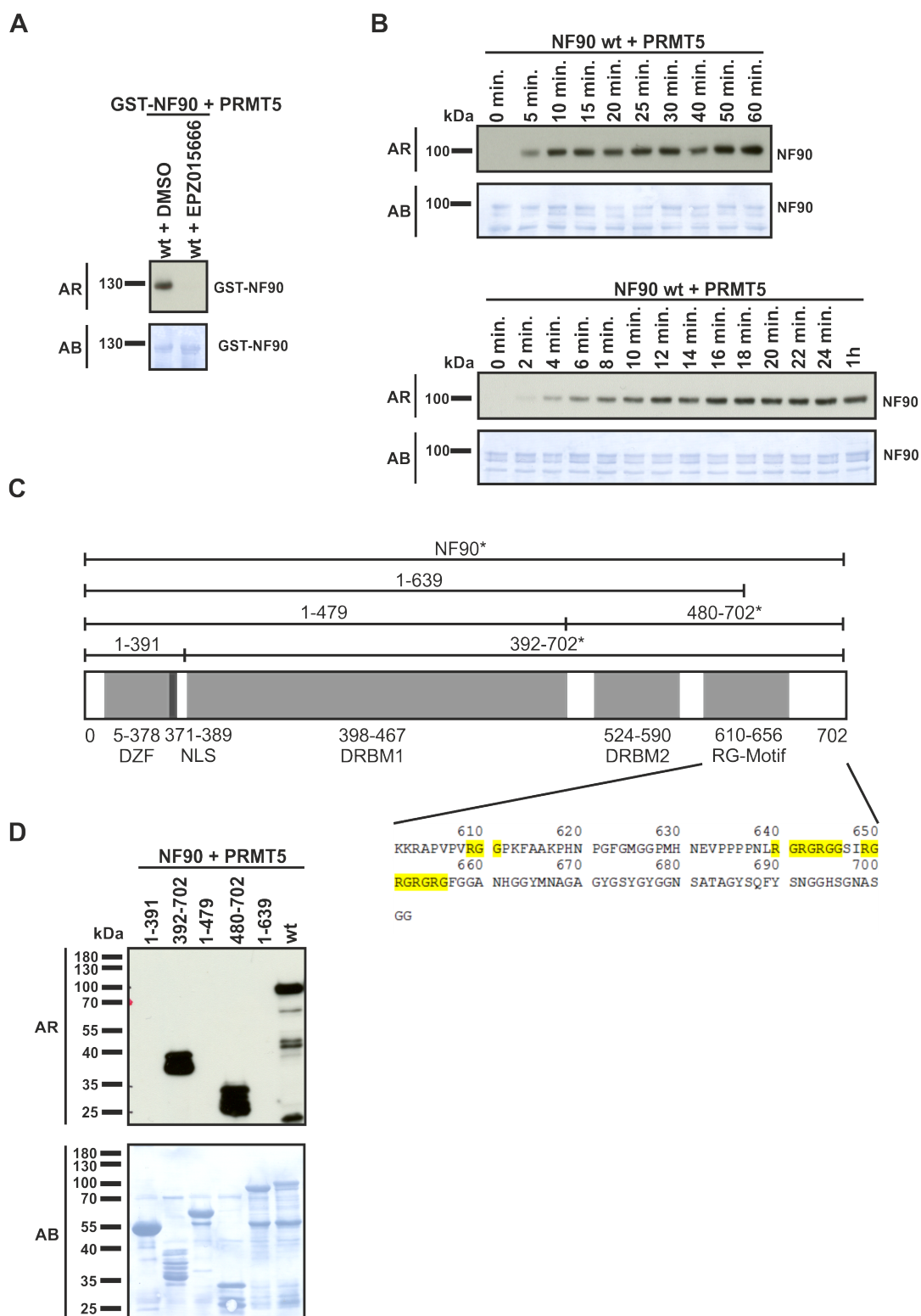


Figure 2: The C-terminus of NF90 is methylated by PRMT5 (A) Radioactive *in vitro* methylation assay using GST-NF90 purified from *E. Coli* and 200 ng recombinant PRMT5 and 1 μ Ci [3-H]-SAM was performed with and without 1 mM PRMT5 inhibitor EPZ015666. Samples were separated by Tris/Glycine-SDS-PAGE and radioactive incorporation was analyzed by western blotting and autoradiography. The addition of 1 mM PRMT5 inhibitor EPZ015666 inhibits the methylation of NF90 by PRMT5. (B) Investigation of the time-dependent methylation of NF90. 880 ng NF90 purified from *E. Coli* without GST-tag was incubated with 200 ng recombinant PRMT5 and 1 μ Ci [3-H]-SAM. The reaction was terminated by addition of SDS sample buffer and the samples were analyzed as described in (A). (C) Schematic overview of the domains and truncated forms of NF90 used in this work. The asterisk indicated methylatable forms and the distinctive RG-boxes have been highlighted in yellow. (D) Methylation assay of truncated NF90 forms purified from *E. Coli* as described in (A). NF90 is methylated in the C-terminus between amino acids 640 and 702 by PRMT5. AR: autoradiography, AB: amido black staining.

NF90 is methylated by PRMT5 in an RG-rich region in the C-terminus

Based on these data, we focused on the RG-motif in the C-terminal region. This RG-rich region contains seven glycine-arginine residues distributed among 17 amino acids that we identified as potentially methylatable (Fig. 2C). We mutated all these arginines at positions 640, 642, 644, 649, 651, 653, and 655 in the RG-rich region to non-active lysines. We then analyzed this NF90-7x R->K mutant in a methylation assay (Fig. 3A) and observed a complete methylation-deficient mutant, which no longer showed incorporation of radioactive ^3H . PRMT5 was no longer able to transfer methyl groups to this mutant, indicating that the methylation site of PRMT5 is localized in the RG-motif in the C-terminal region of NF90. For a deeper insight, we generated single lysine mutants of the seven arginine residues Arg⁶⁴⁰, Arg⁶⁴², Arg⁶⁴⁴, Arg⁶⁴⁹, Arg⁶⁵¹, Arg⁶⁵³, and Arg⁶⁵⁵. After heterologous expression in *E. coli* and cleavage of the GST-tag, a methylation assay was performed using equal amounts (1.5 μg) of every single mutant under identical methylation conditions (Fig. 3B). It could be shown that no single arginine is solely responsible for methylation. Mutation of Arg⁶⁴⁰ and Arg⁶⁵¹ did not affect the methylation status whereas Arg⁶⁴⁴, Arg⁶⁴⁹, Arg⁶⁵³, and Arg⁶⁵⁵ mutation decreased radioactive incorporation (Fig. 3B). This suggests a differential preference of PRMT5 in the methylation of the respective arginines. Thus, arginine 644, 649, 653, and 655 appear to be preferentially methylated. Taken together, our findings clearly show that at least four methylation sites, located in the C-terminal RG-rich region, contribute to the overall methylation status of NF90.

NF90 is fully methylated within the cell

After the experiments with recombinant NF90 from *E. coli*, we further investigated the intracellular methylation status of NF90. The first experiments with endogenous NF90 showed no incorporation of radioactive ^3H . This observation, together with previous findings of Herrmann et al., describing hnRNP U as a protein fully methylated within the cell, leads to the assumption, that NF90 could be completely methylated *in vivo* (Herrmann et al., 2004). Therefore, before the immunoprecipitation of NF90, HEK293 cells were treated with 20 μM adenosine dialdehyde (Adox). Adenosine dialdehyde is a universal methyltransferase inhibitor. Inhibition is indirectly accomplished by inhibition of the S-adenosyl-L-homocysteine hydrolase, resulting in high cytosolic concentrations of S-adenosyl-L-homocysteine (AdoHcy) a natural inhibitor of methyltransferases (Cantoni G.L., 1980, Hoffman, 1980, Chen et al., 2004). Proteins newly synthesized after Adox treatment remain hypomethylated (Chen et al., 2004) and are therefore again receptive for *in vitro* methylation. This allows us to perform methylation studies on immunoprecipitated endogenous NF90 before and after blocking the cellular methylation (Fig. 3C and 3D). Treatment of HEK293 cells with Adox does not alter

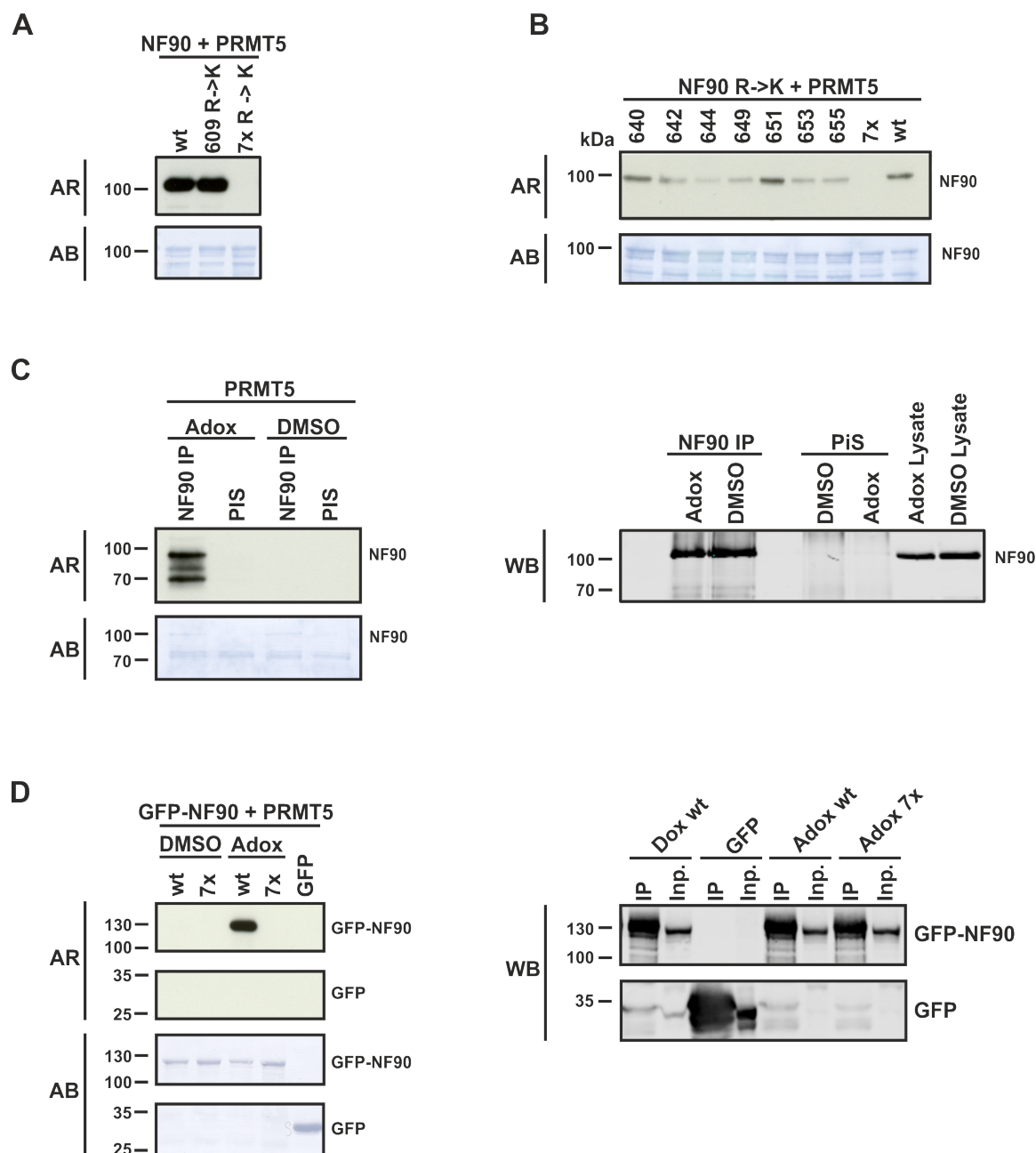


Figure 3: NF90 arginine mutants and *in vivo* inhibitor studies. (A) Recombinant NF90 wt, NF90^{R609K} and NF90 7x from *E. Coli* was incubated with 200 ng recombinant PRMT5 and 1 μ Ci [3-H]-SAM. Samples were separated by Tris/Glycine-SDS-PAGE and radioactive incorporation was analyzed by western blotting and autoradiography. In the NF90 7x mutant, all seven potential arginine methylation sites are mutated to lysines (see Fig. 2C). PRMT5 was not able to methylate the sevenfold arginine to lysine mutant whereas mutation of Arg⁶⁰⁹ to lysine does not influence the methylation status of NF90. (B) Single mutations of all seven arginines were generated and purified from *E. Coli*. 1.5 μ g of the different mutants were subjected to a methylation assay as described above. Only the sevenfold mutant (NF90 7x) shows complete methylation deficiency. (C) HEK293 cells were treated with 20 μ M of the S-adenosylmethionine-dependent methyltransferase inhibitor adenosine dialdehyde (Adox). 500 μ g lysate with 1 μ g NF90 antibody and Protein G Sepharose was incubated for 1.5 h and immunopurified NF90 was subjected to a methylation assay as described in (A). Only NF90 from Adox treated cells could be methylated *in vitro*. (D) Flp-In T-REx 293 cells stably expressing GFP-NF90 wt and GFP-NF90 7x were stimulated with 0.1 μ g/ml doxycycline for 24 h and treated with Adox as described in (C). After GFP-IP, a methylation assay was performed as described previously. No methylation of purified GFP-NF90 occurred in control cells (DMSO), whereas NF90 immunopurified from cells treated with Adox could be methylated *in vitro*. The sevenfold lysine mutant GFP-NF90 7x showed no methylation in all conditions. AR: autoradiography, AB: amido black staining, WB: western blotting.

NF90 expression or immunoprecipitation (Fig. 3C) but does alter the NF90 methylation status. We observed no methylation for NF90 immunoprecipitated from DMSO-treated cells, whereas NF90 immunoprecipitated from Adox treated cells could be methylated by recombinant PRMT5. Apparently, NF90 exhibits free methylation sites only after treatment of cells with adenosine dialdehyde. NF90 precipitated from untreated cells lacks free methylatable arginines, demonstrating that endogenous NF90 is fully methylated in the cell under normal conditions. To confirm this finding, we repeated the experiments with HEK293 Flp-In T-REx cell lines stably overexpressing GFP-NF90 wt and GFP-NF90 7x, the methylation-deficient mutant (Fig. 3D). First, we blocked the intracellular protein methylation by Adox treatment and then induced NF90 protein expression. GFP-immunoprecipitations allowed us to only precipitate and measure newly synthesized proteins and exclude endogenous NF90. The treatment of cells with Adox does not influence the GFP immunoprecipitation (Fig. 3D). Again, no methylation of purified GFP-NF90 occurred in control cells (DMSO), whereas NF90 from Adox treated cells could be methylated *in vitro*. This indicates that the overexpressed NF90 is also completely methylated in the cell. The sevenfold lysine mutant GFP-NF90 7x showed no methylation under all conditions, this further confirms that the methylation sites for PRMT5 are exclusively located in the RG-rich C-terminal region.

DISCUSSION

Although the RG-motif of NF90 has been postulated as a potential methylation site by PRMT5 (Richard et al., 2005), no methylation has yet been detected. In this work, we are the first to describe NF90 as a new interaction partner of the PRMT5-WD45-RioK1 complex and as a new symmetrically methylated substrate of the methyltransferase PRMT5.

In previous studies, we identified RioK1 as an adapter protein for PRMT5 (Guderian et al., 2011). It competes for the same binding site as pICln within PRMT5, resulting in two different complexes (PRMT5-WD45-pICln and PRMT5-WD45-RioK1). Due to the ability of RioK1 to bind numerous proteins containing RG-motifs, it increases the substrate diversity of PRMT5 and recruits new substrates to the methyltransferase. One of these putative RioK1-interacting proteins, determined by mass spectrometry from a pull-down assay using a truncated form of RioK1, was NF90 (Guderian et al., 2011). In this work, we performed interaction studies with PRMT5, WD45, RioK1, and pICln and observed NF90 co-immunoprecipitation with PRMT5 and RioK1 but not with pICln (Fig. 1A, Fig. 1B). These data confirm that NF90 recruitment occurs only via the RioK1-containing complex and not via pICln and therefore, NF90 is a novel

interaction partner of the PRMT5-WD45-RioK1 complex. In more detailed binding studies, the C-terminal region of NF90 (aa 640-702) was identified as the interaction surface with this complex (Fig. 1C). So far, the C-terminal region of ILF3 is already known as a binding site of the methyltransferase PRMT1 (Tang et al., 2000). Surprisingly, NF90 was also studied in this publication, but no interaction with PRMT1 was detected. However, the sequence shown in Tang et al. for NF90 (NM_004516) differs significantly from the current NF90 sequence (NM_004516.4). It lacks the RG-rich region in the C-terminus, which is important for methyltransferases and methylation. The ILF3 sequence studied (AF167570) corresponds closely to the present ILF3 sequence (NM_012218.4) and contains the RG-rich sequences, making a comparison between this and the present NF90 sequence more meaningful. Given the similar target sequences of the methyltransferase family in the form of glycine-arginine-rich sequences, it is convincing that not only PRMT1 but also PRMT5 interaction is mediated by the C-terminal region of NF90 (Bedford and Richard, 2005, Thandapani et al., 2013). The determined dissociation constant (K_D) of 100 ± 29 nM within the protein complex for RioK1 and PRMT5 (Fig. 1D) matches to 34 nM, reported in previous studies (Krzyzanowski et al., 2021). A dissociation constant of 57 ± 18 nM was observed for PRMT5 and NF90, indicating a high affinity of PRMT5 for NF90. The addition of RioK1 did not significantly alter the dissociation constants. Although RioK1 may be required for recruitment to the methyltransferase, it does not appear to play a role in the actual interaction between the enzyme and its substrate. A direct enzyme-substrate interaction was already described for PRMT5 for the histones H2A, H3, and the myelin basic protein, and no adapter proteins are known for PRMT1 either (Pollack et al., 1999, Branscombe et al., 2001, Pal et al., 2004, Zhang and Cheng, 2003). Nevertheless, binding of NF90 and recruitment by RioK1 to the PRMT5 complex may play an essential role *in vivo*.

In radioactive methylation studies, we identified NF90 as a new substrate for PRMT5-mediated methylation (Fig. 2A), which is consistent with our previous observations with truncated NF90 (Guderian et al., 2011). We determined a 17 amino acid long region in the C-terminus between amino acids 640 to 656 as the region of methylation (Fig. 2D). Kinetic studies revealed rapid methylation of NF90 by PRMT5. NF90 is completely methylated after ~15 minutes (Fig. 2B). The observed K_D values for NF90 from MST measurements (Fig. 1D) are consistent with the methylation in our kinetic studies (Fig. 2B) and demonstrate the high affinity of PRMT5 to NF90.

Investigations of the sequence showed that there is a glycine-arginine-rich (GAR) motif in the C-terminal region. These GAR motifs are described as a consensus sequence of protein methylation (Lischwe et al., 1985a, Lapeyre et al., 1986). It is reported that PRMT5 has a stringent substrate specificity. GR repeats that carry a glycine at position -1 are predominantly methylated by PRMT5 (Musiani et al., 2019). In this region of NF90, the sequence “R⁶⁴⁰GRGRGGSIRGRGRGRGF⁶⁵⁷” contains a triple RG repetition followed by a quadruple RG repetition sequence flanked by glycines (Fig. 2C). Our single mutation studies of this motif showed differences between the arginines in their contribution to methylation. It appears that mutation of Arg⁶⁴⁰ does not affect methylation, possibly because Arg⁶⁴⁰ has no preceding glycine. However, Arg⁶⁴⁹ also has no preceding glycine but appears to contribute to overall methylation. Mutations of Arg⁶⁴⁴, Arg⁶⁴⁹, Arg⁶⁵³, and Arg⁶⁵⁵ lead to a significant decrease in methylation, indicating that these arginines are the primary targets of PRMT5 (Fig. 3B). A preference for methylation of individual arginines within an RG-rich region has already been described for the Cellular nucleic acid-binding protein (CNBP), where PRMT5 prefers two of the four arginines (Musiani et al., 2019) or for the Ras GTPase-activating protein-binding protein 1 (G3BP1) (Tsai et al., 2016). The preference of PRMT5 for different arginines also appears to be present for four of the seven arginines in NF90.

So far, the methylation status of NF90 *in vivo* was unclear. We observed that immunoprecipitated NF90 could not be methylated in an *in vitro* methylation assay by recombinant PRMT5 although the IP precipitated a certain amount of protein (Fig. 3C). As the results with Adox showed (Fig. 3C), endogenous NF90 is present as a hypomethylated protein after treatment, since after IP we were able to methylate immunoprecipitated NF90 by PRMT5. The treatment resulted in a loss of methyl groups in newly formed proteins and free methylation sites. Studies with the NF90 7x mutant confirm our previously described findings that the methylation also occurs *in vivo* exclusively at the seven arginine residues in the C-terminus. Under Adox conditions, no methylation was observed in this mutant. This excludes other arginines, for example at positions 90, 247, 537, or 609 as target sequences of PRMT5. Even when strongly overexpressed in HEK293 cells, GFP-NF90 wt is completely methylated. This shows the stringency of the cell's methylation system and supports a general necessity for complete methylation of NF90 *in vivo* (Fig. 3D). We were able to prove within this work that NF90 is fully methylated in the cell under normal conditions and does not harbor any free methyl acceptor sites. These results are supported by examples from the literature where other proteins have been described as highly methylated. For example, is the heterogeneous nuclear ribonucleoprotein U (hnRNP U), a nucleic acid-binding protein, described as fully methylated

by PRMT1 *in vivo* (Herrmann et al., 2004). Also, the proteins in which methylation was first discovered, nucleolin and fibrillarin, exhibit a high degree of methylation (Lischwe et al., 1982, Lischwe et al., 1985b). Sm proteins SmD1, SmD3, SmB, and the U6 snRNA-associated Sm-like protein LSm4 are also described as high methylated proteins. Equal to NF90, these proteins have in common that they carry an RG-rich region in the C-terminus (Brahms et al., 2000, Brahms et al., 2001, Meister et al., 2001, Friesen et al., 2001a).

We currently assume that symmetric methylation of NF90 is irreversible and persists throughout the life of the protein. Little is known about demethylases but the Jumonji domain-containing 6 protein (JMJD6) was described as arginine demethylase (Chang et al., 2007). However, the results could not be reproduced in other studies (Webby et al., 2009, Han et al., 2012) whereas arginine demethylation activity was observed in recent studies (Liu et al., 2013, Poulard et al., 2014, Tsai et al., 2017). Therefore, arginine demethylation by JMJD6 remains highly controversial (Bottger et al., 2015). This raises the question of the biological function of irreversible methylation of NF90. Since many proteins have more than one methylation site but demethylation reactions have rarely been observed and are critically viewed, a regulatory function through turnover as in phosphorylation is unlikely (Simms et al., 1987, Herrmann et al., 2004). However, the production of SAM certainly consumes ATP and the cell does not make this effort unnecessarily in NF90.

DATA AVAILABILITY

All data and constructs are available upon request to christoph.peter@uni-duesseldorf.de.

ACKNOWLEDGEMENTS

We thank Dr. Claudia Hoppen for technical help and critical discussion on the manuscript. We also thank our colleagues David Schlütermann, Niklas Berleth, and Fabian Stuhldreier for comments on the manuscript.

REFERENCES

- ANTONYSAM, S., BONDAY, Z., CAMPBELL, R. M., DOYLE, B., DRUZINA, Z., GHEYI, T., HAN, B., JUNGHEIM, L. N., QIAN, Y., RAUCH, C., RUSSELL, M., SAUDER, J. M., WASSERMAN, S. R., WEICHERT, K., WILLARD, F. S., ZHANG, A. & EMTAGE, S. 2012. Crystal structure of the human PRMT5:MEP50 complex. *Proc Natl Acad Sci U S A*, 109, 17960-5.
- BEDFORD, M. T. & CLARKE, S. G. 2009. Protein arginine methylation in mammals: who, what, and why. *Mol Cell*, 33, 1-13.
- BEDFORD, M. T. & RICHARD, S. 2005. Arginine methylation an emerging regulator of protein function. *Mol Cell*, 18, 263-72.
- BLANC, R. S. & RICHARD, S. 2017. Arginine Methylation: The Coming of Age. *Mol Cell*, 65, 8-24.
- BOTTGER, A., ISLAM, M. S., CHOWDHURY, R., SCHOFIELD, C. J. & WOLF, A. 2015. The oxygenase Jmjd6--a case study in conflicting assignments. *Biochem J*, 468, 191-202.
- BRAHMS, H., MEHEUS, L., DE BRABANDERE, V., FISCHER, U. & LUHRMANN, R. 2001. Symmetrical dimethylation of arginine residues in spliceosomal Sm protein B/B' and the Sm-like protein LSm4, and their interaction with the SMN protein. *RNA*, 7, 1531-42.
- BRAHMS, H., RAYMACKERS, J., UNION, A., DE KEYSER, F., MEHEUS, L. & LUHRMANN, R. 2000. The C-terminal RG dipeptide repeats of the spliceosomal Sm proteins D1 and D3 contain symmetrical dimethylarginines, which form a major B-cell epitope for anti-Sm autoantibodies. *J Biol Chem*, 275, 17122-9.
- BRANSCOMBE, T. L., FRANKEL, A., LEE, J. H., COOK, J. R., YANG, Z., PESTKA, S. & CLARKE, S. 2001. PRMT5 (Janus kinase-binding protein 1) catalyzes the formation of symmetric dimethylarginine residues in proteins. IN VITRO. The role of PRMT5in vivo has yet to be determined. *J Biol Chem*, 276, 32971-6.
- CANTONI G.L., C. P. K. 1980. The Role of S-Adenosylhomocysteine and S-Adenosylhomocysteine Hydrolase in the Control of Biological Methylations. *Natural Sulfur Compounds*. Springer, Boston, MA., pp 67-80.
- CASTELLA, S., BERNARD, R., CORNO, M., FRADIN, A. & LARCHER, J. C. 2015. Ilf3 and NF90 functions in RNA biology. *Wiley Interdiscip Rev RNA*, 6, 243-56.
- CHAN-PENEBRE, E., KUPLAST, K. G., MAJER, C. R., BORIACK-SJODIN, P. A., WIGLE, T. J., JOHNSTON, L. D., RIOUX, N., MUNCHHOF, M. J., JIN, L., JACQUES, S. L., WEST, K. A., LINGARAJ, T., STICKLAND, K., RIBICH, S. A., RAIMONDI, A., SCOTT, M. P., WATERS, N. J., POLLOCK, R. M., SMITH, J. J., BARBASH, O., PAPPALARDI, M., HO, T. F., NURSE, K., OZA, K. P., GALLAGHER, K. T., KRUGER, R., MOYER, M. P., COPELAND, R. A., CHESWORTH, R. & DUNCAN, K. W. 2015. A selective inhibitor of PRMT5 with in vivo and in vitro potency in MCL models. *Nat Chem Biol*, 11, 432-7.
- CHANG, B., CHEN, Y., ZHAO, Y. & BRUICK, R. K. 2007. JMJD6 is a histone arginine demethylase. *Science*, 318, 444-7.
- CHEN, D. H., WU, K. T., HUNG, C. J., HSIEH, M. & LI, C. 2004. Effects of adenosine dialdehyde treatment on in vitro and in vivo stable protein methylation in HeLa cells. *J Biochem*, 136, 371-6.
- COOK, J. R., LEE, J. H., YANG, Z. H., KRAUSE, C. D., HERTH, N., HOFFMANN, R. & PESTKA, S. 2006. FBXO11/PRMT9, a new protein arginine methyltransferase, symmetrically dimethylates arginine residues. *Biochem Biophys Res Commun*, 342, 472-81.
- CORTHESEY, B. & KAO, P. N. 1994. Purification by DNA affinity chromatography of two polypeptides that contact the NF-AT DNA binding site in the interleukin 2 promoter. *J Biol Chem*, 269, 20682-90.

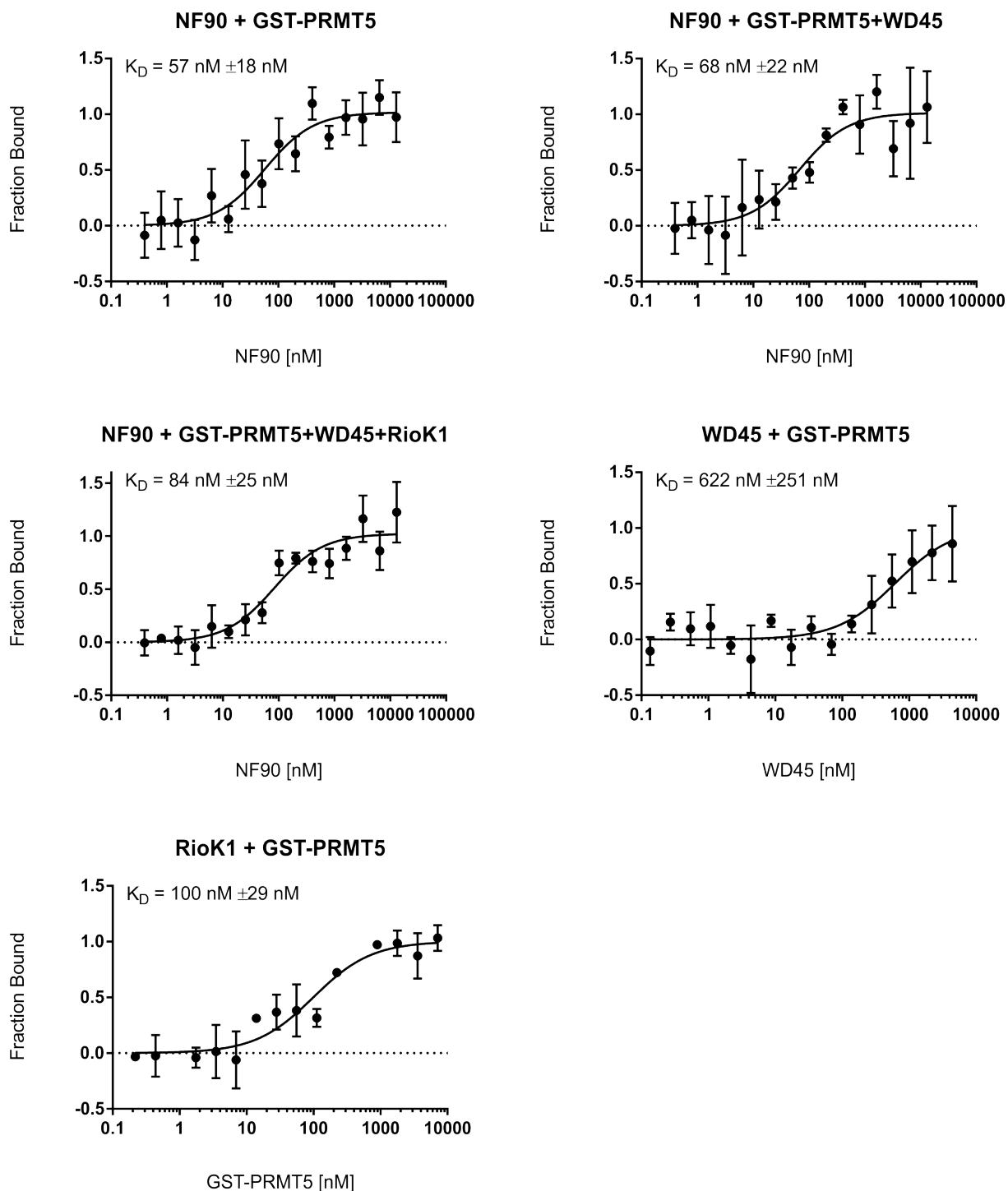
- DUCHANGE, N., PIDOUX, J., CAMUS, E. & SAUVAGET, D. 2000. Alternative splicing in the human interleukin enhancer binding factor 3 (ILF3) gene. *Gene*, 261, 345-53.
- FENG, Y., MAITY, R., WHITELEGGE, J. P., HADJIKYRIACOU, A., LI, Z., ZURITA-LOPEZ, C., AL-HADID, Q., CLARK, A. T., BEDFORD, M. T., MASSON, J. Y. & CLARKE, S. G. 2013. Mammalian protein arginine methyltransferase 7 (PRMT7) specifically targets RXR sites in lysine- and arginine-rich regions. *J Biol Chem*, 288, 37010-25.
- FRIESEN, W. J., MASSENET, S., PAUSHKIN, S., WYCE, A. & DREYFUSS, G. 2001a. SMN, the product of the spinal muscular atrophy gene, binds preferentially to dimethylarginine-containing protein targets. *Mol Cell*, 7, 1111-7.
- FRIESEN, W. J., PAUSHKIN, S., WYCE, A., MASSENET, S., PESIRIDIS, G. S., VAN DUYN, G., RAPPILBER, J., MANN, M. & DREYFUSS, G. 2001b. The methylosome, a 20S complex containing JBP1 and pICln, produces dimethylarginine-modified Sm proteins. *Mol Cell Biol*, 21, 8289-300.
- GUDERIAN, G., PETER, C., WIESNER, J., SICKMANN, A., SCHULZE-OSTHOFF, K., FISCHER, U. & GRIMMLER, M. 2011. RioK1, a new interactor of protein arginine methyltransferase 5 (PRMT5), competes with pICln for binding and modulates PRMT5 complex composition and substrate specificity. *J Biol Chem*, 286, 1976-86.
- HADJIKYRIACOU, A., YANG, Y., ESPEJO, A., BEDFORD, M. T. & CLARKE, S. G. 2015. Unique Features of Human Protein Arginine Methyltransferase 9 (PRMT9) and Its Substrate RNA Splicing Factor SF3B2. *J Biol Chem*, 290, 16723-43.
- HAN, G., LI, J., WANG, Y., LI, X., MAO, H., LIU, Y. & CHEN, C. D. 2012. The hydroxylation activity of Jmjd6 is required for its homo-oligomerization. *J Cell Biochem*, 113, 1663-70.
- HERRMANN, F., BOSSERT, M., SCHWANDER, A., AKGUN, E. & FACKELMAYER, F. O. 2004. Arginine methylation of scaffold attachment factor A by heterogeneous nuclear ribonucleoprotein particle-associated PRMT1. *J Biol Chem*, 279, 48774-9.
- HOFFMAN, J. L. 1980. The rate of transmethylation in mouse liver as measured by trapping S-adenosylhomocysteine. *Arch Biochem Biophys*, 205, 132-5.
- HWANG, J. W., CHO, Y., BAE, G. U., KIM, S. N. & KIM, Y. K. 2021. Protein arginine methyltransferases: promising targets for cancer therapy. *Exp Mol Med*.
- ISKEN, O., GRASSMANN, C. W., SARISKY, R. T., KANN, M., ZHANG, S., GROSSE, F., KAO, P. N. & BEHRENS, S. E. 2003. Members of the NF90/NFAR protein group are involved in the life cycle of a positive-strand RNA virus. *EMBO J*, 22, 5655-65.
- KAO, P. N., CHEN, L., BROCK, G., NG, J., KENNY, J., SMITH, A. J. & CORTHESEY, B. 1994. Cloning and expression of cyclosporin A- and FK506-sensitive nuclear factor of activated T-cells: NF45 and NF90. *Journal of Biological Chemistry*, 269, 20691-20699.
- KHOURY, G. A., BALIBAN, R. C. & FLOUDAS, C. A. 2011. Proteome-wide post-translational modification statistics: frequency analysis and curation of the swiss-prot database. *Sci Rep*, 1.
- KRAPIVINSKY, G., PU, W., WICKMAN, K., KRAPIVINSKY, L. & CLAPHAM, D. E. 1998. pICln binds to a mammalian homolog of a yeast protein involved in regulation of cell morphology. *J Biol Chem*, 273, 10811-4.
- KRZYZANOWSKI, A., GASPER, R., ADIHO, H., T HART, P. & WALDMANN, H. 2021. Biochemical Investigation of the Interaction of pICln, RioK1 and COPR5 with the PRMT5-MEP50 Complex. *Chembiochem*.
- LAPEYRE, B., AMALRIC, F., GHAFARI, S. H., RAO, S. V., DUMBAR, T. S. & OLSON, M. O. 1986. Protein and cDNA sequence of a glycine-rich, dimethylarginine-containing region located near the carboxyl-terminal end of nucleolin (C23 and 100 kDa). *J Biol Chem*, 261, 9167-73.
- LIAO, H. J., KOBAYASHI, R. & MATHEWS, M. B. 1998. Activities of adenovirus virus-associated RNAs: purification and characterization of RNA binding proteins. *Proc Natl Acad Sci U S A*, 95, 8514-9.

- LISCHWE, M. A., COOK, R. G., AHN, Y. S., YEOMAN, L. C. & BUSCH, H. 1985a. Clustering of glycine and NG,NG-dimethylarginine in nucleolar protein C23. *Biochemistry*, 24, 6025-8.
- LISCHWE, M. A., OCHS, R. L., REDDY, R., COOK, R. G., YEOMAN, L. C., TAN, E. M., REICHLIN, M. & BUSCH, H. 1985b. Purification and partial characterization of a nucleolar scleroderma antigen (Mr = 34,000; pI, 8.5) rich in NG,NG-dimethylarginine. *J Biol Chem*, 260, 14304-10.
- LISCHWE, M. A., ROBERTS, K. D., YEOMAN, L. C. & BUSCH, H. 1982. Nucleolar specific acidic phosphoprotein C23 is highly methylated. *J Biol Chem*, 257, 14600-2.
- LIU, W., MA, Q., WONG, K., LI, W., OHGI, K., ZHANG, J., AGGARWAL, A. & ROSENFELD, M. G. 2013. Brd4 and JMJD6-associated anti-pause enhancers in regulation of transcriptional pause release. *Cell*, 155, 1581-1595.
- LOFFLER, A. S., ALERS, S., DIETERLE, A. M., KEPPELER, H., FRANZ-WACHTEL, M., KUNDU, M., CAMPBELL, D. G., WESSELBORG, S., ALESSI, D. R. & STORK, B. 2011. Ulk1-mediated phosphorylation of AMPK constitutes a negative regulatory feedback loop. *Autophagy*, 7, 696-706.
- MEISTER, G., EGGERT, C., BUHLER, D., BRAHMS, H., KAMBACH, C. & FISCHER, U. 2001. Methylation of Sm proteins by a complex containing PRMT5 and the putative U snRNP assembly factor pICln. *Curr Biol*, 11, 1990-4.
- MIRANDA, T. B., MIRANDA, M., FRANKEL, A. & CLARKE, S. 2004. PRMT7 is a member of the protein arginine methyltransferase family with a distinct substrate specificity. *J Biol Chem*, 279, 22902-7.
- MURN, J. & SHI, Y. 2017. The winding path of protein methylation research: milestones and new frontiers. *Nat Rev Mol Cell Biol*, 18, 517-527.
- MUSIANI, D., BOK, J., MASSIGNANI, E., WU, L., TABAGLIO, T., IPPOLITO, M. R., CUOMO, A., OZBEK, U., ZORGATI, H., GHOSHDASTIDER, U., ROBINSON, R. C., GUCCIONE, E. & BONALDI, T. 2019. Proteomics profiling of arginine methylation defines PRMT5 substrate specificity. *Sci Signal*, 12.
- PAL, S., VISHWANATH, S. N., ERDJUMENT-BROMAGE, H., TEMPST, P. & SIF, S. 2004. Human SWI/SNF-associated PRMT5 methylates histone H3 arginine 8 and negatively regulates expression of ST7 and NM23 tumor suppressor genes. *Mol Cell Biol*, 24, 9630-45.
- PATEL, R. C., VESTAL, D. J., XU, Z., BANDYOPADHYAY, S., GUO, W., ERME, S. M., WILLIAMS, B. R. & SEN, G. C. 1999. DRBP76, a double-stranded RNA-binding nuclear protein, is phosphorylated by the interferon-induced protein kinase, PKR. *J Biol Chem*, 274, 20432-7.f
- POLLACK, B. P., KOTENKO, S. V., HE, W., IZOTOVA, L. S., BARNOSKI, B. L. & PESTKA, S. 1999. The human homologue of the yeast proteins Skb1 and Hsl7p interacts with Jak kinases and contains protein methyltransferase activity. *J Biol Chem*, 274, 31531-42.
- POULARD, C., RAMBAUD, J., HUSSEIN, N., CORBO, L. & LE ROMANCER, M. 2014. JMJD6 regulates ERalpha methylation on arginine. *PLoS One*, 9, e87982.
- RICHARD, S., MOREL, M. & CLEROUX, P. 2005. Arginine methylation regulates IL-2 gene expression: a role for protein arginine methyltransferase 5 (PRMT5). *Biochem J*, 388, 379-86.
- SAUNDERS, L. R., JURECIC, V. & BARBER, G. N. 2001. The 90- and 110-kDa human NFAR proteins are translated from two differentially spliced mRNAs encoded on chromosome 19p13. *Genomics*, 71, 256-9.
- SCHMITZ, K., COX, J., ESSER, L. M., VOSS, M., SANDER, K., LOFFLER, A., HILLEBRAND, F., ERKELENZ, S., SCHAAL, H., KAHNE, T., KLINKER, S., ZHANG, T., NAGEL-STEGER, L., WILLBOLD, D., SEGGEWISS, S., SCHLUTERMANN, D., STORK, B., GRIMMLER, M., WESSELBORG, S. & PETER, C. 2021. An essential role of the autophagy activating kinase ULK1 in snRNP biogenesis. *Nucleic Acids Res.*

- SHI, L., ZHAO, G., QIU, D., GODFREY, W. R., VOGEL, H., RANDO, T. A., HU, H. & KAO, P. N. 2005. NF90 regulates cell cycle exit and terminal myogenic differentiation by direct binding to the 3'-untranslated region of MyoD and p21WAF1/CIP1 mRNAs. *J Biol Chem*, 280, 18981-9.
- SHIM, J., LIM, H., J, R. Y. & KARIN, M. 2002. Nuclear export of NF90 is required for interleukin-2 mRNA stabilization. *Mol Cell*, 10, 1331-44.
- SIMMS, S. A., STOCK, A. M. & STOCK, J. B. 1987. Purification and characterization of the S-adenosylmethionine:glutamyl methyltransferase that modifies membrane chemoreceptor proteins in bacteria. *J Biol Chem*, 262, 8537-43.
- SIU, L. L., RASCO, D. W., VINAY, S. P., ROMANO, P. M., MENIS, J., OPDAM, F. L., HEINHUIS, K. M., EGGER, J. L., GORMAN, S. A., PARASRAMPURIA, R., WANG, K., KREMER, B. E. & GOUNDER, M. M. 2019. METEOR-1: A phase I study GSK3326595, a first-in-class protein arginine methyltransferase 5 (PRMT5) inhibitor, in advanced solid tumours. *Annals of Oncology*, 30, 159-159.
- STOPA, N., KREBS, J. E. & SHECHTER, D. 2015. The PRMT5 arginine methyltransferase: many roles in development, cancer and beyond. *Cell Mol Life Sci*, 72, 2041-59.
- TANG, J., KAO, P. N. & HERSCHMAN, H. R. 2000. Protein-arginine methyltransferase I, the predominant protein-arginine methyltransferase in cells, interacts with and is regulated by interleukin enhancer-binding factor 3. *J Biol Chem*, 275, 19866-76.
- THANDAPANI, P., O'CONNOR, T. R., BAILEY, T. L. & RICHARD, S. 2013. Defining the RGG/RG motif. *Mol Cell*, 50, 613-23.
- TSAI, W. C., GAYATRI, S., REINEKE, L. C., SBARDELLA, G., BEDFORD, M. T. & LLOYD, R. E. 2016. Arginine Demethylation of G3BP1 Promotes Stress Granule Assembly. *J Biol Chem*, 291, 22671-22685.
- TSAI, W. C., REINEKE, L. C., JAIN, A., JUNG, S. Y. & LLOYD, R. E. 2017. Histone arginine demethylase JMJD6 is linked to stress granule assembly through demethylation of the stress granule-nucleating protein G3BP1. *J Biol Chem*, 292, 18886-18896.
- WATTS, J. M., BRADLEY, T. J., THOMASSEN, A., BRUNNER, A. M., MINDEN, M. D., PAPADANTONAKIS, N., ABEDIN, S., BAINES, A. J., BARBASH, O., GORMAN, S., KREMER, B. E. & BORTHAKUR, G. M. 2019. A Phase I/II Study to Investigate the Safety and Clinical Activity of the Protein Arginine Methyltransferase 5 Inhibitor GSK3326595 in Subjects with Myelodysplastic Syndrome and Acute Myeloid Leukemia. *Blood*, 134.
- WEBBY, C. J., WOLF, A., GROMAK, N., DREGER, M., KRAMER, H., KESSLER, B., NIELSEN, M. L., SCHMITZ, C., BUTLER, D. S., YATES, J. R., 3RD, DELAHUNTY, C. M., HAHN, P., LENGELING, A., MANN, M., PROUDFOOT, N. J., SCHOFIELD, C. J. & BOTTGER, A. 2009. Jmjd6 catalyses lysyl-hydroxylation of U2AF65, a protein associated with RNA splicing. *Science*, 325, 90-3.
- YANG, Y., HADJIKYRIACOU, A., XIA, Z., GAYATRI, S., KIM, D., ZURITA-LOPEZ, C., KELLY, R., GUO, A., LI, W., CLARKE, S. G. & BEDFORD, M. T. 2015. PRMT9 is a type II methyltransferase that methylates the splicing factor SAP145. *Nat Commun*, 6, 6428.
- ZHANG, X. & CHENG, X. 2003. Structure of the predominant protein arginine methyltransferase PRMT1 and analysis of its binding to substrate peptides. *Structure*, 11, 509-20.
- ZURITA-LOPEZ, C. I., SANDBERG, T., KELLY, R. & CLARKE, S. G. 2012. Human protein arginine methyltransferase 7 (PRMT7) is a type III enzyme forming omega-NG-monomethylated arginine residues. *J Biol Chem*, 287, 7859-70.

SUPPLEMENTARY DATA

Supplementary Data 1



Supplementary Data Figure 1

Quantitative binding studies of NF90, PRMT5, WD45, and RioK1 by microscale thermophoresis. Related to figure 1D. Purified recombinant proteins GST-PRMT5, NF90 or RioK1 were labeled with AlexaFluor488-NHS (A20000, Invitrogen) in 50 mM HEPES, 300 mM NaCl, pH 7.5. 50 nM of labeled proteins and 4-14 μM of unlabeled proteins were used for interaction studies. All measurements were run in triplicates. Data acquisition was performed on a Nanotemper Monolith NT.115. Curve fitting was done using GraphPad Prism version 7.

8 Discussion

PRMT5 is the major methyltransferase that catalyzes symmetric dimethylations of arginine residues (SDMA) in cells (Hadjikyriacou et al., 2015). Depending on its cellular function, the enzyme methylates substrates directly (e.g. histones) (Pollack et al., 1999, Pal et al., 2004, Migliori et al., 2012) or methylates new substrates recruited via the adapter proteins pICln (e.g. Sm proteins) (Brahms et al., 2000, Meister et al., 2001b, Brahms et al., 2001, Friesen et al., 2001b) or RioK1 (e.g. nucleolin) (Guderian et al., 2011). The focus of this thesis lies on the composition of the PRMT5 complex and the adapter proteins pICln and RioK1, which form the PRMT5-WD45-pICln complex (Chapter 7.1) and the PRMT5-WD45-RioK1 complex (Chapter 7.2). In the first part of this thesis (Chapter 7.1), we identified ULK1 as a new interaction partner of pICln, which was previously known mainly for its function in the regulation of autophagy (Akers et al., 2012). Here, we described a novel role of ULK1 in snRNP biosynthesis as a pICln-phosphorylating kinase. This phosphorylation of pICln leads to the breakup of the 6S ring structure by lowering SmG binding, a process essential for successful UsnRNP biosynthesis. In the second part of this thesis (Chapter 7.2), we identified and characterized NF90 as a new PRMT5 substrate, interacting via the adapter protein RioK1. We determined the PRMT5 methylation sites of NF90 and found that NF90 is present in the cell in a fully methylated state.

8.1 Impaired splicing and autophagy - associations between ULK1, AMPK, and mTOR

In our studies, we demonstrated that ULK1, in addition to its role in autophagy, plays an important role in the UsnRNP biogenesis. ULK1 phosphorylates pICln, resulting in ring opening of the 6S complex at the protein SmG, which is essential for efficient snRNP core assembly. We also showed that the role of ULK1 in UsnRNP biosynthesis is independent of its function in autophagy (Fig. 1A, B; Chapter 7.1), as ULK1 binds to the FIP200, ATG13, and ATG101 complexes through its C-terminal domain (Chan et al., 2009), whereas binding of the PRMT5 complex occurs in a C-terminally independent manner (Fig. 1C, D; Chapter 7.1). Nevertheless, the same ULK1 protein cannot simultaneously perform both functions in the respective complexes, but it is unknown how ULK1 activity is regulated between these two different complexes. Due to the activating or inhibitory effect of the mTOR complex on ULK1 by phosphorylation (Shimobayashi and Hall, 2014), ULK1 acts as a switch and is probably permanently required in the autophagy inducing FIP200-ATG13-ATG101 complex. In

contrast, ULK1 in the PRMT5-pICln complex is required only as long as UsnRNP biosynthesis is activated.

The connection between the spliceosomal proteins and autophagy has already been demonstrated (Quidville et al., 2013, Prusty et al., 2017, Piras et al., 2017). A link between disturbed splicing and autophagy was observed for neurodegenerative diseases such as spinal muscular atrophy (SMA) (Piras et al., 2017). In SMA, degeneration of motor neurons occurs due to disturbed splicing and studies showed, that autophagy is also dysregulated in SMA, leading to an increased occurrence of autophagic vesicles. Furthermore, the life span of SMA mice could be prolonged by an autophagy inhibitor (Piras et al., 2017). It has also been shown that after pICln knockdown, Sm proteins are downregulated and degraded via the autophagy pathway, preventing the uncontrolled accumulation of Sm proteins (Prusty et al., 2017). In turn, knockdown of the spliceosomal protein SmE decreased the cellular mTOR mRNA levels and mTOR protein expression, leading to deregulated mTOR signaling and induction of autophagy (Quidville et al., 2013). Further studies showed that knockdown of SmE not only leads to autophagy but also impaired splicing activity (Chen et al., 2019). This initially suggests that in the absence of SmE, mTOR mRNA processing simply does not occur anymore, thus lowering the mTOR levels and inducing autophagy. However, the absence of SmD1, another spliceosomal protein, does not have the same effect on mTOR but still leads to autophagy (Quidville et al., 2013). In summary, knockdown of pICln, as well as SmE or SmD1, triggers autophagy which suggests that there is an unknown link between UsnRNP biosynthesis and autophagy. All of these proteins, in addition to ULK1, are involved in the formation of the 6S complex and ULK1 represents a cross-link between the two pathways. Possibly, the disturbed assembly of the 6S complex due to the absence of SmE or SmD1 changes the activity of ULK1 in the cell. In combination with impaired mTOR activity, there is an excess of active ULK1 in the cell, leading to induction of autophagy. It is also possible that a yet unknown kinase affects the activity of ULK1 since it is known that the activity of ULK1 is regulated by phosphorylation (Kim et al., 2011, Egan et al., 2011). An enzyme involved in the regulation of autophagy and linked to ULK1 is the AMP-activated protein kinase (AMPK). AMPK measures the energy level in the cell and maintains energy homeostasis (Hardie et al., 2012). Under starvation conditions, AMPK directly phosphorylates ULK1, thereby activating ULK1 and inducing autophagy (Kim et al., 2011, Egan et al., 2011). It is known that after autophagy activation, protein synthesis is downregulated (Hay and Sonenberg, 2004, Hardie et al., 2012) to allow the cell to conserve energy. Due to reduced protein synthesis, also less mRNA needs to be processed and the ATP-dependent process of RNA splicing (Newman, 1998, Meister et al., 2001a) could also be downregulated even though no mechanism for this has yet been

discovered. Furthermore, AMPK inhibits the mTOR complex, leading to ULK1 activation through loss of mTOR phosphorylation (Shimobayashi and Hall, 2014). This leads to an altered phosphorylation pattern of ULK1 upon autophagy induction. ULK1 loses phosphorylation of mTOR at Ser757 and is in turn phosphorylated by AMPK at Ser317, Ser777, Ser467, Ser555, Thr574, and Ser637 (Kim et al., 2011, Egan et al., 2011, Alers et al., 2012). However, the phosphorylation pattern of our discovered ULK1 in snRNP biosynthesis is unknown. We could show that ULK1 is present in the PRMT5-WD45-pICln complex independently of autophagy (Fig. 1A, B; Chapter 7.1). Either the phosphorylation pattern of autophagy does not affect the activity of ULK1 in snRNP biosynthesis or ULK1 in the complex with PRMT5 is not a target of AMPK and mTORC1 and is regulated by other mechanisms. An unknown kinase may regulate the activity of ULK1 in snRNP biosynthesis, similar to AMPK or mTOR in autophagy. An autophagy independent inhibition of ULK1 would result in reduced phosphorylation of pICln and a lack of ring breakage in the 6S complex. This may represent a regulatory mechanism of UsnRNP biosynthesis in autophagy, as an influence of autophagy on spliceosomal processes for energy conservation would be conclusive. Based on our discoveries, ULK1 now represents an enzyme that is directly involved in both processes and could therefore play a crucial role in regulation.

8.2 PRMT5-RioK1 and mTOR

In mass spectrometry studies, an enrichment of PRMT5 was detected in the mTOR interactome (Schwarz et al., 2015). Likewise, interaction partners WD45 and RioK1 were detected, but no pICln. Since no pICln but only RioK1 was found, it does not seem to be a nonspecific interaction with PRMT5 and indicates an unknown cross-link between mTOR and the PRMT5-RioK1 complex. Currently, only two substrates are known to interact with the PRMT5-RioK1 complex, the previously known nucleolin discovered in 2011 (Guderian et al., 2011) and NF90 discovered in this work (Chapter 7.2). Both proteins were also found in the interactome of mTOR (Schwarz et al., 2015), providing further evidence for a link between the PRMT5-RioK1 complex and the mTOR signaling pathway. A crosslink between PRMT5 and mTOR was already detected in murine hematopoietic stem cells (Tan et al., 2019). Tan et al. lowered PRMT5 levels by treatment with PRMT5 inhibitor and observed a higher protein synthesis rate and an increase in cell size. These effects could be reversed by the addition of the mTOR inhibitor rapamycin (Tan et al., 2019). They also observed an increase in mTOR signaling and mTOR phosphorylation upon PRMT5 reduction. It is known that ribosome biosynthesis can be regulated by the mTOR signaling pathway, affecting cell size and protein biosynthesis

(Shimobayashi and Hall, 2014). Therefore, Tan et al. speculated that PMRT5 reduction activates mTOR, which in turn increases ribosome biogenesis, leading to higher protein synthesis and cell size (Tan et al., 2019). RioK1 is also known for its role in ribosome biogenesis. It is involved in the maturation of the 40S ribosomal subunit, but its function there is described as independent of PRMT5 (Widmann et al., 2012). In the search for how PRMT5 affects mTOR, RioK1 may play a role, potentially recruiting so far unknown substrates of the mTORC1 complex to PRMT5. However, it is as yet unknown how PRMT5 affects mTOR.

8.3 Protein arginine methylation of NF90 – a fully methylated substrate

So far, only nucleolin was known to be recruited via the PRMT5-RioK1 complex (Guderian et al., 2011). In this work, NF90 was discovered as a novel substrate that interacts with RioK1 and is methylated by PRMT5. In radioactive methylation assays using recombinant NF90 from *E. coli*, we detected methylation of NF90 by PRMT5. In contrast, the detection was more difficult with endogenous NF90, immunoprecipitated from cell lysates. Initially, no methylation was detected in the methylation assay, although immunoprecipitation was successful (Fig. 3 C, D, Chapter 7.2). We suspected that endogenous NF90 from the cells was already fully methylated by endogenous PRMT5. Thus, methylation in the *in-vitro* assay would not be possible. To test this hypothesis, we treated cells with adenosine dialdehyde a general methyltransferase inhibitor (Chen et al., 2004). Surprisingly, we were able to methylate the immunoprecipitated NF90 after cell treatment, indicating a previously fully methylated protein (Fig. 3C, D, Chapter 7.2). Complete or high methylation of proteins has already been described in the literature. For example, fully methylation of heterogeneous nuclear ribonucleoprotein U (hnRNP U), a substrate of PRMT1, is known (Herrmann et al., 2004). Although other substrates of PRMT5 such as fibrillarin, nucleolin, or the Sm proteins SmD1, D3, and B have been described as highly methylated (Lischwe et al., 1982, Lischwe et al., 1985b, Brahms et al., 2000, Brahms et al., 2001, Friesen et al., 2001a), NF90 is the only substrate of PRMT5 for which complete methylation has been demonstrated to date. This raises the question of the biological effect of the methylation. Currently, methylations are considered irreversible, as the presence of demethylases is controversially discussed (Bottger et al., 2015). This fact and the complete methylation speak rather against a regulatory function and more for a general functional modification. For example, NF90 is known as an RNA-binding protein and binds the mRNA of the 3'-untranslated region of p21 mRNA (Shi et al., 2005) or interleukin-2 mRNA (Shim et al., 2002). Arginine residues are known to play an important role in RNA-protein interactions (Bedford and Richard, 2005). A motif of RNA binding is the arginine-glycine-rich sequence (RG-motif)

found in many other RNA-binding proteins (Kiledjian and Dreyfuss, 1992), which are also targets of arginine methylation (Lischwe et al., 1985a, Lapeyre et al., 1986). Therefore, arginine methylation of NF90 possibly affects affinity for RNAs.

8.4 Conclusions and further perspectives

The links between spliceosomal activity and autophagy presented in this discussion represent an interesting overlap. Through the newly discovered function of ULK1, we were able to provide information about a possible link between the two signaling pathways. However, it remains unclear how the presented connections are regulated at the protein level. A key question is how the ULK1 activity is regulated in the cell between the two complexes, PRMT5-pICln-ULK1 and ULK1-FIP200-ATG13-ATG101. Moreover, it is not known whether the phosphorylation pattern of ULK1 in autophagy affects the complex composition of PRMT5-pICln-ULK1 during splicing. Further studies examining the phosphorylation status of ULK1 in the different complexes are needed.

A broad field of new potential interaction partners emerges for the PRMT5-RioK1 complex. Thus, additional new PRMT5 substrates recruited via RioK1 may be discovered in the future. It will be interesting to see whether NF90, as a fully methylated protein, is an exception or the normal case. It remains to be seen if protein methylation will continue to be considered irreversible or if demethylases will be found in the cell. Since no demethylases are known to date, it must be assumed that methylations of proteins such as NF90 are irreversible and therefore have less of a switch function but may represent a general functional modification. The next step in NF90 research would be to study the biological function of the methylation, particularly the binding of RNA via the RG-rich sequences.

9 Bibliography

- ADAMS, J. A. 2001. Kinetic and catalytic mechanisms of protein kinases. *Chem Rev*, 101, 2271-90.
- AEBERSOLD, R., AGAR, J. N., AMSTER, I. J., BAKER, M. S., BERTOZZI, C. R., BOJA, E. S., COSTELLO, C. E., CRAVATT, B. F., FENSELAU, C., GARCIA, B. A., GE, Y., GUNAWARDENA, J., HENDRICKSON, R. C., HERGENROTHER, P. J., HUBER, C. G., IVANOV, A. R., JENSEN, O. N., JEWETT, M. C., KELLEHER, N. L., KIESSLING, L. L., KROGAN, N. J., LARSEN, M. R., LOO, J. A., OGORZALEK LOO, R. R., LUNDBERG, E., MACCOSS, M. J., MALLICK, P., MOOHA, V. K., MRKSICH, M., MUIR, T. W., PATRIE, S. M., PESAVENTO, J. J., PITTERI, S. J., RODRIGUEZ, H., SAGHATELIAN, A., SANDOVAL, W., SCHLUTER, H., SECHI, S., SLAVOFF, S. A., SMITH, L. M., SNYDER, M. P., THOMAS, P. M., UHLEN, M., VAN EYK, J. E., VIDAL, M., WALT, D. R., WHITE, F. M., WILLIAMS, E. R., WOHLSCHLAGER, T., WYSOCKI, V. H., YATES, N. A., YOUNG, N. L. & ZHANG, B. 2018. How many human proteoforms are there? *Nat Chem Biol*, 14, 206-214.
- ALERS, S., LOFFLER, A. S., WESSELBORG, S. & STORK, B. 2012. Role of AMPK-mTOR-Ulk1/2 in the regulation of autophagy: cross talk, shortcuts, and feedbacks. *Mol Cell Biol*, 32, 2-11.
- AMBLER, R. P. & REES, M. W. 1959. Epsilon-N-Methyl-lysine in bacterial flagellar protein. *Nature*, 184, 56-7.
- AMEISMEIER, M., CHENG, J., BERNINGHAUSEN, O. & BECKMANN, R. 2018. Visualizing late states of human 40S ribosomal subunit maturation. *Nature*, 558, 249-253.
- ANTONYSAMY, S., BONDAY, Z., CAMPBELL, R. M., DOYLE, B., DRUZINA, Z., GHEYI, T., HAN, B., JUNGHEIM, L. N., QIAN, Y., RAUCH, C., RUSSELL, M., SAUDER, J. M., WASSERMAN, S. R., WEICHERT, K., WILLARD, F. S., ZHANG, A. & EMTAGE, S. 2012. Crystal structure of the human PRMT5:MEP50 complex. *Proc Natl Acad Sci U S A*, 109, 17960-5.
- ARDITO, F., GIULIANI, M., PERRONE, D., TROIANO, G. & LO MUZIO, L. 2017. The crucial role of protein phosphorylation in cell signaling and its use as targeted therapy (Review). *Int J Mol Med*, 40, 271-280.
- BACHAND, F. 2007. Protein arginine methyltransferases: from unicellular eukaryotes to humans. *Eukaryot Cell*, 6, 889-98.
- BALDWIN, G. S. & CARNEGIE, P. R. 1971a. Isolation and partial characterization of methylated arginines from the encephalitogenic basic protein of myelin. *Biochem J*, 123, 69-74.
- BALDWIN, G. S. & CARNEGIE, P. R. 1971b. Specific enzymic methylation of an arginine in the experimental allergic encephalomyelitis protein from human myelin. *Science*, 171, 579-81.
- BEADLE, G. W. & TATUM, E. L. 1941. Genetic Control of Biochemical Reactions in Neurospora. *Proc Natl Acad Sci U S A*, 27, 499-506.
- BEDFORD, M. T. & CLARKE, S. G. 2009. Protein arginine methylation in mammals: who, what, and why. *Mol Cell*, 33, 1-13.
- BEDFORD, M. T. & RICHARD, S. 2005. Arginine methylation an emerging regulator of protein function. *Mol Cell*, 18, 263-72.
- BERGET, S. M., MOORE, C. & SHARP, P. A. 1977. Spliced segments at the 5' terminus of adenovirus 2 late mRNA. *Proc Natl Acad Sci U S A*, 74, 3171-5.
- BLANC, R. S. & RICHARD, S. 2017. Arginine Methylation: The Coming of Age. *Mol Cell*, 65, 8-24.
- BLUDAU, I. & AEBERSOLD, R. 2020. Proteomic and interactomic insights into the molecular basis of cell functional diversity. *Nat Rev Mol Cell Biol*, 21, 327-340.

- BORCHARDT, R. T., PATEL, U. G. & BARTEL, R. L. 1982. Adenosine dialdehyde: a potent inhibitor of S-adenosylhomocysteine hydrolase. *Biochemistry of S-adenosylmethionine and related compounds*. Springer.
- BOTTGER, A., ISLAM, M. S., CHOWDHURY, R., SCHOFIELD, C. J. & WOLF, A. 2015. The oxygenase Jmjd6--a case study in conflicting assignments. *Biochem J*, 468, 191-202.
- BRAHMS, H., MEHEUS, L., DE BRABANDERE, V., FISCHER, U. & LUHRMANN, R. 2001. Symmetrical dimethylation of arginine residues in spliceosomal Sm protein B/B' and the Sm-like protein LSm4, and their interaction with the SMN protein. *RNA*, 7, 1531-42.
- BRAHMS, H., RAYMACKERS, J., UNION, A., DE KEYSER, F., MEHEUS, L. & LUHRMANN, R. 2000. The C-terminal RG dipeptide repeats of the spliceosomal Sm proteins D1 and D3 contain symmetrical dimethylarginines, which form a major B-cell epitope for anti-Sm autoantibodies. *J Biol Chem*, 275, 17122-9.
- BRANSCOMBE, T. L., FRANKEL, A., LEE, J. H., COOK, J. R., YANG, Z., PESTKA, S. & CLARKE, S. 2001. PRMT5 (Janus kinase-binding protein 1) catalyzes the formation of symmetric dimethylarginine residues in proteins. IN VITRO. The role of PRMT5 in vivo has yet to be determined. *J Biol Chem*, 276, 32971-6.
- BROSTOFF, S. & EYLAR, E. H. 1971. Localization of methylated arginine in the A1 protein from myelin. *Proc Natl Acad Sci U S A*, 68, 765-9.
- BURNETT, G. & KENNEDY, E. P. 1954. The enzymatic phosphorylation of proteins. *J Biol Chem*, 211, 969-80.
- CANTONI G.L., C. P. K. 1980. The Role of S-Adenosylhomocysteine and S-Adenosylhomocysteine Hydrolase in the Control of Biological Methylations. *Natural Sulfur Compounds*. Springer, Boston, MA., pp 67-80.
- CHAN, E. Y., LONGATTI, A., MCKNIGHT, N. C. & TOOZE, S. A. 2009. Kinase-inactivated ULK proteins inhibit autophagy via their conserved C-terminal domains using an Atg13-independent mechanism. *Mol Cell Biol*, 29, 157-71.
- CHARI, A., GOLAS, M. M., KLINGENHAGER, M., NEUENKIRCHEN, N., SANDER, B., ENGLBRECHT, C., SICKMANN, A., STARK, H. & FISCHER, U. 2008. An assembly chaperone collaborates with the SMN complex to generate spliceosomal SnRNPs. *Cell*, 135, 497-509.
- CHEN, D. H., WU, K. T., HUNG, C. J., HSIEH, M. & LI, C. 2004. Effects of adenosine dialdehyde treatment on in vitro and in vivo stable protein methylation in HeLa cells. *J Biochem*, 136, 371-6.
- CHEN, T., ZHANG, B., ZIEGENHALS, T., PRUSTY, A. B., FROHLER, S., GRIMM, C., HU, Y., SCHAEFKE, B., FANG, L., ZHANG, M., KRAEMER, N., KAINDL, A. M., FISCHER, U. & CHEN, W. 2019. A missense mutation in SNRPE linked to non-syndromal microcephaly interferes with U snRNP assembly and pre-mRNA splicing. *PLoS Genet*, 15, e1008460.
- CHOW, L. T., GELINAS, R. E., BROKER, T. R. & ROBERTS, R. J. 1977. An amazing sequence arrangement at the 5' ends of adenovirus 2 messenger RNA. *Cell*, 12, 1-8.
- COOK, J. R., LEE, J. H., YANG, Z. H., KRAUSE, C. D., HERTH, N., HOFFMANN, R. & PESTKA, S. 2006. FBXO11/PRMT9, a new protein arginine methyltransferase, symmetrically dimethylates arginine residues. *Biochem Biophys Res Commun*, 342, 472-81.
- CORTHESEY, B. & KAO, P. N. 1994. Purification by DNA affinity chromatography of two polypeptides that contact the NF-AT DNA binding site in the interleukin 2 promoter. *J Biol Chem*, 269, 20682-90.
- DE KLERK, E. & T HOEN, P. A. 2015. Alternative mRNA transcription, processing, and translation: insights from RNA sequencing. *Trends Genet*, 31, 128-39.
- DUCHANGE, N., PIDOUX, J., CAMUS, E. & SAUVAGET, D. 2000. Alternative splicing in the human interleukin enhancer binding factor 3 (ILF3) gene. *Gene*, 261, 345-53.

- EGAN, D. F., SHACKELFORD, D. B., MIHAYLOVA, M. M., GELINO, S., KOHNZ, R. A., MAIR, W., VASQUEZ, D. S., JOSHI, A., GWINN, D. M., TAYLOR, R., ASARA, J. M., FITZPATRICK, J., DILLIN, A., VIOLLET, B., KUNDU, M., HANSEN, M. & SHAW, R. J. 2011. Phosphorylation of ULK1 (hATG1) by AMP-activated protein kinase connects energy sensing to mitophagy. *Science*, 331, 456-61.
- EVICH, M., STROEVA, E., ZHENG, Y. G. & GERMANN, M. W. 2016. Effect of methylation on the side-chain pKa value of arginine. *Protein Sci*, 25, 479-86.
- FENG, Y., MAITY, R., WHITELEGGE, J. P., HADJIKYRIACOU, A., LI, Z., ZURITA-LOPEZ, C., AL-HADID, Q., CLARK, A. T., BEDFORD, M. T., MASSON, J. Y. & CLARKE, S. G. 2013. Mammalian protein arginine methyltransferase 7 (PRMT7) specifically targets RXR sites in lysine- and arginine-rich regions. *J Biol Chem*, 288, 37010-25.
- FIELENBACH, N., GUARDAVACCARO, D., NEUBERT, K., CHAN, T., LI, D., FENG, Q., HUTTER, H., PAGANO, M. & ANTEBI, A. 2007. DRE-1: an evolutionarily conserved F box protein that regulates *C. elegans* developmental age. *Dev Cell*, 12, 443-55.
- FITCH, C. A., PLATZER, G., OKON, M., GARCIA-MORENO, B. E. & MCINTOSH, L. P. 2015. Arginine: Its pKa value revisited. *Protein Sci*, 24, 752-61.
- FRIESEN, W. J., MASSENET, S., PAUSHKIN, S., WYCE, A. & DREYFUSS, G. 2001a. SMN, the product of the spinal muscular atrophy gene, binds preferentially to dimethylarginine-containing protein targets. *Mol Cell*, 7, 1111-7.
- FRIESEN, W. J., PAUSHKIN, S., WYCE, A., MASSENET, S., PESIRIDIS, G. S., VAN DUYN, G., RAPPILBER, J., MANN, M. & DREYFUSS, G. 2001b. The methylosome, a 20S complex containing JBP1 and pICln, produces dimethylarginine-modified Sm proteins. *Mol Cell Biol*, 21, 8289-300.
- GALLOWAY, A. & COWLING, V. H. 2019. mRNA cap regulation in mammalian cell function and fate. *Biochim Biophys Acta Gene Regul Mech*, 1862, 270-279.
- GANLEY, I. G., LAM DU, H., WANG, J., DING, X., CHEN, S. & JIANG, X. 2009. ULK1.ATG13.FIP200 complex mediates mTOR signaling and is essential for autophagy. *J Biol Chem*, 284, 12297-305.
- GHOSH, S. K., PAIK, W. K. & KIM, S. 1988. Purification and molecular identification of two protein methylases I from calf brain. Myelin basic protein- and histone-specific enzyme. *J Biol Chem*, 263, 19024-33.
- GONSALVEZ, G. B., TIAN, L., OSPINA, J. K., BOISVERT, F. M., LAMOND, A. I. & MATERA, A. G. 2007. Two distinct arginine methyltransferases are required for biogenesis of Sm-class ribonucleoproteins. *J Cell Biol*, 178, 733-40.
- GRIMM, C., CHARI, A., PELZ, J. P., KUPER, J., KISKER, C., DIEDERICHS, K., STARK, H., SCHINDELIN, H. & FISCHER, U. 2013. Structural basis of assembly chaperone-mediated snRNP formation. *Mol Cell*, 49, 692-703.
- GRIMMLER, M., BAUER, L., NOUSIAINEN, M., KORNER, R., MEISTER, G. & FISCHER, U. 2005. Phosphorylation regulates the activity of the SMN complex during assembly of spliceosomal U snRNPs. *EMBO Rep*, 6, 70-6.
- GRUSS, O. J., MEDURI, R., SCHILLING, M. & FISCHER, U. 2017. UsnRNP biogenesis: mechanisms and regulation. *Chromosoma*, 126, 577-593.
- GUDERIAN, G., PETER, C., WIESNER, J., SICKMANN, A., SCHULZE-OSTHOFF, K., FISCHER, U. & GRIMMLER, M. 2011. RioK1, a new interactor of protein arginine methyltransferase 5 (PRMT5), competes with pICln for binding and modulates PRMT5 complex composition and substrate specificity. *J Biol Chem*, 286, 1976-86.
- GWINN, D. M., SHACKELFORD, D. B., EGAN, D. F., MIHAYLOVA, M. M., MERY, A., VASQUEZ, D. S., TURK, B. E. & SHAW, R. J. 2008. AMPK phosphorylation of raptor mediates a metabolic checkpoint. *Mol Cell*, 30, 214-26.
- HADJIKYRIACOU, A., YANG, Y., ESPEJO, A., BEDFORD, M. T. & CLARKE, S. G. 2015. Unique Features of Human Protein Arginine Methyltransferase 9 (PRMT9) and Its Substrate RNA Splicing Factor SF3B2. *J Biol Chem*, 290, 16723-43.

- HARDIE, D. G., ROSS, F. A. & HAWLEY, S. A. 2012. AMPK: a nutrient and energy sensor that maintains energy homeostasis. *Nat Rev Mol Cell Biol*, 13, 251-62.
- HAY, N. & SONENBERG, N. 2004. Upstream and downstream of mTOR. *Genes Dev*, 18, 1926-45.
- HERRMANN, F., BOSSERT, M., SCHWANDER, A., AKGUN, E. & FACKELMAYER, F. O. 2004. Arginine methylation of scaffold attachment factor A by heterogeneous nuclear ribonucleoprotein particle-associated PRMT1. *J Biol Chem*, 279, 48774-9.
- HOFFMAN, J. L. 1980. The rate of transmethylation in mouse liver as measured by trapping S-adenosylhomocysteine. *Arch Biochem Biophys*, 205, 132-5.
- HOSKINS, A. A. & MOORE, M. J. 2012. The spliceosome: a flexible, reversible macromolecular machine. *Trends Biochem Sci*, 37, 179-88.
- HOSOKAWA, N., HARA, T., KAIZUKA, T., KISHI, C., TAKAMURA, A., MIURA, Y., IEMURA, S., NATSUME, T., TAKEHANA, K., YAMADA, N., GUAN, J. L., OSHIRO, N. & MIZUSHIMA, N. 2009. Nutrient-dependent mTORC1 association with the ULK1-Atg13-FIP200 complex required for autophagy. *Mol Biol Cell*, 20, 1981-91.
- HUSEDZINOVIC, A., OPPERMANN, F., DRAEGER-MEURER, S., CHARI, A., FISCHER, U., DAUB, H. & GRUSS, O. J. 2014. Phosphoregulation of the human SMN complex. *Eur J Cell Biol*, 93, 106-17.
- HWANG, J. W., CHO, Y., BAE, G. U., KIM, S. N. & KIM, Y. K. 2021. Protein arginine methyltransferases: promising targets for cancer therapy. *Exp Mol Med*.
- INOKI, K., ZHU, T. & GUAN, K. L. 2003. TSC2 mediates cellular energy response to control cell growth and survival. *Cell*, 115, 577-90.
- ISKEN, O., GRASSMANN, C. W., SARISKY, R. T., KANN, M., ZHANG, S., GROSSE, F., KAO, P. N. & BEHRENS, S. E. 2003. Members of the NF90/NFAR protein group are involved in the life cycle of a positive-strand RNA virus. *EMBO J*, 22, 5655-65.
- JAIN, J., LOH, C. & RAO, A. 1995. Transcriptional regulation of the IL-2 gene. *Curr Opin Immunol*, 7, 333-42.
- JENSEN, O. N. 2004. Modification-specific proteomics: characterization of post-translational modifications by mass spectrometry. *Curr Opin Chem Biol*, 8, 33-41.
- JUNG, C. H., JUN, C. B., RO, S. H., KIM, Y. M., OTTO, N. M., CAO, J., KUNDU, M. & KIM, D. H. 2009. ULK-Atg13-FIP200 complexes mediate mTOR signaling to the autophagy machinery. *Mol Biol Cell*, 20, 1992-2003.
- KAMBACH, C., WALKE, S., YOUNG, R., AVIS, J. M., DE LA FORTELLE, E., RAKER, V. A., LUHRMANN, R., LI, J. & NAGAI, K. 1999. Crystal structures of two Sm protein complexes and their implications for the assembly of the spliceosomal snRNPs. *Cell*, 96, 375-87.
- KAO, P. N., CHEN, L., BROCK, G., NG, J., KENNY, J., SMITH, A. J. & CORTHESEY, B. 1994. Cloning and expression of cyclosporin A- and FK506-sensitive nuclear factor of activated T-cells: NF45 and NF90. *Journal of Biological Chemistry*, 269, 20691-20699.
- KHOURY, G. A., BALIBAN, R. C. & FLOUDAS, C. A. 2011. Proteome-wide post-translational modification statistics: frequency analysis and curation of the swiss-prot database. *Sci Rep*, 1.
- KILEDJIAN, M. & DREYFUSS, G. 1992. Primary structure and binding activity of the hnRNP U protein: binding RNA through RGG box. *EMBO J*, 11, 2655-64.
- KIM, J., KUNDU, M., VIOLLET, B. & GUAN, K. L. 2011. AMPK and mTOR regulate autophagy through direct phosphorylation of Ulk1. *Nat Cell Biol*, 13, 132-41.
- KIM, S. & PAIK, W. K. 1965. Studies on the origin of epsilon-N-methyl-L-lysine in protein. *J Biol Chem*, 240, 4629-34.
- KRAPIVINSKY, G., PU, W., WICKMAN, K., KRAPIVINSKY, L. & CLAPHAM, D. E. 1998. pICln binds to a mammalian homolog of a yeast protein involved in regulation of cell morphology. *J Biol Chem*, 273, 10811-4.

- KRZYŻANOWSKI, A., GASPER, R., ADIHO, H., THART, P. & WALDMANN, H. 2021. Biochemical Investigation of the Interaction of pICln, RioK1 and COPR5 with the PRMT5-MEP50 Complex. *Chembiochem*.
- LACROIX, M., EL MESSAOUDI, S., RODIER, G., LE CAM, A., SARDET, C. & FABBRIZIO, E. 2008. The histone-binding protein COPR5 is required for nuclear functions of the protein arginine methyltransferase PRMT5. *EMBO Rep*, 9, 452-8.
- LAPEYRE, B., AMALRIC, F., GHAFFARI, S. H., RAO, S. V., DUMBAR, T. S. & OLSON, M. O. 1986. Protein and cDNA sequence of a glycine-rich, dimethylarginine-containing region located near the carboxyl-terminal end of nucleolin (C23 and 100 kDa). *J Biol Chem*, 261, 9167-73.
- LAPLANTE, M. & SABATINI, D. M. 2012. mTOR signaling in growth control and disease. *Cell*, 149, 274-93.
- LARONDE-LEBLANC, N., GUSZCZYNSKI, T., COPELAND, T. & WLODAWER, A. 2005. Structure and activity of the atypical serine kinase Rio1. *FEBS J*, 272, 3698-713.
- LARONDE-LEBLANC, N. & WLODAWER, A. 2005. A family portrait of the RIO kinases. *J Biol Chem*, 280, 37297-300.
- LEE, J. H., COOK, J. R., YANG, Z. H., MIROCHNITCHENKO, O., GUNDERSON, S. I., FELIX, A. M., HERTH, N., HOFFMANN, R. & PESTKA, S. 2005. PRMT7, a new protein arginine methyltransferase that synthesizes symmetric dimethylarginine. *J Biol Chem*, 280, 3656-64.
- LIAO, H. J., KOBAYASHI, R. & MATHEWS, M. B. 1998. Activities of adenovirus virus-associated RNAs: purification and characterization of RNA binding proteins. *Proc Natl Acad Sci U S A*, 95, 8514-9.
- LISCHWE, M. A., COOK, R. G., AHN, Y. S., YEOMAN, L. C. & BUSCH, H. 1985a. Clustering of glycine and NG,NG-dimethylarginine in nucleolar protein C23. *Biochemistry*, 24, 6025-8.
- LISCHWE, M. A., OCHS, R. L., REDDY, R., COOK, R. G., YEOMAN, L. C., TAN, E. M., REICHLIN, M. & BUSCH, H. 1985b. Purification and partial characterization of a nucleolar scleroderma antigen (Mr = 34,000; pI, 8.5) rich in NG,NG-dimethylarginine. *J Biol Chem*, 260, 14304-10.
- LISCHWE, M. A., ROBERTS, K. D., YEOMAN, L. C. & BUSCH, H. 1982. Nucleolar specific acidic phosphoprotein C23 is highly methylated. *J Biol Chem*, 257, 14600-2.
- LUSCOMBE, N. M., LASKOWSKI, R. A. & THORNTON, J. M. 2001. Amino acid-base interactions: a three-dimensional analysis of protein-DNA interactions at an atomic level. *Nucleic Acids Res*, 29, 2860-74.
- MACIAN, F. 2005. NFAT proteins: key regulators of T-cell development and function. *Nat Rev Immunol*, 5, 472-84.
- MANN, M., ONG, S. E., GRONBORG, M., STEEN, H., JENSEN, O. N. & PANDEY, A. 2002. Analysis of protein phosphorylation using mass spectrometry: deciphering the phosphoproteome. *Trends Biotechnol*, 20, 261-8.
- MATERA, A. G. & WANG, Z. 2014. A day in the life of the spliceosome. *Nat Rev Mol Cell Biol*, 15, 108-21.
- MEISTER, G., BUHLER, D., PILLAI, R., LOTTSPREICH, F. & FISCHER, U. 2001a. A multiprotein complex mediates the ATP-dependent assembly of spliceosomal U snRNPs. *Nat Cell Biol*, 3, 945-9.
- MEISTER, G., EGGERT, C., BUHLER, D., BRAHMS, H., KAMBACH, C. & FISCHER, U. 2001b. Methylation of Sm proteins by a complex containing PRMT5 and the putative U snRNP assembly factor pICln. *Curr Biol*, 11, 1990-4.
- MIGLIORI, V., MULLER, J., PHALKE, S., LOW, D., BEZZI, M., MOK, W. C., SAHU, S. K., GUNARATNE, J., CAPASSO, P., BASSI, C., CECATIELLO, V., DE MARCO, A., BLACKSTOCK, W., KUZNETSOV, V., AMATI, B., MAPELLI, M. & GUCCIONE, E.

2012. Symmetric dimethylation of H3R2 is a newly identified histone mark that supports euchromatin maintenance. *Nat Struct Mol Biol*, 19, 136-44.
- MIRANDA, T. B., MIRANDA, M., FRANKEL, A. & CLARKE, S. 2004. PRMT7 is a member of the protein arginine methyltransferase family with a distinct substrate specificity. *J Biol Chem*, 279, 22902-7.
- MURN, J. & SHI, Y. 2017. The winding path of protein methylation research: milestones and new frontiers. *Nat Rev Mol Cell Biol*, 18, 517-527.
- MURRAY, K. 1964. The Occurrence of Epsilon-N-Methyl Lysine in Histones. *Biochemistry*, 3, 10-5.
- NEWMAN, A. 1998. RNA splicing. *Curr Biol*, 8, R903-5.
- NISHIOKA, K. & REINBERG, D. 2003. Methods and tips for the purification of human histone methyltransferases. *Methods*, 31, 49-58.
- PAIK, W. K. & KIM, S. 1968. Protein methylase I. Purification and properties of the enzyme. *J Biol Chem*, 243, 2108-14.
- PAKNIA, E., CHARI, A., STARK, H. & FISCHER, U. 2016. The Ribosome Cooperates with the Assembly Chaperone pICln to Initiate Formation of snRNPs. *Cell Rep*, 16, 3103-3112.
- PAL, S., VISHWANATH, S. N., ERDJUMENT-BROMAGE, H., TEMPST, P. & SIF, S. 2004. Human SWI/SNF-associated PRMT5 methylates histone H3 arginine 8 and negatively regulates expression of ST7 and NM23 tumor suppressor genes. *Mol Cell Biol*, 24, 9630-45.
- PATEL-THOMBRE, U. & BORCHARDT, R. T. 1985. Adenine nucleoside dialdehydes: potent inhibitors of bovine liver S-adenosylhomocysteine hydrolase. *Biochemistry*, 24, 1130-6.
- PATEL, R. C., VESTAL, D. J., XU, Z., BANDYOPADHYAY, S., GUO, W., ERME, S. M., WILLIAMS, B. R. & SEN, G. C. 1999. DRBP76, a double-stranded RNA-binding nuclear protein, is phosphorylated by the interferon-induced protein kinase, PKR. *J Biol Chem*, 274, 20432-7.
- PAULMICHL, M., LI, Y., WICKMAN, K., ACKERMAN, M., PERALTA, E. & CLAPHAM, D. 1992. New mammalian chloride channel identified by expression cloning. *Nature*, 356, 238-41.
- PIRAS, A., SCHIAFFINO, L., BOIDO, M., VALSECCHI, V., GUGLIELMOTTO, M., DE AMICIS, E., PUYAL, J., GARCERA, A., TAMAGNO, E., SOLER, R. M. & VERCELLI, A. 2017. Inhibition of autophagy delays motoneuron degeneration and extends lifespan in a mouse model of spinal muscular atrophy. *Cell Death Dis*, 8, 3223.
- POLLACK, B. P., KOTENKO, S. V., HE, W., IZOTOVA, L. S., BARNOSKI, B. L. & PESTKA, S. 1999. The human homologue of the yeast proteins Skb1 and Hsl7p interacts with Jak kinases and contains protein methyltransferase activity. *J Biol Chem*, 274, 31531-42.
- PRUSTY, A. B., MEDURI, R., PRUSTY, B. K., VANSELOW, J., SCHLOSSER, A. & FISCHER, U. 2017. Impaired spliceosomal UsnRNP assembly leads to Sm mRNA down-regulation and Sm protein degradation. *J Cell Biol*, 216, 2391-2407.
- PU, W. T., KRAPIVINSKY, G. B., KRAPIVINSKY, L. & CLAPHAM, D. E. 1999. pICln inhibits snRNP biogenesis by binding core spliceosomal proteins. *Mol Cell Biol*, 19, 4113-20.
- PU, W. T., WICKMAN, K. & CLAPHAM, D. E. 2000. ICln is essential for cellular and early embryonic viability. *J Biol Chem*, 275, 12363-6.
- QUIDVILLE, V., ALSAFADI, S., GOUBAR, A., COMMO, F., SCOTT, V., PIOCHE-DURIEU, C., GIRAULT, I., BACONNAIS, S., LE CAM, E., LAZAR, V., DELALOGUE, S., SAGHATCHIAN, M., PAUTIER, P., MORICE, P., DESSEN, P., VAGNER, S. & ANDRE, F. 2013. Targeting the deregulated spliceosome core machinery in cancer cells triggers mTOR blockade and autophagy. *Cancer Res*, 73, 2247-58.
- RAMAZI, S. & ZAHIRI, J. 2021. Posttranslational modifications in proteins: resources, tools and prediction methods. *Database (Oxford)*, 2021.

- REICHMAN, T. W., MUNIZ, L. C. & MATHEWS, M. B. 2002. The RNA binding protein nuclear factor 90 functions as both a positive and negative regulator of gene expression in mammalian cells. *Mol Cell Biol*, 22, 343-56.
- ROBBINS, J., DILWORTH, S. M., LASKEY, R. A. & DINGWALL, C. 1991. Two interdependent basic domains in nucleoplasmin nuclear targeting sequence: identification of a class of bipartite nuclear targeting sequence. *Cell*, 64, 615-23.
- SANCHEZ-OLEA, R., EMMA, F., COGHLAN, M. & STRANGE, K. 1998. Characterization of pICln phosphorylation state and a pICln-associated protein kinase. *Biochim Biophys Acta*, 1381, 49-60.
- SATO, M., SHAHEEN, V. M., KAO, P. N., OKANO, T., SHAW, M., YOSHIDA, H., RICHARDS, H. B. & REEVES, W. H. 1999. Autoantibodies define a family of proteins with conserved double-stranded RNA-binding domains as well as DNA binding activity. *J Biol Chem*, 274, 34598-604.
- SAUNDERS, L. R., JURECIC, V. & BARBER, G. N. 2001. The 90- and 110-kDa human NFAR proteins are translated from two differentially spliced mRNAs encoded on chromosome 19p13. *Genomics*, 71, 256-9.
- SCHMITZ, K., COX, J., ESSER, L. M., VOSS, M., SANDER, K., LOFFLER, A., HILLEBRAND, F., ERKELENZ, S., SCHAAL, H., KAHNE, T., KLINKER, S., ZHANG, T., NAGEL-STEGER, L., WILLBOLD, D., SEGGEWISS, S., SCHLUTERMANN, D., STORK, B., GRIMMLER, M., WESSELBORG, S. & PETER, C. 2021. An essential role of the autophagy activating kinase ULK1 in snRNP biogenesis. *Nucleic Acids Res.*
- SCHWARZ, J. J., WIESE, H., TOLLE, R. C., ZAREI, M., DENGJEL, J., WARSCHIED, B. & THEDIECK, K. 2015. Functional Proteomics Identifies Acinus L as a Direct Insulin- and Amino Acid-Dependent Mammalian Target of Rapamycin Complex 1 (mTORC1) Substrate. *Mol Cell Proteomics*, 14, 2042-55.
- SHATKIN, A. J. 1976. Capping of eucaryotic mRNAs. *Cell*, 9, 645-53.
- SHAW, J. P., UTZ, P. J., DURAND, D. B., TOOLE, J. J., EMMEL, E. A. & CRABTREE, G. R. 1988. Identification of a putative regulator of early T cell activation genes. *Science*, 241, 202-5.
- SHI, L., ZHAO, G., QIU, D., GODFREY, W. R., VOGEL, H., RANDO, T. A., HU, H. & KAO, P. N. 2005. NF90 regulates cell cycle exit and terminal myogenic differentiation by direct binding to the 3'-untranslated region of MyoD and p21WAF1/CIP1 mRNAs. *J Biol Chem*, 280, 18981-9.
- SHIM, J., LIM, H., J. R. Y. & KARIN, M. 2002. Nuclear export of NF90 is required for interleukin-2 mRNA stabilization. *Mol Cell*, 10, 1331-44.
- SHIMOBAYASHI, M. & HALL, M. N. 2014. Making new contacts: the mTOR network in metabolism and signalling crosstalk. *Nat Rev Mol Cell Biol*, 15, 155-62.
- STEWART, M. 2019. Polyadenylation and nuclear export of mRNAs. *J Biol Chem*, 294, 2977-2987.
- SUN, L., WANG, M., LV, Z., YANG, N., LIU, Y., BAO, S., GONG, W. & XU, R. M. 2011. Structural insights into protein arginine symmetric dimethylation by PRMT5. *Proc Natl Acad Sci U S A*, 108, 20538-43.
- TAN, D. Q., LI, Y., YANG, C., LI, J., TAN, S. H., CHIN, D. W. L., NAKAMURA-ISHIZU, A., YANG, H. & SUDA, T. 2019. PRMT5 Modulates Splicing for Genome Integrity and Preserves Proteostasis of Hematopoietic Stem Cells. *Cell Rep*, 26, 2316-2328 e6.
- TEWARY, S. K., ZHENG, Y. G. & HO, M. C. 2019. Protein arginine methyltransferases: insights into the enzyme structure and mechanism at the atomic level. *Cell Mol Life Sci*, 76, 2917-2932.
- UVERSKY, V. N. 2013. Posttranslational Modification. *Brenner's Encyclopedia of Genetics*, 425-430.

- VIRÁG, D., DALMADI-KISS, B., VÉKEY, K., DRAHOS, L., KLEBOVICH, I., ANTAL, I. & LUDÁNYI, K. 2020. Current trends in the analysis of post-translational modifications. *Chromatographia*, 83, 1-10.
- WALSH, C. T., GARNEAU-TSODIKOVA, S. & GATTO, G. J., JR. 2005. Protein posttranslational modifications: the chemistry of proteome diversifications. *Angew Chem Int Ed Engl*, 44, 7342-72.
- WANG, E. T., SANDBERG, R., LUO, S., KHREBTUKOVA, I., ZHANG, L., MAYR, C., KINGSMORE, S. F., SCHROTH, G. P. & BURGE, C. B. 2008. Alternative isoform regulation in human tissue transcriptomes. *Nature*, 456, 470-6.
- WESSELBORG, S. & STORK, B. 2015. Autophagy signal transduction by ATG proteins: from hierarchies to networks. *Cell Mol Life Sci*, 72, 4721-57.
- WIDMANN, B., WANDREY, F., BADERTSCHER, L., WYLER, E., PFANNSTIEL, J., ZEMP, I. & KUTAY, U. 2012. The kinase activity of human Rio1 is required for final steps of cytoplasmic maturation of 40S subunits. *Mol Biol Cell*, 23, 22-35.
- WU, W., WANG, X., BERLETH, N., DEITERSEN, J., WALLOT-HIEKE, N., BOHLER, P., SCHLUTERMANN, D., STUHLREIER, F., COX, J., SCHMITZ, K., SEGGEWISS, S., PETER, C., KASOF, G., STEFANSKI, A., STUHLER, K., TSCHAPEK, A., GODECKE, A. & STORK, B. 2020. The Autophagy-Initiating Kinase ULK1 Controls RIPK1-Mediated Cell Death. *Cell Rep*, 31, 107547.
- WU, W., WANG, X., SUN, Y., BERLETH, N., DEITERSEN, J., SCHLUTERMANN, D., STUHLREIER, F., WALLOT-HIEKE, N., JOSE MENDIBURO, M., COX, J., PETER, C., BERGMANN, A. K. & STORK, B. 2021. TNF-induced necroptosis initiates early autophagy events via RIPK3-dependent AMPK activation, but inhibits late autophagy. *Autophagy*, 1-18.
- YANG, Y., HADJIKYRIACOU, A., XIA, Z., GAYATRI, S., KIM, D., ZURITA-LOPEZ, C., KELLY, R., GUO, A., LI, W., CLARKE, S. G. & BEDFORD, M. T. 2015. PRMT9 is a type II methyltransferase that methylates the splicing factor SAP145. *Nat Commun*, 6, 6428.
- ZHANG, R., SO, B. R., LI, P., YONG, J., GLISOVIC, T., WAN, L. & DREYFUSS, G. 2011. Structure of a key intermediate of the SMN complex reveals Gemin2's crucial function in snRNP assembly. *Cell*, 146, 384-95.
- ZURITA-LOPEZ, C. I., SANDBERG, T., KELLY, R. & CLARKE, S. G. 2012. Human protein arginine methyltransferase 7 (PRMT7) is a type III enzyme forming omega-NG-monomethylated arginine residues. *J Biol Chem*, 287, 7859-70.

10 Acknowledgments

Zuallererst möchte ich mich bei Dr. Christoph Peter für die Betreuung dieser Doktorarbeit bedanken. Du hast durch deine Ideen und deine Geduld maßgeblich zum Gelingen dieser Arbeit beigetragen. Bedanken möchte ich mich nicht nur für den steten wissenschaftlichen Input und die immer vorhandene Unterstützung, sondern auch für zahlreiche gute Gespräche über Wein, Uhren und Fahrräder. Ich habe viel bei dir gelernt.

Bedanken möchte ich mich auch bei Prof. Dr. Sebastian Wesselborg für die Übernahme der Tätigkeit als 1. Gutachter und die Möglichkeit, die Doktorarbeit in seinem Institut anzufertigen. Danke für dein Vertrauen und deinen wissenschaftlichen Rat.

Mein besonderer Dank gilt auch Prof. Dr. Lutz Schmitt, nicht nur für die Übernahme der 2. Gutachtertätigkeit, sondern auch für die Mentorengespräche und den wissenschaftlichen Diskurs zum Thema. Als Biochemiker möchte ich auch die Gelegenheit nutzen, mich für ein interessantes, abwechslungsreiches und gut organisiertes Studium zu bedanken, sodass ich die Entscheidung nach Düsseldorf zu gehen nie bereut habe.

Nicht unerwähnt bleiben darf in diesem Zusammenhang auch Herr PD Dr. Ulrich Schulte für die gute Organisation des Biochemie Studienganges. Von der ersten Begrüßung im Hörsaal, über alle Semester hinweg haben Sie nicht nur mir, sondern allen Studierenden der Biochemie mit Rat und Tat zur Seite gestanden.

Bedanken möchte ich mich auch bei den Kolleginnen und Kollegen des Instituts für Molekulare Medizin I für die Unterstützung und den wissenschaftlichen Austausch, für Tipps zu Experimenten und für die gute Versorgung mit Kuchen. Besonders der alten Garde der Doktoranden der MolMed und MolRadOnk gebührt mein Dank für Biertastings, Abende im Strandbad Süd am U-See, Stand Up Paddling, laute Musik in den Laboren, Karnevalsfeiern und Abende in der Kasette. Es hat mir sehr viel Spaß gemacht mit euch zusammenzuarbeiten.

Ein besonderer Dank gilt dem Lehrerkollegium der Abteilung Biowissenschaften des Berufskolleg Hilden für ihr Engagement, ihre Begeisterung für die Naturwissenschaften und die gute Ausbildung. Vielen Dank für den ersten Kontakt mit der Wissenschaft, ohne den ich mich möglicherweise nie für ein Studium entschieden hätte. Ich denke sehr gerne an die zwei Jahre in der BTA zurück.

Auf der zweiten Seite soll Platz sein für die Wegbegleiter in meinem privaten Umfeld:

Ich danke meinen langjährigen Freunden, die mich auf dem Weg zu dieser Arbeit begleitet haben. Claudia, ich danke dir für deine Unterstützung in den letzten Jahren, für die schöne Zeit mit dir und deiner wunderbaren Familie und für das Lesen meiner Arbeit. Auf dein Gedächtnis war immer Verlass, wenn ich wieder mal meinte, dass wir etwas Bestimmtes ganz sicher nicht im Studium behandelt hatten. Dennis, für deine immer lustige Art, für unvergessliche Urlaube und für viele Abende in Heidelberg und Düsseldorf und den straffen Zeitplan auf der Zielgeraden, den ich nicht ganz eingehalten habe. Thomas, als bester Wegbegleiter im Studium, in der Fachschaft und bei der GBM. Danke für die allererste Bleibe in Düsseldorf bei den vielen Veranstaltungen und Feiern im 1. Semester, als ich noch nicht in Düsseldorf gewohnt habe. Danke für die vielen spontanen „lass mal was machen“, ausgedehnte Laufrunden und das eine Glas Bier in der Altstadt, bei dem die Größe des Glases immer variabel war. Daniel, meinem Reisepartner für Rucksack und Zelt, für viele Abenteuer außerhalb des Uni Alltags ob in Schweden oder andern Teilen der Welt, aber auch für die vielen schönen Dinge in Düsseldorf als fast Nachbarn. Michael, seit der 5. Klasse bist du ein treuer Freund. Danke für viele Gespräche und Hilfe in allen Lebenslagen. David, für die schöne Zeit im Labor, viele Kilometer gemeinsam mit den Laufschuhen, Radtouren, zahlreichen Feierabendbieren und besonders für nächtliche spontane Flugbuchungen im Schaukelstühlchen. Bei Ann Cathrin für die langjährige Freundschaft auch über große Distanzen, für deine Ratschläge und eine unvergessliche Ausbildungszeit. Bei Inga für die Unterstützung im Studium und Anja und Melanie, ihr drei wart Wegbeleiter der ersten Stunde an der HHU und habt mir den Einstieg in die Uniwelt durch eure fröhliche Art leicht gemacht. Danke für eure Unterstützung bei zahlreichen Praktika, Übungen und dem Schreiben von Protokollen bis in die Nacht hinein.

Ein riesiger Dank gebührt auch meiner ganzen Familie. Meiner Mutter, die mir im Leben so vieles ermöglicht hat. Danke, für deine stetige Unterstützung und dass wir immer als eine Einheit unterwegs waren. Meinen Großeltern, als riesiger Fels in der Brandung auch in turbulenten Zeiten. Auf euch ist immer verlass! Meinem Vater, meiner Schwester und meinen Großeltern für ihre immerwährende Unterstützung auf meinem Lebensweg. Meinen Cousins Martin und Christian, mit denen ich meine Kindheit verbracht habe und die wie Brüder für mich sind. Am Ende möchte ich mich noch bedanken bei den vielen, die hier persönlich keine Erwähnung fanden. An euch ist gedacht, ich weiß, dass es euch gibt! Danke!

11 Declaration

Ich versichere an Eides Statt, dass die Dissertation von mir selbständig und ohne unzulässige fremde Hilfe unter Beachtung der „Grundsätze zur Sicherung guter wissenschaftlicher Praxis an der Heinrich-Heine-Universität Düsseldorf“ erstellt worden ist. Die Dissertation wurde in der vorgelegten oder in ähnlicher Form noch bei keiner anderen Fakultät eingereicht. Ich habe bisher keine erfolglosen und erfolgreichen Promotionsversuche unternommen.

Ort, Datum

Jan Cox